Precambrian Research 422 (2025) 107707

Contents lists available at ScienceDirect

Precambrian Research

journal homepage: www.elsevier.com/locate/precamres

50th Anniversary Invited Review

Review of Paleoproterozoic tectonics in the southern West African Craton: Insights from multi-disciplinary data integration

Julien Perret [a,*], Mark W. Jessell [a], Quentin Masurel [a], Patrick C. Hayman [b], Nicolas Thébaud [a], Lenka Baratoux [c,d], Alain Kouamélan [d], Aurélien Eglinger [e,f], Anne-Sylvie André-Mayer [e], Augustin Y. Koffi [d], Ibrahima Dia [g], Jacques Koné [h], James Davis [a], Ousmane Wane [i], Prince O. Amponsah [j], Seta Naba [k], Oliver Vanderhaeghe [c]

[a] Centre for Exploration Targeting, School of Earth and Oceans, The University of Western Australia, Western Australia 6009, Australia
[b] School of Earth and Atmospheric Sciences, Queensland University of Technology, Brisbane, QLD 4000, Australia
[c] GET, Université de Toulouse, CNRS, IRD, UPS, Toulouse, France
[d] Université Félix Houphouët-Boigny Abidjan-Cocody, UFR-STRM, 22 BP 582 Abidjan 22, Côte d'Ivoire
[e] GeoRessources, Université de Lorraine-CNRS, Nancy, France
[f] InnovExplo – Norda Stelo, Québec, Canada
[g] Amadou Mahtar Mbow University, Dakar, Senegal
[h] Department of Geology, Faculty of Science and Technology, Cheikh Anta Diop University, Dakar, Senegal
[i] Laboratoire de Géodynamique et de Cartographie, D.E.R de Géologie, FST, Université des Sciences, des Techniques et des Technologies de Bamako, Bamako, Mali
[j] University of Ghana, School of Physical and Mathematical Sciences, Department of Earth Science, P.O. Box LG 58, Legon Accra, Ghana
[k] Laboratoire Géosciences et Environnement (LaGE), Université Joseph KI-ZERBO, Département des Sciences de la Terre, Unité de Formation et de Recherche en Sciences de la Vie et de la Terre, 03 BP 7021, Ouaga 03, Burkina Faso

ARTICLE INFO

Keywords:
southern West African Craton
Paleoproterozoic
Tectonics
Geodynamics
Multi-disciplinary data integration

ABSTRACT

For over a century, research has focused on the southern West African Craton (sWAC), aiming to unravel its lithological, geochemical, geochronological, structural, metamorphic, and metallogenic record. Yet, the late Siderian to early Rhyacian (c. 2350–2265 Ma) geodynamic setting of the sWAC remains poorly constrained due to (i) the unresolved configuration of adjacent Archean blocks; (ii) limited geochronological data for the lowermost stratigraphic units; and (iii) extensive overprinting by subsequent magmatic, tectonic, and thermal events. Using a multidisciplinary data integration approach, it is however possible to conduct the analysis of tectonic processes governing the emplacement of the Paleoproterozoic granite-greenstone belts of West Africa.

In this review, we integrate all available published datasets and knowledge to provide new insights on the late Siderian to Rhyacian tectonic evolution of the sWAC. This data compilation is presented and discussed in the form of key time slices (c. 2350–2265 Ma, 2265–2200 Ma, 2200–2135 Ma, 2135–2120 Ma, 2120–2095 Ma and 2095–2060 Ma), which mark evolutionary stages in the geological history of the region. The results of our analysis support the shift from enigmatic Archean tectonic modes to plate tectonics, with the onset of subduction at c. 2265 Ma.

However, critical knowledge gaps remain, particularly regarding the tectonic significance of greenstone belts and the role of the West African Craton in potential configurations of the Eburnean–Transamazonian Orogen during the assembly of Nuna. To address these issues, future research directions are proposed to conclude this synthesis.

1. Introduction

The transition from the Archean to the dawn of the Paleoproterozoic marks a pivotal period in Earth's history, reflected by significant changes in the lithosphere. With relatively few rocks from the Siderian (2500–2300 Ma) and Rhyacian (2300–2050 Ma) periods preserved in the geological record, this transition remains poorly understood (Condie, 2018; Shields et al., 2022). This transition was characterised by

* Corresponding author.
E-mail address: julien.perret@uwa.edu.au (J. Perret).

https://doi.org/10.1016/j.precamres.2025.107707
Received 25 September 2024; Received in revised form 16 January 2025; Accepted 19 January 2025
Available online 22 March 2025

(i) the rapid emergence of subaerial landmasses, leading to changes in weathering and erosion rates (e.g. Kusky et al., 2016; Bindeman et al., 2018; Huang et al., 2022; Huang et al., 2023); (ii) the increase in continental alkali basalts around 2.1 Ga, coinciding with a sharp reduction in mantle melting and compositional changes in komatiites (Liu et al., 2019); (iii) a pronounced shift in granitoid geochemistry, including increased large-ion lithophile elements (LILE) and rare earth elements (REE), decreased Eu anomaly, Zr/Sm and Sr/Y ratios, and reduced Mg and Ni concentrations, collectively interpreted to reflect decreasing magma generation depth and crustal thickness (Condie et al., 2024); and (iv) the emergence of a sustained, large-scale deep carbon cycle, evidenced by associations of Paleoproterozoic carbonatites with high-pressure metamorphic rocks in orogenic belts (e.g. Zhao et al., 2024; Xu et al., 2018). Yet, the tectonic regimes that operated during this transitional period in Earth's history remain widely debated, with both uniformitarian and non-uniformitarian models proposed (Nebel et al., 2018; Cawood et al., 2022; Stern, 2023; Hawkesworth et al., 2024).

The late Siderian to Rhyacian terrains of the southern West African Craton (sWAC) provide a rare natural laboratory to investigate this enigmatic period of Precambrian Earth history. Firstly, the overall tectonic evolution of the Paleoproterozoic part of the sWAC can be summarised as two periods. The c. 2350–2265 Ma period is marked by a fragmental geological record limited to the lowermost mafic stratigraphic units, with tectonic models including: (i) eruption of tholeiitic basalts at a mid-oceanic ridge (Leube et al., 1990); (ii) rapid outpouring primitive magmas forming an oceanic plateau (Lompo, 2009; Hayman et al., 2023); and (iii) eruption of basalts within an incipient intra-oceanic subduction zone (e.g. Salah et al., 1996). The c. 2265–2050 Ma period is equally contentious, with proponents of subduction-driven tectonics (e.g. Pouclet et al., 2006; Baratoux et al., 2011; Eglinger et al., 2017; Wane et al., 2018; Grenhölm et al., 2019a,b; Hayman et al., 2023) opposed to those advocating vertical tectonics including sagduction and dripping (e.g. Vidal et al., 2009; Lompo, 2009, 2010). Secondly, the relative position of the West African Craton (WAC) in the Nuna supercontinent remains poorly constrained (Gong et al., 2021; Cao et al., 2024). Age-equivalent terrains have been identified across the Guiana Shield (Vianna et al, 2020; Neto and Lafon, 2020; Pinto et al., 2024), Borborema Province (de Lira Santos et al., 2023), São Luis Cratonic Fragment (Klein et al., 2020), São Francisco Craton (Bruno et al., 2020, 2021; Almeida et al., 2022), and Ukrainian Shield (Bogdanova et al., 2008; Terentiev and Santosh, 2020). However, the spatial configuration of these lithospheric blocks remains contentious due to limited robust paleogeographic indicators (e.g. Gong et al., 2021; D'Agrella-Filho et al., 2021). Lastly, Paleoproterozoic terrains across the sWAC host a variety of mineral systems, including orogenic Au, Cu-Zn volcanic-hosted massive sulphides (VMS), porphyry Cu, Fe skarn, and Li-Cs-Ta (LCT) pegmatites (Goldfarb et al., 2017; Markwitz et al., 2016; Milési et al., 1992; Eglinger et al., 2022; Thébaud et al., 2020; Masurel et al., 2022). Despite significant metallogenic syntheses (Thébaud et al., 2020; Masurel et al., 2022), the space–time-integrated metallogenic inventory of the sWAC has yet to be incorporated as a proxy to track secular changes in tectonic processes during the Paleoproterozoic Era (Huston et al., 2023).

Over the last decade, abundant lithological, geochemical, geochronological, structural, metamorphic, and metallogenic data for the Paleoproterozoic sWAC have been acquired through the ongoing AMIRA Global West African eXploration Initiative (WAXI). In numbers, this integrated research and training program involved 11 countries and more than 70 partner organisations by the end of Stage 3 (after running for 12 years), and resulted in the training and upskilling of > 90 African and international PhD/MSc/Hons students and postdoctoral geoscientists (https://waxi4.org). The collected multi-disciplinary data and integrated geological knowledge have resulted in a step change in our ability to decipher the tectonics of the sWAC during Paleoproterozoic times. In this review and synopsis, we present the status of the knowledge on the Paleoproterozoic part of the sWAC and discuss key knowledge gaps to stimulate future research.

2. Geological background

The West African Craton (WAC), as defined by Kennedy (1964), consists of two Archean nuclei in the north-western and south-western parts of the craton, respectively the Reguibat and Kénéma-Man Domains, against which an array of Paleoproterozoic domains is juxtaposed (Fig. 1). These Paleoproterozoic domains consist of greenstone belts separated by sedimentary basins or regions of extensive tonalite-trondhjemite-granodiorite (TTG) plutons, all dissected by major faults and shear zones (Fig. 1). These Paleoproterozoic domains are overlain by Mesoproterozoic and younger sedimentary basins. The northern extent of the WAC is marked by the Paleoproterozoic Anti-Atlas Inliers. The borders of the WAC were largely defined by a combination of surface geology and gravity signatures (Burke and Whiteman, 1973; Bayer and Lesquer, 1978; Ennih and Liégeois, 2008a,b). However, it has been suggested that the western craton margin extended further to the west at the time of its formation (Jessell et al., 2016). To the east, the WAC is separated from the Archean Benino-Nigerian Shield by the southern portion of the 1000 km-long Pan-African suture zone of the Dahomeyide belt. This suture zone represents the closure of the Pharusian Ocean and the subsequent continental collision during the Neoproterozoic (c. 800–580 Ma; Guillot et al., 2009).

The southern West African Craton (sWAC) consists of the Paleoproterozoic (historically referred to as "Birimian" by Kitson, 1918) Baoulé-Mossi Domain (Bonhomme, 1962; Bessoles, 1977) juxtaposed against the Archean Kénéma-Man Domain (Bessoles, 1977; Boher et al., 1992; Fig. 1). The Kénéma-Man Domain consists of exposed, c. 3500–2600 Ma Archean crust in Liberia and Sierra Leone (Rollinson, 2016), as well as crust of similar age reworked during the Paleoproterozoic in southern Guinea and western Côte d'Ivoire (Kouamélan et al., 1997, 2015; Eglinger et al., 2017; Koffi et al., 2020, 2022). A segment of this crust, known as the SASCA Domain, is situated in south-western Côte d'Ivoire (Fig. 1). The Baoulé-Mossi Domain extends from western Niger and south-eastern Ghana in the east to the Kédougou-Kénieba Inlier on the Mali-Senegal border in the west (Abouchami et al., 1990; Boher et al., 1992; Diallo et al., 2020; Salah et al., 1996). The Paleoproterozoic terrains of this domain have been divided into linear to arcuate greenstone belts, sedimentary basins, and intrusive domains (Bessoles, 1977; Feybesse et al., 1989; Feybesse and Milési, 1994; Kouamélan et al., 1997; Caby et al., 2000; Egal et al., 2002; Baratoux et al., 2011, 2024; Perrouty et al., 2012; Grenhölm et al., 2019a). This nomenclature is adopted throughout this manuscript (Fig. 1).

3. Stratigraphic, plutonic, structural, and metallogenic evolution of the sWAC from 2350 to 2060 Ma

This section provides a review and synopsis of the geological evolution of the sWAC over 290 Myr from 2350 to 2060 Ma. The latest Siderian (2350–2300 Ma) and most of the Rhyacian (2300–2060 Ma) evolution are discussed hereafter through key time slices, focusing on

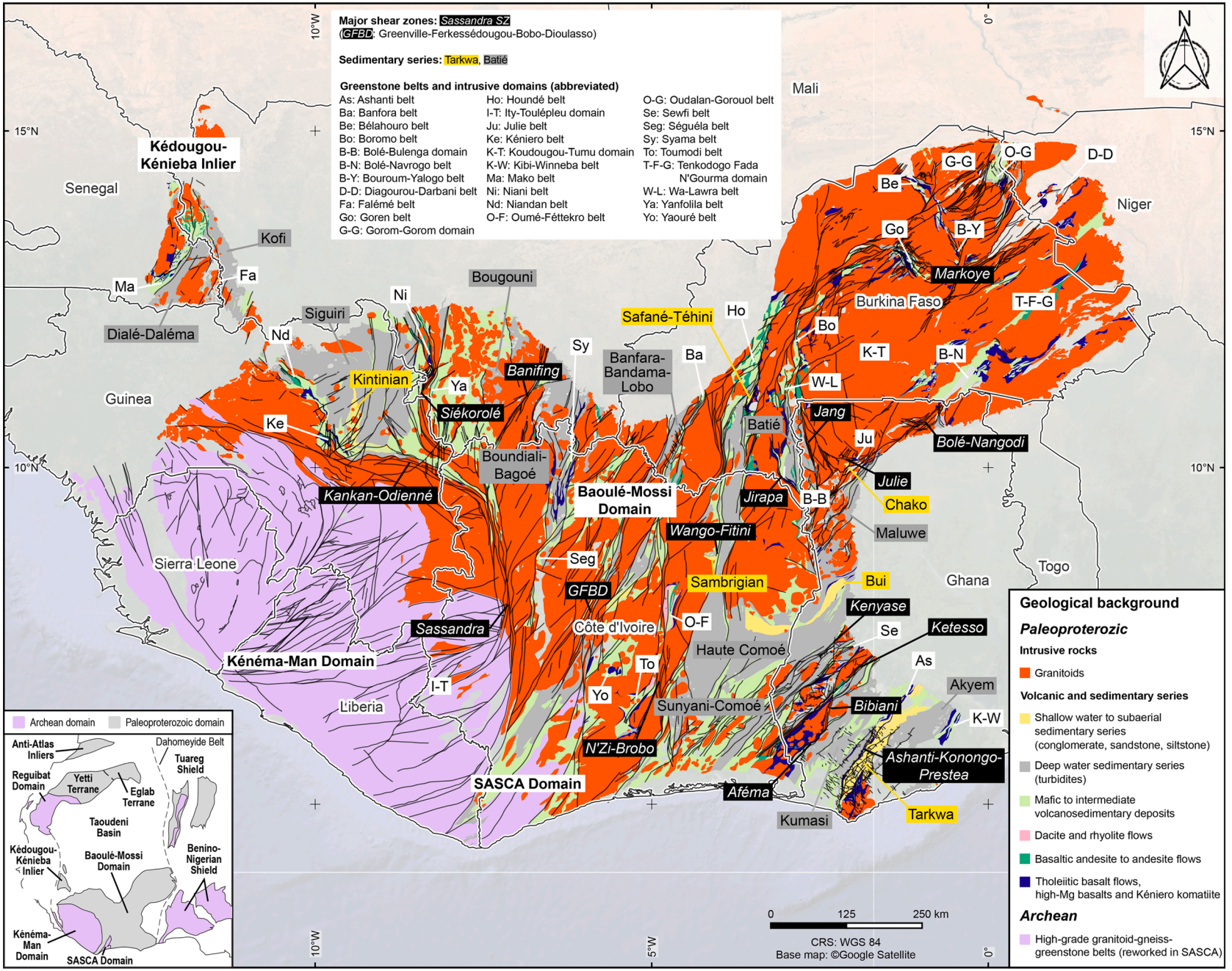

Fig. 1. Geological map of the southern West African Craton (sWAC), including the Paleoproterozoic Baoulé-Mossi Domain and Kédougou-Kénieba Inlier, and Archean Kénéma-Man Domain and SASCA Domain (modified after Milési et al., 2010; Masurel et al., 2022). Names of key shear zones, sedimentary series, greenstone belts, and plutonic domains are shown for reference. The bottom-left inset displays the extent of the WAC including the Anti-Atlas Inliers, Reguibat Domain and Yetti-Eglab Terranes to the north of the sWAC. Dashed lines represent the western limit of the WAC, and the Pan-African Dahomeyide belt juxtaposing the WAC and the Archean Benino-Nigerian Shield to the east.

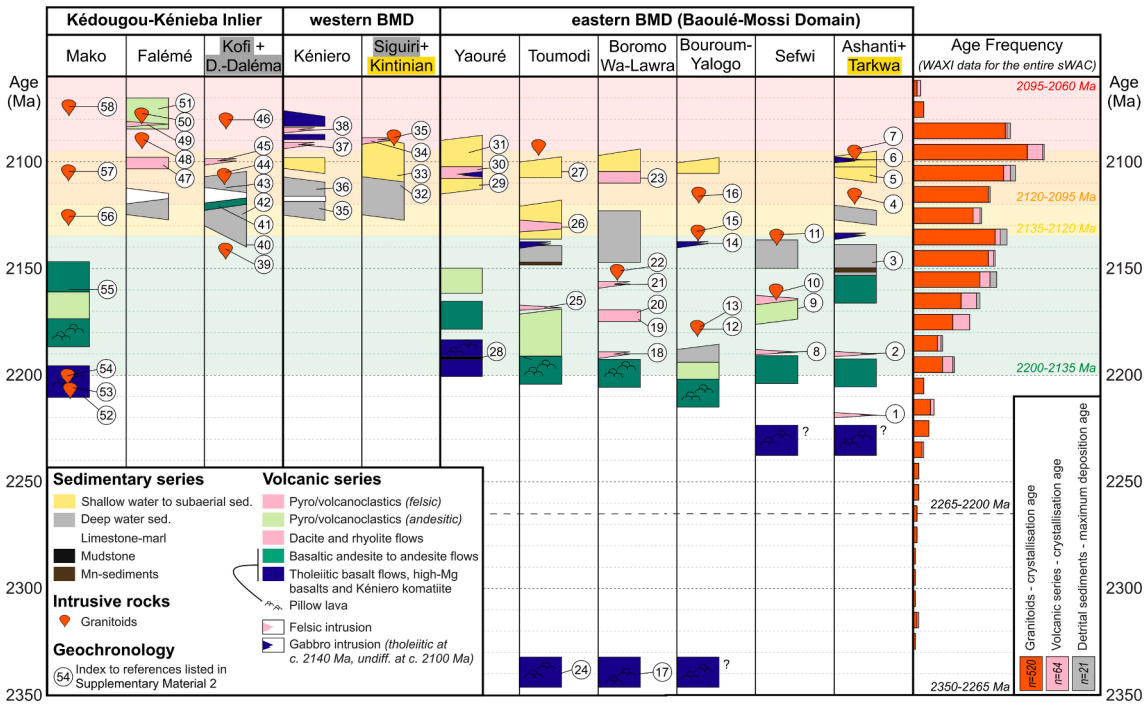

Fig. 2. Space-time-integrated Rhyacian stratigraphic evolution of belts and basins representative of the sWAC. Geochronological constraints on stratigraphy labelled as circled numbers are compiled in Electronic Supplementary Material 2. Greenstone belts and sedimentary basins are labelled in Fig. 1 and arranged from west to east. Coloured time intervals in the background refer to time-slices introduced to present the stratigraphic, plutonic and tectonic evolution of the sWAC. Granitoids in stratigraphic summary panels only include intra-belt intrusions. Stratigraphic data are modified from various sources, including Dabo et al. (2017) – Mako greenstone belt; Masurel et al. (2017a) – Falémé greenstone belt; Hein et al. (2015) – Kofi and Dialé-Daléma series; Feybesse et al. (1999) – Kéniero greenstone belt; Lebrun et al. (2016) – Siguiri and Kintinian series; Mériaud et al. (2020) – Yaouré greenstone belt; Hayman et al. (2023) – Toumodi greenstone belt; Baratoux et al. (2011), Senyah (2021) – Boromo and Wa-Lawra greenstone belts; McCuaig et al. (2016) – Bouroum-Yalogo greenstone belt; McFarlane et al. (2019) – Sefwi Belt; Loh and Hirdes (1999), Dampare et al. (2008), Perrouty et al. (2012) – Ashanti greenstone belt and Tarkwa series.

space–time-integrated patterns in stratigraphy (Fig. 2), plutonism (Fig. 3), metamorphism (Fig. 4), deformation, and mineral systems (Figs. 5-10). This approach enables robust geological interpretations by minimising uncertainties, resolving potential geological paradoxes, and facilitating the cross-validation of findings. The transitions between the proposed time slices are aligned with changes in the magmatic, stratigraphic, structural, isotopic, and metallogenic records across the sWAC, collectively marking evolutionary stages in the geological history of the sWAC. It is important to note that the proposed time brackets for each time slice are applicable at the scale of the sWAC but may vary at the scale of individual greenstone belts due to diachroneity in geological development. Table 1 summarises the stratigraphic, plutonic, tectono-metamorphic and metallogenic record of the sWAC for each of these time slices.

Details on the methodology used to interpret whole-rock geochemical signatures and U-Pb and Lu-Hf zircon isotopic data for igneous rocks are provided in Electronic Supplementary Material 1. A comprehensive compilation of geochronological constraints on stratigraphy, deformation, and mineralisation can be found in Electronic Supplementary Material 2. Note that only robust ages with 2σ errors obtained through absolute dating have been reported after cross-checking against original publications. This rigorous approach led us to exclude some geochronological data compiled in previous reviews that did not meet these criteria. Finally, Electronic Supplementary Material 3 presents a time-lapse at 5 Myr intervals depicting the stratigraphic, magmatic, structural, and metallogenic evolution of the sWAC (extended between c. 2350–2020 Ma).

3.1. *c. 2350–2265 Ma time slice (Fig. 5)*

3.1.1. *Stratigraphy*

The earliest record of magmatism in the Paleoproterozoic Baoulé-Mossi Domain corresponds to a period of tholeiitic mafic volcanism (Hayman et al., 2023; Hirdes and Davis, 1998; Masurel et al., 2022). Tholeiitic basalts and volumetrically minor co-magmatic intrusive rocks consistently form the basal part of the lithostratigraphic record in various greenstone belts across the Baoulé-Mossi Domain (Fig. 2). These mafic volcanic successions include both massive and pillow basalts collectively erupted under subaqueous conditions, but with different discharge rates in space and time (Hayman et al., 2023).

The only robust age extracted from these basal mafic igneous rocks is provided by the Kokumbo Hills dolerite in the Oumé-Féttekro

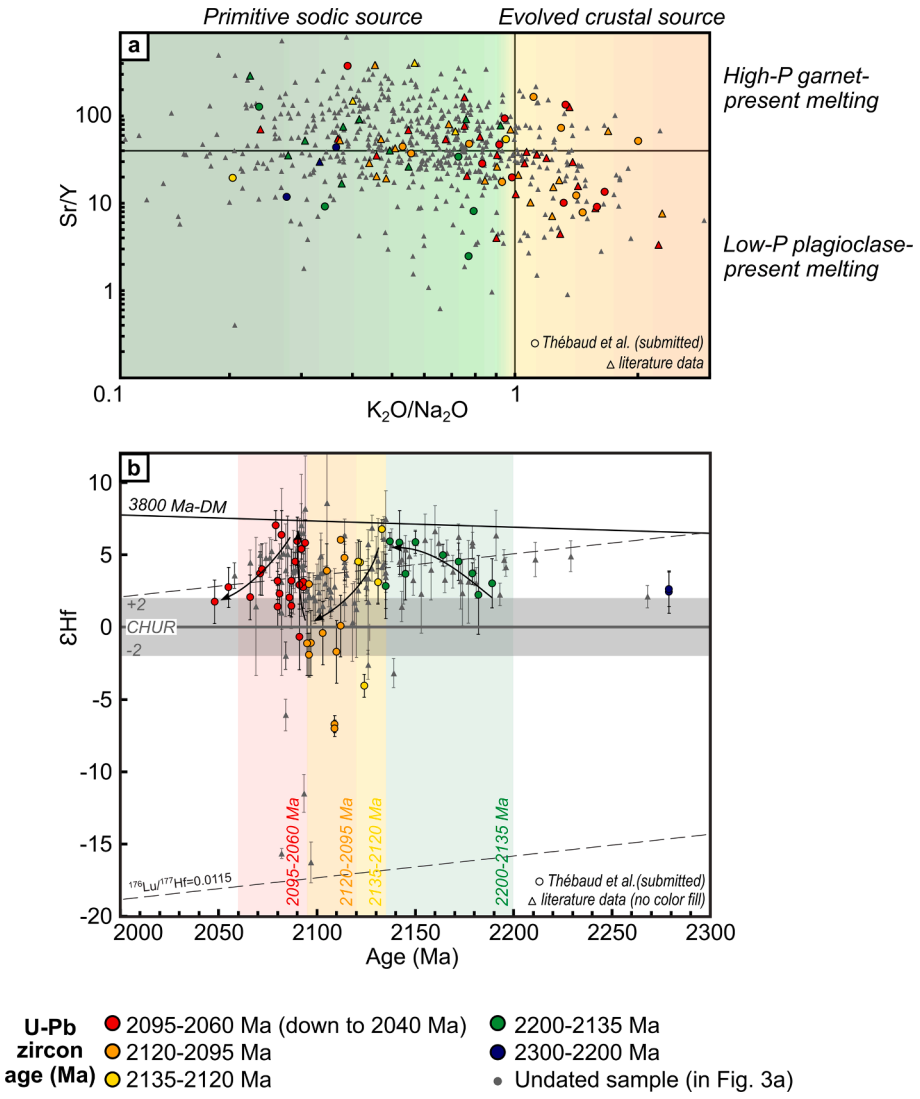

Fig. 3. Geochemical and isotopic record of petrogenetic processes involved in Paleoproterozoic intrusive rock emplacement in the sWAC, modified from Thébaud et al. (submitted). Igneous intrusive rocks are colour-coded based on their interpreted U-Pb zircon age of emplacement. References for literature data are listed in Thébaud et al. (submitted). **a.** Sr/Y vs. K_2O/Na_2O crossplot providing insights into the evolution of melt sources and petrogenetic processes through time. **b.** U-Pb zircon age vs. εHf(t) isotopic signature crossplot, with insights into mixing trends between juvenile and reworked melt source components through time. Coloured time intervals in the background refer to time-slices introduced to present the stratigraphic, plutonic and tectonic evolution of the sWAC.

greenstone belt of central Côte d'Ivoire, which is hosted by tholeiitic basalts and yielded an igneous crystallisation age of 2343 ± 2 Ma (Hayman et al., 2023). At the scale of the Baoulé-Mossi Domain, the age of this mafic crust is indirectly constrained by igneous inheritance in post-2265 Ma intermediate to felsic plutons emplaced in greenstone belts, which includes xenocrystic zircon cores dated at 2386 ± 42 Ma (Ifantayire granitic gneiss, De Kock et al., 2011), 2350 ± 27 Ma (Anikro rhyolite, Hayman et al., 2023), 2337 ± 11 Ma (Mengwe tonalite, Nunoo et al., 2022); 2323 ± 10 Ma (Gondo rhyolite, Nunoo et al., 2022), 2313 ± 34 Ma (TTG felsic pluton, Tapsoba et al., 2013), 2312 ± 17 Ma (Dabakala tonalitic gneiss, Gasquet et al., 2003), and 2286 ± 17 Ma (Kel Enguef migmatitic orthogneiss, Tshibubudze et al., 2013). Model ages obtained from Lu-Hf analyses on magmatic zircon grains (Petersson et al., 2016; Parra-Avila et al., 2017) and Sm-Nd whole-rock analyses (Abouchami et al., 1990; Boher et al., 1992; Doumbia et al., 1998) in post-2265 Ma igneous rocks overlap in age with the above-described range of xenocrystic zircon cores. The minimum age for tholeiitic mafic volcanism remains poorly constrained but is interpreted to be marked by the emergence of abundant diorite-tonalite-granodiorite plutons after c. 2265 Ma (De Kock et al., 2011; Tshibubudze et al., 2013, 2015; Parra-Avila et al., 2017). For now, we estimate the minimum age for tholeiitic mafic volcanism at 2265 ± 17 Ma, i.e. the

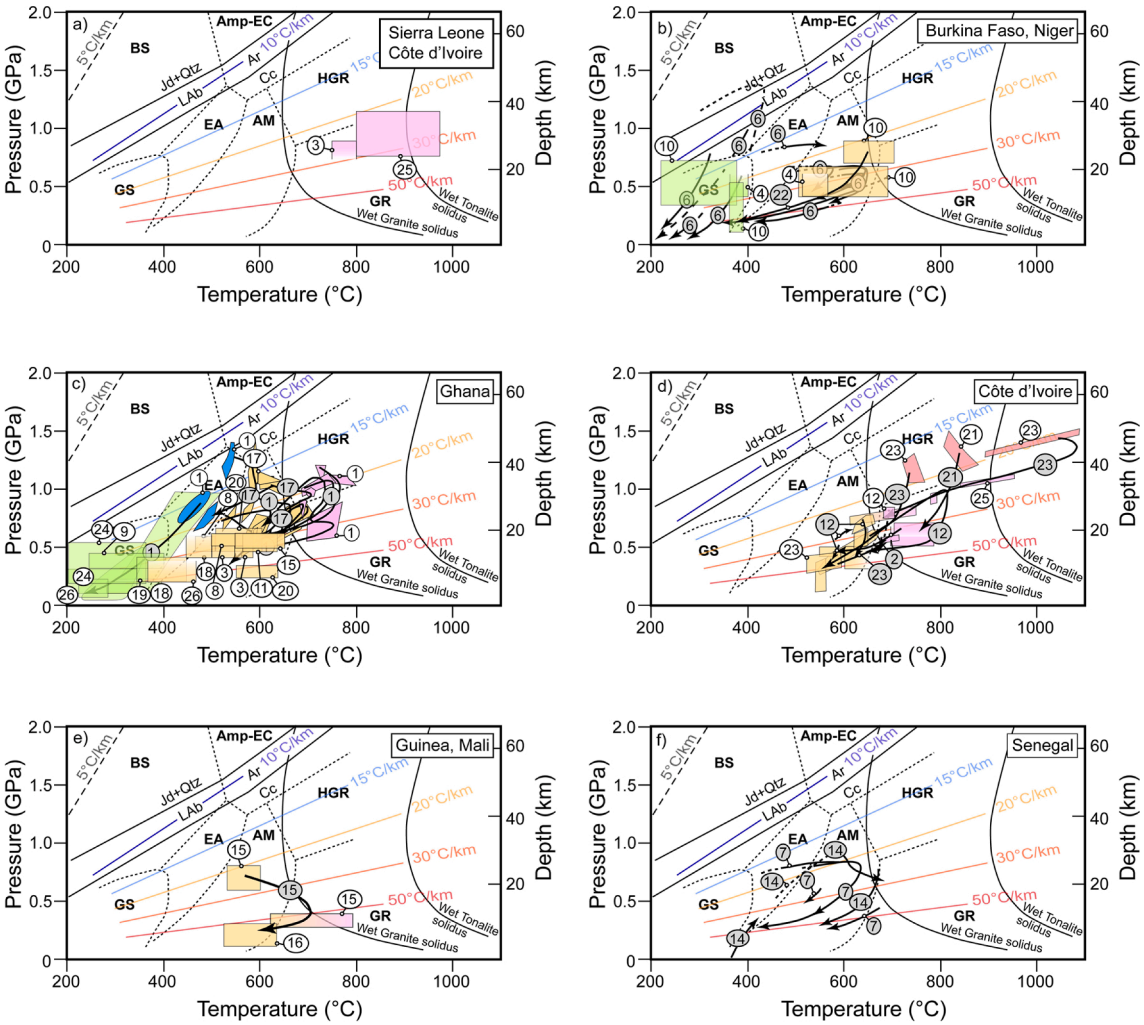

Fig. 4. Bibliography *P-T* synthesis for a) Archean Leonian (3400–3100 Ma) and Liberian (2850–2700 Ma) metamorphism, and b), c), d), e), f) Paleoproterozoic Eburnean (2200–2000) metamorphism in the WAC (Baratoux et al., 2024). The grey numbers refer to *P-T* paths, white numbers are *P-T* boxes from the references as follows: 1) Block et al. (2015); 2) Caby et al. (2000); 3) Camil et al. (1983); 4) Debat et al. (2003); 5) Galipp et al. (2003); 6) Ganne et al. (2012); 7) John et al. (1999); 8) Kleinschrot et al. (1994); 9) Klemd et al. (1993); 10) Klemd et al. (1997); 11) Klemd et al. (2002); 12) Koffi et al. (2023) (13) Koné (2020) 14) Ledru et al. (1994); 15) Lerouge et al. (2004); 16) McFarlane et al. (2011); 17) McFarlane (2018); 18) Mumin et al. (1996); 19) Oberthür et al. (1996); 20) Opare-Addo et al. (1993); 21) Pitra et al. (2010); 22) Soumaila and Garba (2006); 23) Triboulet and Feybesse (1998); 24) Wille and Klemd (2004); 25) Williams (1988); 26) Yao et al. (2001); Mineral abbreviations: Ar = aragonite; Cc = calcite; Jd = jadeite; Qtz = quartz; LAb = low albite; and HAb = high albite. Metamorphic facies abbreviations: AM = amphibolite; Amp-EC = amphibolite-eclogite; BS = blueschist; EA = epidote–amphibolite; Ep-EC = Epidote Eclogite; GR = sillimanite-granulite; HGR = kyanite-granulite; GS = greenschist; Lw-EC = lawsonite-eclogite (*P-T* diagram modified after Liou et al., 1998; Ernst and Liou, 2008).

crystallisation age of a granodiorite in the Tenkodogo Fada N'Gourma domain of eastern Burkina Faso (Parra-Avila et al., 2017).

Where reported, igneous rocks assigned to this lowermost mafic stratigraphy are characterised by a tholeiitic affinity, relatively flat to slightly depleted REE patterns with low $(La/Yb)_n$ ratios, and no pronounced heavy REE (HREE) depletion, features collectively interpreted to be consistent with these primitive melts being derived through partial melting in the spinel (± garnet) lherzolite stability field (Salah et al., 1996; Lompo, 2009; Hayman et al., 2023). The geodynamic setting for these basalts is largely interpreted from geochemical data and thus remains debated, with models including (i) mid-ocean ridge basalts (Leube et al., 1990); oceanic flood basalts (Lompo, 2009; Hayman et al., 2023); and intra-oceanic island arc basalts (e.g. Salah et al., 1996).

3.2. c. 2265–2200 Ma time slice (Fig. 6)

3.2.1. Stratigraphy

Transitional to calc-alkaline, bimodal volcanic successions conformably overlie older tholeiitic units in most, if not all, greenstone belts across the Baoulé-Mossi Domain, although basal unconformities are recognised locally (Fig. 2). These mafic-intermediate-felsic volcanic suites (basalt-andesite-dacite-rhyolite series) and associated pyroclastic-

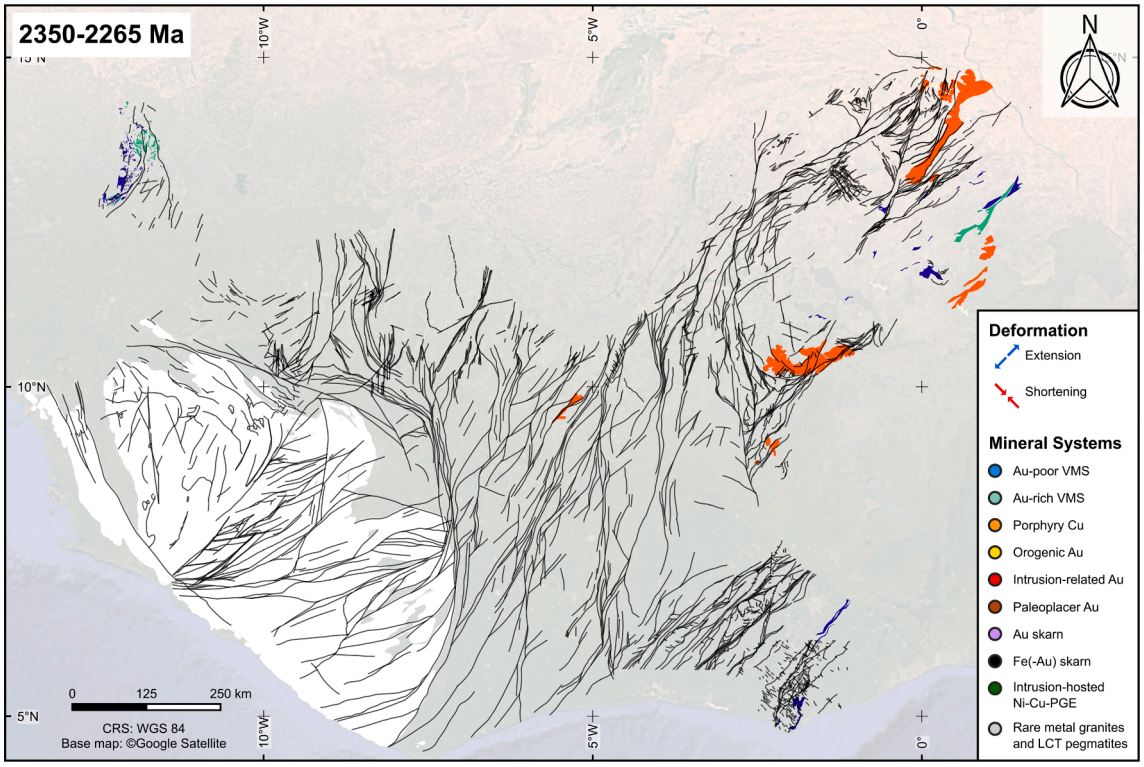

Fig. 5. Summary of the c. 2350–2265 Ma time slice. Refer to the legend in Fig. 1 for details on the background geological map. Only the Paleoproterozoic units of known age and emplaced during the specified time slice are coloured, while others are shown in transparent grey shades (note that some units may appear coloured in successive time slices due to age uncertainties, which result in overlapping age ranges across multiple time slices). The Archean Kénéma-Man domain is depicted in white. Arrows indicate the predominant shortening and/or extension paleodirection(s) at the centres of belts where the deformation stages have been identified. When present, mineral deposits emplaced during the time slice are represented. They are labelled in grey if the timing of emplacement considered is less robustly constrained. Deformation, metallogenic inventory, and related geochronological constraints are compiled in Electronic Supplementary Material 2.

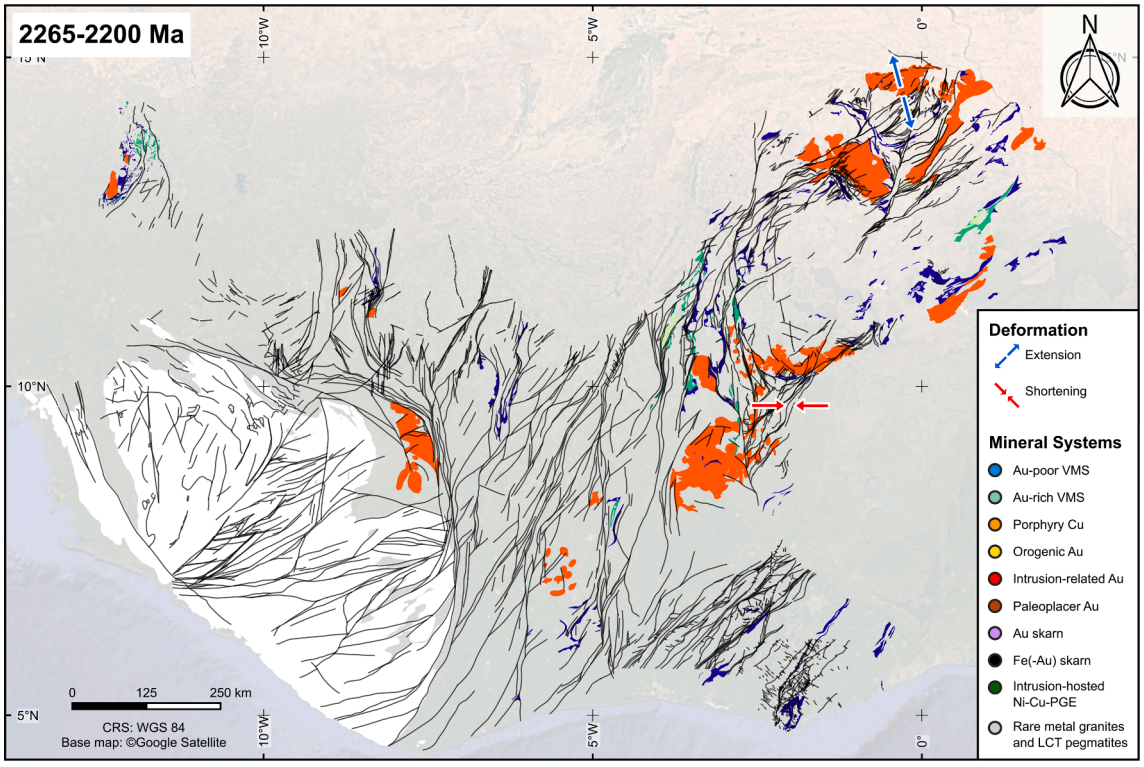

Fig. 6. Summary of the c. 2265–2200 Ma time slice. Caption as per Fig. 5.

volcanoclastic deposits are locally associated with co-magmatic gabbro and pyroxenite complexes (Hayman et al., 2023; Masurel et al., 2022). These transitional to calc-alkaline volcanic successions were interpreted to reflect subaqueous deposits transitioning into emergent (subaerial) volcanic centres (Salah et al., 1996; Hayman et al., 2023).

As a corollary to the point made for tholeiitic mafic volcanism, the exact onset of calc-alkaline bimodal volcanism remains poorly constrained and may have been diachronous between the eastern and western Baoulé-Mossi Domain. The related volcanic successions have likely erupted coevally with the emplacement of calc-alkaline, metaluminous to peraluminous, biotite-hornblende-bearing diorite-granodiorite-tonalite plutonic bodies within greenstone belts across the Baoulé-Mossi Domain (de Kock et al., 2011; Tapsoba et al., 2013; Petersson et al., 2016; Parra-Avila et al., 2017; Grenhölm et al., 2019a). Although the discernible onset of such plutonism occurred at c. 2265 Ma (De Kock et al., 2011; Parra-Avila et al., 2017), it only became voluminous after c. 2200 Ma. The higher geochronological data density towards younger ages for these plutons, i.e. 2210–2200 Ma, may yet reflect a preservation and/or sampling bias only. Micaschists associated with calc-alkaline geochemical affinities and interlayered with talc-chlorite schists and amphibolites in the Diagourou-Darbani greenstone belt of Niger yielded protolith/detrital ages between c. 2278 ± 5 and 2273 ± 19 Ma, εNd(T) values of +0.3 to +1.7, and T_{DM} close to 2300 Ma (Soumaila et al., 2008). Furthermore, a rhyolitic tuff in the Goren greenstone belt of northern Burkina Faso yielded a crystallisation age of 2238 ± 5 Ma (Castaing et al., 2003). Lastly, polymict conglomerates in the Oudalan-Gorouol belt of north-eastern Burkina Faso were deposited prior to c. 2200 Ma and contain granitic detritus as old as 2255 ± 26 Ma (Tshibubudze et al., 2013, 2015).

Geochemical features associated with these bimodal calc-alkaline volcanic rocks include enrichment in LILE relative to high-field strength elements (HFSE), negative HFSE (e.g. Nb-Ta-Ti) anomalies, fractionated REE patterns with moderate to high $(La/Yb)_n$ ratios, no Eu anomaly, and moderate to high Sr/Y ratios (Béziat et al., 2000; Pawlig et al., 2006; Dampare et al., 2008; Baratoux et al., 2011; Block et al., 2016a; Nunoo et al., 2022). Statistically representative isotopic datasets for these calc-alkaline volcanic successions remain lacking. The available Sm-Nd whole-rock data, however, reflects some degree of isotopic heterogeneity between different greenstone belts. For instance, basalts and andesites-rhyolites in the Mako greenstone belt of Senegal yielded εNd(T) values of +2.1 to +3.7 and T^2_{DM} between 2245–2133 Ma (Pawlig et al., 2006) whereas basalts and basaltic-andesites in the Wa-Lawra greenstone belt of north-western Ghana yielded εNd(T) values of +0.8 to +2.86 and T^2_{DM} between 2470–2310 Ma (Sakyi et al., 2020).

3.2.2. Plutonism

Felsic plutonism between c. 2265–2200 Ma was predominantly recognised in Ghana, Burkina Faso, and eastern Côte d'Ivoire, although more spatially restricted plutons of similar ages were reported in Mali and Senegal across the Kédougou-Kénieba Inlier. A representative selection of plutonic rocks for this period is listed hereafter.

In the Oudalan-Gorouol greenstone belt of north-eastern Burkina Faso, the Kel Enguef migmatitic orthogneiss, the Lilengo granodioritic orthogneiss, and the Mrs Pink granite yielded crystallisation ages of 2253 ± 15, 2253 ± 9, and 2203 ± 12 Ma, respectively (Tshibubudze et al., 2013, 2015). In the Kibi-Winneba greenstone belt of south-eastern Ghana, the West Accra biotite-hornblende-granodiorite yielded a crystallisation age of 2229 ± 4 Ma (Petersson et al., 2016). In the Julie greenstone belt of north-western Ghana, the Chaggupani biotite-hornblende-granodiorite yielded a crystallisation age of 2209 ± 5 Ma (Nunoo et al., 2022). In the Bolé-Bulenga plutonic domain of north-western Ghana, the Gondo granitic orthogneiss yielded a precursor age of 2187 ± 5 Ma and two inherited zircon grains dated at 2217 ± 21 Ma (De Kock et al., 2011), whereas the Lambonga biotite-bearing granitic orthogneiss yielded a crystallisation age of 2193 ± 4 Ma and three inherited zircon grains dated at 2211 ± 6 Ma (De Kock et al., 2011). In the Mako greenstone belt of the Kédougou-Kénieba Inlier, the Sandikounda hornblende-biotite-bearing tonalitic and dioritic orthogneisses yielded a crystallisation age of 2205 ± 15 (Gueye et al., 2007) and 2202 ± 6 Ma (Dia et al., 1997), and the Badon granodiorite yielded crystallisation ages of 2213 ± 3 and 2198 ± 2 Ma (Gueye et al., 2007).

3.2.3. Deformation

Field evidence argues for a cryptic increment of deformation that occurred prior to c. 2200 Ma in the eastern part of the Baoulé-Mossi Domain. This increment of deformation, however, is commonly overlooked during geological mapping due to the subsequent tectono-thermal overprint and associated reorientation of mineral fabrics. In the Oudalan-Gorouol greenstone belt of north-eastern Burkina Faso, the 2253 ± 9 Ma Lilengo granodioritic orthogneiss is unconformably overlain by lower-grade volcanosedimentary rocks (e.g. dolomite, BIF, basalt, greywacke, siltstone, mudstone, conglomerate) of the Oudalan basin, with both units intruded by the 2203 ± 12 Ma Mrs Pink granite (Tshibubudze et al., 2013, 2015). In the Bolé-Navrogo greenstone belt of north-western Ghana, tectonically foliated xenoliths in an amphibolite and a paragneiss were documented within the 2195 ± 4 Ma Ifanteyire and 2187 ± 3 Ma Gondo granitic orthogneisses (Siegfried et al., 2009; De Kock et al., 2011, 2012). The far-field boundary stress conditions and tectonic style associated with this early increment of deformation remain uncertain, but, if correct, would push back the onset of the Eoeburnean Tectonic Event at least ~ 25 Myr older than currently recognised at c. 2175 Ma (Masurel et al., 2022).

3.2.4. Metallogenic inventory

The identification of mineralisation older than c. 2200 Ma across the sWAC is particularly challenging due to the intensity of the subsequent tectono-thermal overprint, the limited amount of robust geochronological constraints on multi-commodity ores, and the low preservation potential of some mineral systems such as volcanic-hosted massive sulphides and epithermal gold. The only potential candidate recognised to date is the Nsuta Mn deposit, which is interpreted to have formed at c. 2200 Ma based on relative chronological constraints (Grenhölm et al., 2019a and references therein).

3.3. c. 2200–2135 Ma time slice (Fig. 7)

3.3.1. Stratigraphy

Calc-alkaline bimodal volcanism appears to have peaked, in terms of volumetric abundance, between c. 2200 and 2175 Ma in the eastern-central Baoulé-Mossi Domain (Feybesse et al., 2006; Gueye et al., 2007; Hirdes et al., 2009; de Kock et al., 2011; Baratoux et al., 2011; Perrouty et al., 2012; Tshibubudze et al., 2015; Block et al., 2016a; McFarlane et al., 2019; Grenhölm et al., 2019a; Nunoo et al., 2022). Voluminous intermediate to felsic magmatism followed in the eastern-central Baoulé-Mossi Domain between c. 2175 and 2135 Ma (Fig. 2). A rhyolitic lava in the Houndé greenstone belt of south-western Burkina Faso yielded a crystallisation age of 2171 ± 7 Ma (Castaing et al., 2003), which falls within error of rhyolites dated at 2166 ± 2 Ma in the Sefwi greenstone belt of south-eastern Ghana (Hirdes et al., 2007) and 2170 ± 6 Ma in the Oumé-Féttekro greenstone belt of central Côte d'Ivoire (Hayman et al., 2023). Andesitic to dacitic lavas in the Bolé-Navrogo greenstone belt of north-eastern Ghana yielded crystallisation ages between 2155 ± 6 and 2149 ± 7 Ma (Block et al., 2016a). The reworking of felsic volcanic edifices (e.g. dacite-rhyolite lava flows, lapilli tuffs, and ignimbrites) led to the onset of deposition of volcanoclastic and epiclastic rocks in sedimentary depocentres in the eastern Baoulé-Mossi Domain (e.g. Sunyani-Comoé, Kumasi, Maluwe; Grenhölm et al., 2019a; Masurel et al., 2022). The complete internal stratigraphy of these basins has yet to be unravelled due to a combination of factors including the lack of lithological variation, weathering and exposure conditions, and the intensity of overprinting strain. The emerging view, however, is that the base of these series consists of volcanic-derived material progressing

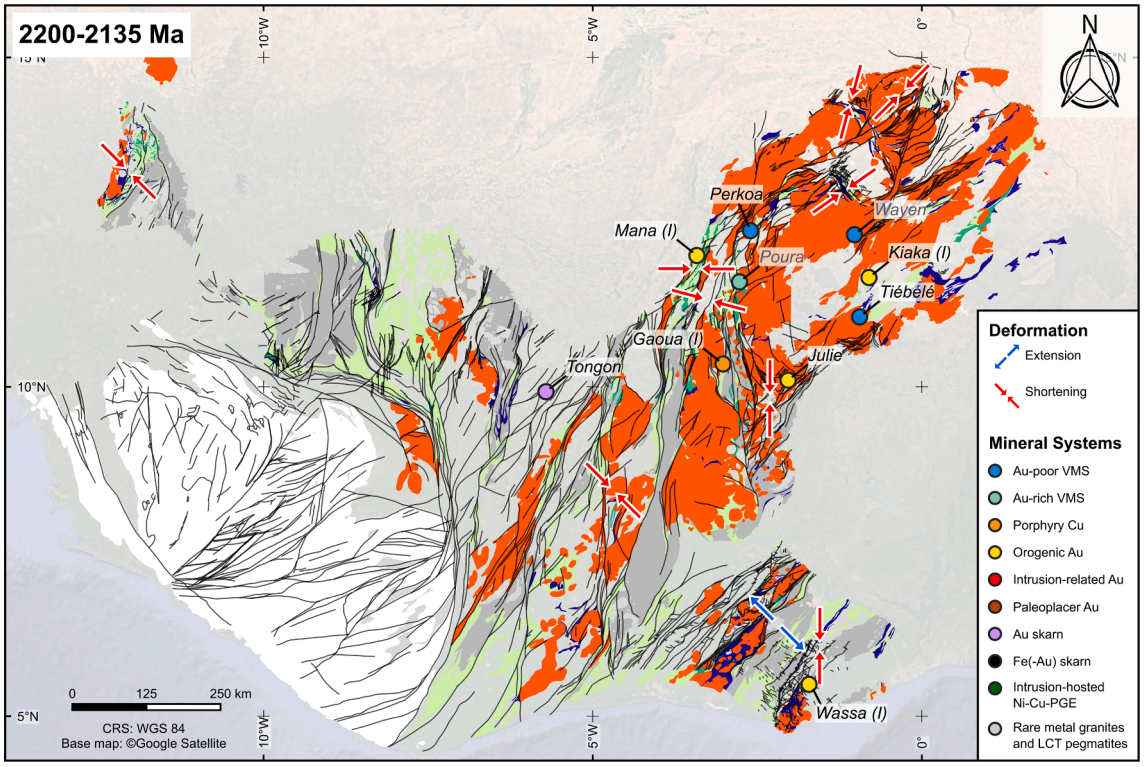

Fig. 7. Summary of the c. 2200–2135 Ma time slice. Caption as per Fig. 5.

upwards into epiclastic sedimentary rocks (e.g. greywacke, sandstone, siltstone) characterised by a gradual decrease in volcanic material input (Davis et al., 2015; Grenhölm et al., 2019a). Importantly, the cessation of volcanism across the eastern-central Baoulé-Mossi Domain is constrained to c. 2135 Ma and marks a fundamental change in the geological evolution of the sWAC (Grenhölm et al., 2019b and references therein).

3.3.2. *Plutonism*

Felsic plutonism between c. 2200–2135 Ma was recognised across the Baoulé-Mossi Domain. Key plutons of this age in south-eastern Ghana include the 2195 ± 6 Ma Wassa felsic porphyry (Parra-Avila et al., 2015), 2193 ± 9 Ma Kibi-Winneba granitic orthogneiss (Anum et al., 2015), 2176 ± 3 Ma Papoase granodiorite (Hirdes et al., 1993), 2174 ± 2 Ma Dixcove tonalite (Hirdes et al., 1992), 2172 ± 4 Ma Ketan granodioritic orthogneiss (Opare-Addo et al., 1993), 2159 ± 4 Ma Kenyase monzogranite (Feybesse et al., 2006), 2157 ± 5 Benso granodiorite (Parra-Avila et al., 2015), 2159 ± 2 Ma Prince Town granite (Attoh et al., 2006), and 2158 ± 5 Ma monzonitic orthogneiss (Feybesse et al., 2006). Plutons of similar ages in Burkina Faso include the 2182 ± 3 Ma Tougan-Thiou tonalite (Castaing et al., 2003), 2181 ± 7 Ma Yalago granodiorite (Tapsoba et al., 2013), 2168 ± 10 to 2149 ± 12 Ma Iridiaka Suite (Parra-Avila et al., 2015), 2146 ± 9 Ma Tin-Taradat granodiorite and 2148 ± 9 Ma Dori Batholith (Tshibubudze et al., 2015), 2140 ± 7 Ma Kiaka diorite (Fontaine et al., 2017). In Côte d'Ivoire, and Mali, these include the 2154 ± 1 Ma Dabakala tonalitic orthogneiss (Gasquet et al., 2003) and 2150 ± 15 Ma Tienko orthogneiss (Liégeois and De Waele, 2005), respectively. In the Kédougou-Kénieba Inlier, representative plutons of this age include the 2158 ± 8 Ma amphibolite-biotite-bearing tonalite of the Sandikounda layered plutonic complex (Dia et al., 1997) and 2147 ± 8 Ma Finman horblende-granodiorite (Masurel et al., 2017a).

K_2O/Na_2O ratio for these plutonic rocks displays a mean value of 0.4, indicating a predominantly sodic composition. Sr/Y mean values of 65 suggest that these magmas were derived from a source region where hornblende and/or garnet were stable, indicative of relatively thick crust (Thébaud et al., submitted). U-Pb-Hf data show an increase of εHf (t) with a mean value of 4.2, indicating dominantly juvenile material in central and western Ghana, Côte d'Ivoire, and Burkina Faso (Fig. 3; Thébaud et al., submitted). However, the juvenile signature is contrasted by negative εHf(t) values in the south-easternmost Baoulé-Mossi Domain in both Ghana and Togo, indicating local reworking of Archean crust at c. 2135 Ma (e.g. Suhum basin, not visible in Fig. 1, Petersson et al., 2016; Kibi-Winneba greenstone belt, Petersson et al., 2018; Amponsah et al., 2023; Thébaud et al., submitted).

These biotite-hornblende-bearing, metaluminous to peraluminous, I-type, calc-alkaline plutonic rocks are not strictly TTGs as per the definition of Moyen and Martin (2012) and were defined as TTG-like by Parra-Avila et al. (2019). TTG-like plutons in the Baoulé-Mossi Domain are inferred to have been generated either by high-pressure (garnet-bearing residue) or low-pressure (garnet-free residue) partial melting of young and warm subducted slab (McFarlane et al., 2019) or by partial melting at the base of volcanic island arcs following dehydration of the deep slab and heat transfer from the mantle wedge (Ganne et al., 2014).

3.3.3. *Deformation*

The first, major increment of deformation recorded in the Baoulé-Mossi Domain is referred to as the Eoeburnean Tectonic Event (De Kock et al., 2011). This tectonic event was underway at c. 2175 Ma and associated with deformation features widely recognised in the north-eastern Baoulé-Mossi Domain (Naba et al., 2004; Vanin et al., 2004; Vegas et al., 2008; Hein, 2010; De Kock et al., 2012; Perrouty et al., 2012; Tshibubudze et al., 2015; McCuaig et al., 2016; Block et al. 2016b; McFarlane et al. 2019). Two kinematic views have been proposed for the Eoeburnean Tectonic Event. In one view, abundant ENE-striking tectonic fabrics and shear zones were interpreted to reflect NNW-SSE-directed bulk crustal shortening (Perrouty et al., 2012; Tshibubudze et al., 2015; Block et al., 2016b). In an alternative view, the regional-scale deformation features were interpreted to reflect incremental/progressive NW-SE-directed bulk crustal shortening (Feybesse et al.,

2006; Grenhölm et al., 2019b; Chardon et al., 2020).

3.3.4. Metamorphism

Although variability in kinematics has been documented across distinct greenstone belts and granitoid domains, this major increment of deformation is correlated with crustal thickening (clockwise pressure–temperature (*P-T*) paths) and upper greenschist-, amphibolite- to granulite-facies metamorphism (Fig. 4). Peak metamorphic conditions of 12–14 kbar at 550–600 °C followed by 7–10 kbar at 600–650 °C were reported in the Bolé-Bulenga domain of north-western Ghana (Block et al., 2016b); 10–12 kbar and 400–450 °C in the Tenkodogo Fada N'Gourma and neighbouring domains of Burkina Faso (Ganne et al., 2012), 7–9 kbar and 560-680°C in the Diagourou-Darbani greenstone belt in Niger (Soumaila and Garba, 2006). Only a few studies, however, have combined structural, metamorphic, and geochronological analyses thus achieving a complete record of the pressure–temperature-timing-deformation (*P-T-t-d*) paths. The timing of peak regional metamorphism was constrained to 2137 ± 8 Ma (U-Pb on monazite in leucosome) in north-western Ghana (Block et al., 2016b) and 2135 ± 11 Ma (U-Pb on metamorphic zircon grains) in Burkina Faso (Augustin et al., 2017).

3.3.5. Metallogenic inventory

A range of economically significant mineral systems formed across the central-eastern part of the Baoulé-Mossi Domain during this period. Gold systems formed in two distinct pulses over this period and are tentatively referred to as early Eoeburnean (c. 2190–2170 Ma; VMS, porphyry-Cu-(Au-Mo) and orogenic Au) and late Eoeburnean (c. 2140 Ma; Au skarn).

VMS systems are best represented by the Perkoa and Tiébelé deposits in Burkina Faso. Mineralisation at Perkoa is constrained to have occurred between the crystallisation of the host rhyolite at 2171 ± 7 Ma (Le Métour et al., 2003) and a crosscutting quartz-diorite dated at 2175 ± 1 Ma (Schwartz and Melcher, 2004). Mineralisation at Tiébelé is interpreted to have occurred broadly synchronously with eruption of A-type rhyolites dated at 2156 ± 9 Ma (Ilboudo et al., 2017).

Porphyry systems include Cu-(Au) mineralisation at Gaoua in northwest Ghana, dated at 2165 ± 24 Ma via Re-Os on hydrothermal pyrite (Le Mignot et al., 2017b), and Cu-(Mo) mineralisation at Kourki in south-western Niger, dated at 2144 ± 40 Ma, also by the Re-Os method, with an emplacement age for associated granitoids at c. 2137 Ma (Léger et al., 1992; Hallarou et al., 2021).

At Mana in Burkina Faso, early Eoeburnean orogenic Au mineralisation occurred contemporaneously with the intrusion of syn-tectonic plutons such as the 2172 ± 6 Ma Wona-Kona and 2176 ± 8 Ma Siou plutons (Augustin et al., 2017). At Wassa in Ghana, early Eoeburnean orogenic Au mineralisation is constrained by the crystallisation of the host porphyry at 2191 ± 6 Ma and the crosscutting Benso granodiorite at 2157 ± 5 Ma, and ore-related hydrothermal pyrite dated at 2164 ± 14 Ma (Parra-Avila et al., 2015; Le Mignot et al., 2017a).

The only recognised late Eoeburnean gold deposit to date is the Tongon Au skarn deposit in northern Côte d'Ivoire. It formed during peak metamorphism and deformation at c. 2140 Ma, immediately prior to the emplacement of the 2139 ± 21 Ma Tongon granodiorite (Lawrence et al., 2017).

3.4. c. 2135–2120 Ma time slice (Fig. 8)

3.4.1. Stratigraphy

This period was marked by deposition of shallow to deep water volcanoclastic and/or epiclastic sedimentary series in large (~50–200 km wide) depocentres in the eastern-central Baoulé-Mossi Domain (Figs. 1,2). Some of these sedimentary series unconformably overlie Birimian packages locally whereas the nature of the basal contact appears conformable to disconformable elsewhere (Grenhölm et al., 2019a). Key examples include the c. 2135–2125 Ma Maluwe series (De Kock et al., 2011; Block et al., 2016a); c. 2135–2115 Ma Kumasi and Sunyani-Comoé series (Oberthür et al., 1998; Hirdes et al., 2007; Adadey et al., 2009); and the c. 2140–2125 Ma Akyem series (Grenhölm et al., 2019a). Note that basin infill may have however started as early as c. 2150 Ma based on (i) maximum depositional age constraints (e.g.

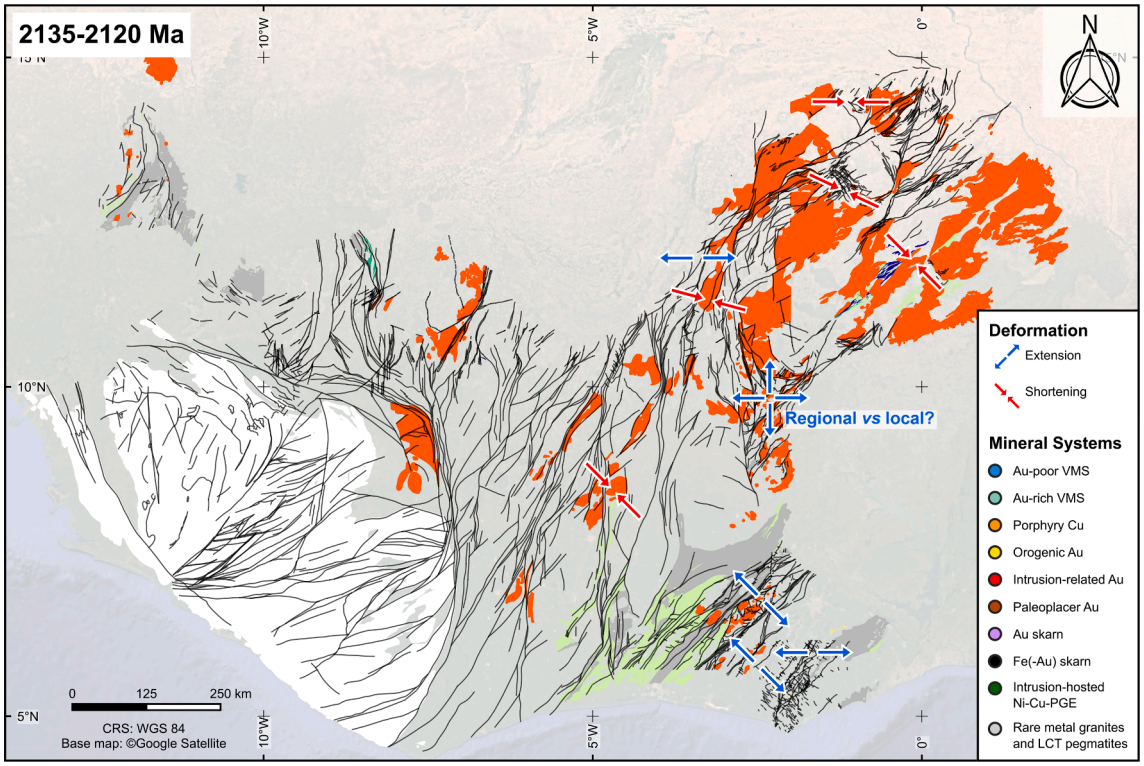

Fig. 8. Summary of the c. 2135–2120 Ma time slice. Caption as per Fig. 5.

Sunyani basin: 2151 ± 5 Ma, Grenhölm et al., 2019a and 2141 ± 7 Ma, Adou et al., 1995; Kumasi basin: 2158 ± 3 Ma, Nunoo et al., 2022, 2155 ± 2 Ma, Oberthür et al., 1998 and 2154 ± 7 Ma, Grenhölm et al., 2019a); and (ii) crosscutting intrusive rocks (e.g. Maluwe basin: 2145 ± 1 Ma granite, Zitzmann 1997; Sunyani basin: 2145 ± 2 Ma granite, de Kock et al., 2012).

The c. 2135–2120 Ma period was also marked by deposition of shallow water to subaerial sedimentary series in narrow depocentres in the eastern-central Baoulé-Mossi Domain, although at a slightly younger time (Fig. 2). Key examples include the c. 2125–2120 Ma Chako series deposited in an intra-orogenic depocentre flanking anatectic migmatite domes (Block et al., 2016b) and the c. 2125–2115 Ma Safané-Téhini series deposited along a crustal-scale shear zone (Baratoux et al., 2011).

3.4.2. Plutonism

Available geochronological constraints for this time slice may not allow an accurate definition of the spatial distribution of such plutonism and its potential chemical heterogeneity. Yet, it is likely that voluminous felsic volcanism (e.g. rhyolite, ignimbrite) was contemporaneous with co-magmatic felsic plutons and shallow intrusive rocks. For instance, the syn-kinematic 2128 ± 6 Ma Tenkodogo-Yamba granite (Castaing et al., 2003) in eastern Burkina Faso emplaced during a period of transcurrent tectonics (Naba et al., 2004; Vegas et al., 2008). In north-western Ghana, the 2122 ± 6 Marsipe granite (Adadey et al., 2009) transects fabrics associated with Eoeburnean (c. 2200–2135 Ma) deformation (De Kock et al., 2011; Block et al., 2016b). In northern Burkina Faso, 2129 ± 7 Ma and 2123 ± 6 Ma syn-kinematic granites emplaced during a period of bulk crustal shortening (Parra-Avila et al., 2015; McCuaig et al., 2016).

3.4.3. Deformation

The deposition of both shallow to deep water sedimentary series in large-scale depocentres and molasse in narrower depocentres in the central-eastern Baoulé-Mossi Domain occurred shortly after the tectono-thermal peak associated with the Eoeburnean Tectonic Event. The mechanism(s) of large-scale basin formation remain uncertain, with proposed models including: (i) indentation-triggered extension/transtension by lateral escape and rotation of the crustal blocks around rigid indenter (Grenhölm et al., 2019b); (ii) fore-arc, back-arc, and intra-arc basins (Perrouty et al., 2012); and (iii) foreland basins (Feybesse et al., 2006; Block et al., 2016b). Adding to the problem, transpressional tectonics recorded along the margins of the north-eastern Burkina Faso occurred contemporaneously with basin-fill under predominantly extensional/transtensional tectonics in the central-eastern Baoulé-Mossi Domain (Castaing et al., 2003; Naba et al., 2004; Vegas et al., 2008; Tshibubudze et al., 2015).

3.4.4. Metamorphism

In north-western Ghana, tectonic exhumation of amphibolite-facies rocks from ~ 12 kbar to ~ 5 kbar at temperatures reaching 700–800 °C expressed as migmatisation was dated at 2127 ± 7 Ma (U-Pb on metamorphic monazite; Block et al., 2015, 2016b) (Fig. 5) and occurred within an increment of extensional deformation (Fig. 8).

3.5. c. 2120–2095 Ma time slice (Fig. 9)

3.5.1. Stratigraphy

This period was marked by deposition of shallow to deep water volcanoclastic and/or epiclastic sedimentary series in large depocentres in the western-central Baoulé-Mossi Domain (Fig. 2). Key examples include the c. 2115–2100 Ma Siguiri series (Lebrun et al., 2016); c. 2120–2105 Ma Kofi and Dialé-Daléma series (Masurel et al., 2017a; Allibone et al., 2020); c. 2115–2095 Ma Boundiali-Bagoé series (Wane et al., 2018); c. 2110–2095 Ma Bougouni series (McFarlane et al., 2011); and c. 2107–2095 Ma Banfora-Bandama-Lobo series (Doumbia et al., 1998). This period was also marked by deposition of shallow water to subaerial sedimentary series in narrow depocentres (Fig. 2). Key examples include the c. 2107–2097 Ma Tarkwa series (Pigois et al., 2003; Oberthür et al., 1998; Adadey et al., 2009); c. 2120–2115 Ma Bui series (Kiessling et al., 1997; Grenhölm et al., 2019a); c. 2115–2105 Ma Sambrigian series (Hirdes et al., 1996; Lüdtke et al., 1999); c.

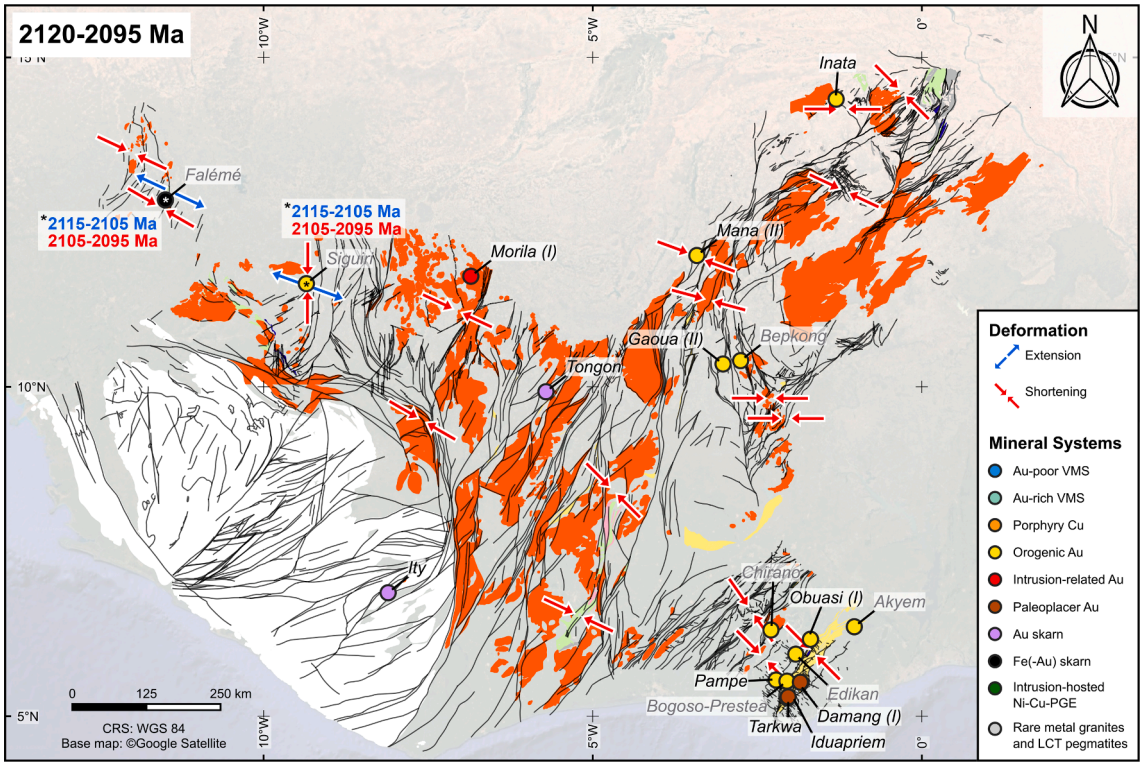

Fig. 9. Summary of the c. 2120–2095 Ma time slice. Caption as per Fig. 5.

2105–2095 Ma Kintinian series (Lebrun et al., 2016); and Tarkwaian-type sedimentary rocks in Burkina Faso over a shorter-lived event constrained at c. 2124 Ma (Bossière et al., 1996).

3.5.2. Plutonism

From 2120 to 2095 Ma, plutonic activity spread from eastern Burkina Faso through to Mali and Senegal. Plutonism during this time slice exhibits K_2O/Na_2O ratio with a mean value of 0.57, but spreading a range from 0.20 to 0.90, suggesting mixed composition involving both primitive sodic and reworked alkaline sources (Thébaud et al., submitted). Sr/Y ratio returns a mean value of 52, indicating magmas were derived from a source region where hornblende and/or garnet were stable (Fig. 3; Thébaud et al., submitted). U-Pb-Hf data show a downward trend in εHf(t) values (i.e. "isotopic pull-down"), compatible with crustal thickening and reworking of Eoeburnean juvenile suites. Very negative εHf(t) values (∼ −7) and along the eastern and northern margin of the Kénéma-Man Domain indicate localised reworking of Meso- to Paleoarchean crust (Eglinger et al., 2017; Koffi et al., 2023).

3.5.3. Deformation

The second, major increment of deformation recorded in the Baoulé-Mossi Domain is referred to as the Eburnean Tectonic Event or Eburnean orogeny (Bonhomme, 1962). This tectonic event started at c. 2120 Ma and is associated with deformation features widely recognised across two-thirds of the Baoulé-Mossi Domain (Fig. 9). Based on whole rock geochemistry of felsic magmas and associated U-Pb-Hf isotopic constraints (Fig. 3), the Eburnean orogeny may be extended to c. 2135 Ma. It encompassed both deposition and inversion of large-scale volcanosedimentary series in the north-western Baoulé-Mossi Domain (Masurel et al., 2022 and references therein). There, inversion of carbonate-rocks-bearing flysch basins between c. 2110–2095 Ma resulted in clockwise *P-T* paths and the development of 1–10-km-scale NNE- to NE-trending isoclinal folds, associated axial-planar cleavage, major intra-basin reverse shear zones, and reactivation of the basin margin faults as major reverse shear zones (Hirdes et al., 1992; Allibone et al., 2002a,b; Masurel et al., 2017a; Allibone et al., 2020; Oliver et al., 2020).

It has been proposed that the collision between the Baoulé-Mossi Domain and the Archean Kénéma-Man Domain occurred at c. 2095 Ma after NW-SE-directed oblique convergence (Chardon et al., 2020; Grenhölm et al., 2019b; Mériaud et al., 2020; Traoré et al., 2022; Wane et al., 2018; Masurel et al., 2022). Such collision was coeval with oblique-slip reactivation of the crustal-scale Sassandra, Banifing, Siékorolé, and Greenville-Ferkessédougou-Bobo-Dioulasso shear zones across the central and western parts of the Baoulé-Mossi Domain (Egal et al., 2002; Feybesse et al., 2006; Eglinger et al., 2017; Wane et al., 2018).

3.5.4. Metamorphism

In southern Guinea, the peak *P-T* conditions at 5–7 kbar and 700–800 °C were estimated at 2115–2075 Ma based on U-Pb zircon ages of adjacent *syn*-tectonic granites (Lerouge et al., 2004; Fig. 4).

3.5.5. Metallogenic inventory

This time slice marks one the most prolific periods of gold mineralisation across the eastern-central part of the Baoulé-Mossi Domain, and broadly correlates with peak collisional orogenesis in its western counterpart (Masurel et al., 2022). This apparent volumetric peak in gold deposition was referred to by Thébaud et al. (2020) as the "*early Eburnean gold stage*", and accounts for the bulk of the sWAC's gold endowment, including both orogenic Au and paleoplacer Au systems.

Paleoplacer Au deposits are exemplified by the auriferous quartz-pebble conglomerates of the Tarkwaian Banket Formation (c. 2107–2097 Ma) both at Tarkwa and Damang. The gold-bearing coarse-clastic rock successions were deposited in a fluvial-lacustrine foreland basin and unconformably overlie Eoeburnean basement (Hirdes and Nunoo, 1994; White, 2011; Thébaud et al., 2020). These paleoplacer Au systems formed broadly synchronous with orogenic Au systems. For instance, the giant (>60 Moz) Obuasi Au deposit formed contemporaneously with greenschist-facies metamorphism at c. 2095 Ma (Oberthür et al., 1998; Fougerouse et al., 2017; Oliver et al., 2020). Orogenic Au mineralisation at Bogoso-Prestea and Chirano in south-eastern Ghana are interpreted to have formed at the same time as the Obuasi deposit at 2098 ± 7 Ma (Allibone et al., 2002a; 2004). Other, less economically significant orogenic Au deposits formed at similar times include Bepkong in the Wa-Lawra greenstone belt (Ghana) and Mana in the Houndé-Boromo greenstone belt (Burkina Faso). The Bepkong gold deposit formed synchronously with sinistral movement along the Jirapa shear zone at c. 2100 Ma (Amponsah et al., 2016; Block et al., 2016b). The Mana gold deposit similarly formed coeval with sinistral displacement along the Wona-Kona shear zone and intrusion of the 2090 ± 8 Ma Kokoï diorite (Augustin et al., 2017).

Although orogenic Au and paleoplacer Au systems dominate the metallogenic inventory associated with this time slice, other mineralisation styles also formed during this period. For instance, the Ity Au skarn in northern Côte d'Ivoire was formed at 2104 ± 3 Ma (Béziat et al., 2016) and a hypothesised intrusion-related Au stage at Morila in south-eastern Mali is constrained to have occurred between 2098 ± 4 Ma and 2091 ± 4 Ma (McFarlane et al., 2011). The genesis of the Goulamina spodumene pegmatite field is tentatively correlated with a suite of post-2100 Ma collisional granitoids similar to the Morila intrusion (Parra-Avila et al. 2017; Wilde et al., 2021).

3.6. c. 2095–2060 Ma time slice (Fig. 10)

3.6.1. Stratigraphy

A resurgence in volcanism was restricted to the north-western margin of the Kénéma-Man Domain along the WNW-striking Kankan-Odienné shear zone (Fig. 10) and represented by the Niandan and Kéniero volcanic suites (Thiéblemont, 1989; Hirdes et al., 1996). The Kéniero bimodal (mafic-felsic) volcanic rocks have been dated between 2098 ± 4 and 2093 ± 2 Ma (Guérrot, in Feybesse et al., 1999). The Niandan komatiitic basalts cut across the Kéniero volcanic rocks but these are themselves cut by hypovolcanic intrusions dated at 2085 ± 2 Ma (Guérrot, in Feybesse et al., 1999). Eruption of such juvenile mafic–ultramafic volcanic rocks through crust thickened during Eburnean collision was interpreted to reflect upwelling of the asthenosphere and associated extension caused by lithospheric delamination or slab break-off (Eglinger et al., 2017; Mériaud et al., 2020).

This resurgence in volcanism extended up to the Kédougou-Kénieba Inlier, where it is represented by the c. 2085–2075 Ma Falémé magmatic belt (Lahondère et al., 2002; Hirdes and Davis, 2002; Lambert-Smith et al., 2016a; Allibone et al., 2020). There, an andesitic volcaniclastic rock and a rhyolite yielded crystallisation ages of 2078 ± 7 Ma (Allibone et al., 2020) and 2082 ± 8 Ma (Delor et al., 2010), respectively. A pyroclastic rock from the vicinity yielded a maximum depositional age of 2096 ± 7 Ma (Allibone et al., 2020). These geochronological constraints are consistent with crystallisation ages obtained from plutons, plugs, and dykes of the Falémé batholith, including the 2082 ± 1 Ma Boto tonalite and 2080 ± 1 Ma Boboti granodiorite (Hirdes and Davis, 2002), 2080 ± 11 Ma Highway monzonite and 2070 ± 6 Ma Balangouma quartz-monzodiorite (Allibone et al., 2020).

These geochronological constraints collectively indicate a magma flare-up event along the north-eastern margin of the Kénéma-Man Domain between c. 2095 and 2075 Ma. The timing of this magma flare-up event is consistent with emplacement of the Samapleu-Yacouba layered igneous complex (e.g. websterites, pyroxenites, and gabbronorites) along the eastern Kénéma-Man Domain margin between 2091 ± 18 and 2080 ± 13 Ma (Gouedji et al., 2014). This magma flare-up event was interpreted as the consequence of the collision between the Archean Kénéma-Man Domain and the Baoulé-Mossi Domain (Wane et al., 2018).

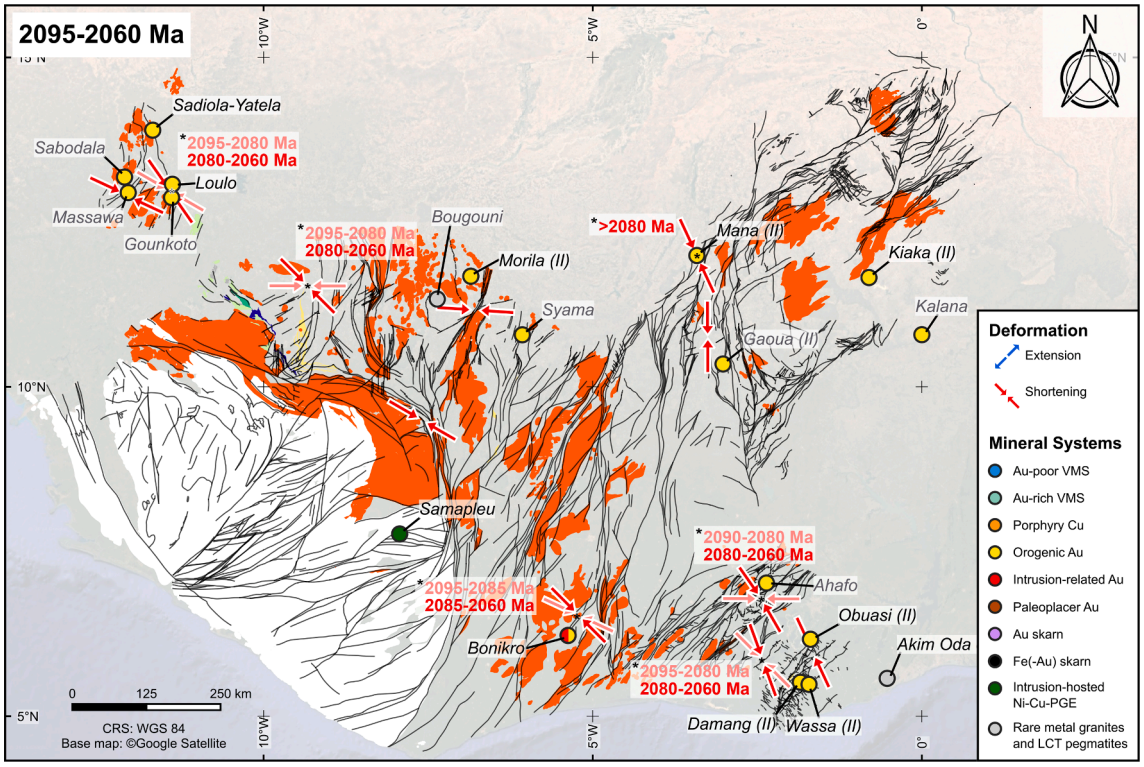

Fig. 10. Summary of the c. 2095–2060 Ma time slice. Caption as per Fig. 5.

3.6.2. *Plutonism*

Plutonic activity in the north-eastern Baoulé-Mossi Domain ceased soon after the end of the peak Eburnean orogeny at c. 2095 Ma (Augustin et al., 2017; Parra-Avila et al., 2017; Grenhölm et al., 2019b). In contrast, the north-western Baoulé-Mossi Domain recorded abundant plutonism during this time slice, as represented by c. 2090–2080 Ma voluminous S-type granites emplaced in the Dialé-Daléma and Siguiri basins (Hirdes and Davis, 2002; Parra-Avila et al., 2017), c. 2085–2075 Ma Falémé batholith in the Kédougou-Kénieba Inlier (Lahondère et al., 2002; Hirdes et al., 1996; Hirdes and Davis, 2002; Lambert-Smith et al., 2016a; Allibone et al., 2020), and 2097 ± 7 to 2082 ± 6 Ma high-K, calc-alkaline to shoshonitic granitic plutonism along the Baoulé-Mossi – Kénéma-Man boundary (Lebrun et al., 2016; Eglinger et al., 2017). Importantly, plutons, plugs, and dykes of the Falémé batholith intruded into sedimentary rocks of the Kofi series but do not record structural evidence associated with its inversion, whereas Kofi sedimentary rocks and Falémé intrusive rocks were both affected by low-strain, sinistral transcurrent deformation (Masurel et al., 2017a; Allibone et al., 2020). The potassic granite of San Pedro located in the SASCA Domain yielded a similar age (2084 ± 5 Ma; Koffi et al., 2022), and showcases the spread of this magmatic event as far as the south-western Baoulé-Mossi Domain.

Plutonic rocks from 2095 to 2060 Ma show metaluminous, calc-alkalic to alkali-calcic affinities, and both magnesian and ferroan compositions. K_2O/Na_2O ratio returns a mean value of 1.0, indicating a clearly potassic evolved crustal source composition (Fig. 3; Thébaud et al., submitted). Trace element composition for these plutons shows Sr/Y and Gb/Yb mean values of 54 and 3.3, respectively, suggesting mixed source regions (Thébaud et al., submitted). U-Pb-Hf data for this period show positive εHf(t) at c. 2095 Ma, marking the introduction of juvenile material into the crust, along with ongoing reworking of older crustal components around existing Archean continental blocks (Thébaud et al., submitted). The reworked crustal material is not only Paleoproterozoic, but also Archean as evidenced by abundant inherited Archean zircon grains in these rocks (Egal et al., 2002; Kouamélan et al., 1997; Thiéblemont et al., 2004; Eglinger et al., 2017). This resurgence in bimodal magmatism involved both crustal- and mantle-derived melts and was followed by a downward trend in εHf(t) values ("isotopic pull-down") suggesting further reworking of Archean and Paleoproterozoic crust in a convergent setting. Wane et al. (2018) attributed this resurgence of volcanism and the geochemical characteristics of felsic plutonism along the northern margin of the Kénéma-Man Domain to metacratonisation processes, involving the reworking of Archean crust and preexisting structures. This interpretation aligns partially with the model recently proposed by Chardon et al. (2024) for Paleoproterozoic accretion-collision tectonics in the Reguibat Shield, which suggests that collision was controlled by thermal erosion and the mechanical softening of the craton edge by the accretionary orogen.

3.6.3. *Deformation*

Tectono-thermal activity appears to have shut down by c. 2080 Ma in the north-eastern Baoulé-Mossi Domain (Augustin et al., 2017; Parra-Avila et al., 2017; Grenhölm et al., 2019b). Except for this region, the rest of the Baoulé-Mossi Domain similarly underwent transcurrent tectonics (Fig. 10), with sinistral displacement recorded along several crustal-scale shear zones including the NNE-striking Banifing shear zone in Mali (Wane et al., 2018), N'Zi Brobo shear zone in Côte d'Ivoire, and Ashanti-Konongo-Prestea shear zones in Ghana (Masurel et al., 2022). Deformation along the Archean Kénéma-Man Domain margin operated at higher temperatures than further away in the eastern Baoulé-Mossi Domain, as evidenced by granulite-facies metamorphism along ductile shear zones (Feybesse et al., 2000; Lerouge et al., 2004) and metacratonisation (Wane et al., 2018).

3.6.4. *Metamorphism*

In the Sefwi greenstone belt, peak regional metamorphic conditions of 8–10 kbar and 550–600 °C have been dated at c. 2073 Ma (U-Pb on monazite, McFarlane, 2018; McFarlane et al., 2019), which is similar to the inferred age of a major episode of shearing parallel to the Sefwi greenstone belt (Jessell et al., 2012) and high-grade metamorphism

Table 1
Summary table of the stratigraphic, plutonic, tectonic, and metallogenic record of the sWAC between c. 2350–2060 Ma.

	Stratigraphy	Plutonism	Tectonics: Deformation-Metamorphism	Metallogeny
c. 2095–2060 Ma	Resurgence in bimodal and juvenile mafic–ultramafic volcanism confined to the north-western margin of the Kénéma-Man Domain (e.g. Niandan komatiitic basalts).	Cessation of the plutonic activity in the north-eastern Baoulé-Mossi Domain after the peak Eburnean orogeny (c. 2095 Ma)	**Eburnean tectono-thermal shutdown** in the northeastern Baoulé-Mossi Domain at c. 2080 Ma	**Late Eburnean Mineralisation Event:** diverse mineralisation styles associated with retrograde *P-T-t* paths and late collisional tectonics.
	Volcanism induced by local asthenospheric upwelling and extension triggered by lithospheric delamination or slab break-off	Significant S-type and high-K, calc-alkaline to shoshonitic granitic plutonism in the north-western Baoulé-Mossi Domain	**Late Eburnean transcurrent tectonics** with sinistral displacement along crustal shear zones in the rest of the Baoulé-Mossi Domain	**Late Eburnean Gold Deposits:** orogenic and intrusion Au mostly expressed in the western sWAC, newly formed deposits (Bonikro (I), Massawa, Sabodala, Loulo, Sadiola-Yatela) vs overprinting of preexisting mineralisation until c. 2035 Ma (Bonikro (II), Damang (II), Wassa (II), Gaoua (II))
		Mixed source regions: introduction of mantle-derived melts into the crust, along with ongoing reworking of older crustal components around existing Archean continental blocks, followed by further reworking of Paleoproterozoic crust	Peak regional metamorphism at 8–10 kbar and 550–600 °C in the Baoulé-Mossi Domain and the Kénéma-Man Domain margin, and at 4.5–6 kbar and 500–650 °C in the south-eastern Ghana	**Other Deposits:** intrusion-hosted Ni-Cu-PGE (Samapleu), LCT pegmatites (Winneba-Mankoadze, Mangodara, Issia complex) and rare metal granites (Akim Oda district) emplaced until c. 2035 Ma
			Post-tectonic metamorphism after 2060 Ma: generalised retrogression, and granulite-facies metamorphism and crustal reworking along the eastern margin of the Kénéma-Man Domain (4–14 kbar − 600–1000 °C) at c. 2060–2030 Ma, during metacratonisation	
c. 2120–2095 Ma	Deposition of shallow to deep water volcanoclastic and epiclastic sedimentary series in the western-central Baoulé-Mossi Domain	Felsic plutonism from eastern Burkina Faso to the Kedoudou-Kéniéba Inlier	**Eburnean Tectonic Event:** started around 2120 Ma (up to 2135 Ma), resulted in the collision of the Baoulé-Mossi Domain and the Kénéma-Man Domain around 2095 Ma	**Early Eburnean Mineralisation Event:** maximum mineralisation overlapping with the onset of Eburnean deformation, peak metamorphism, and magmatism, particularly in the eastern sWAC (Burkina Faso, Ghana, and Côte d'Ivoire)
	Ongoing deposition of shallow water to subaerial sedimentary series in narrow depocentres, initiated in the previous time slice	Reworking of Eoeburnean juvenile suites coeval with crustal thickening, except for the eastern and northern margins of the Kénéma-Man Domain, and the south-eastern Baoulé-Mossi Domain, with evidence for local reworking of Archean crust	NW-SE oblique convergence: inversion and folding of volcano-sedimentary series, reverse- to oblique-slip reactivation of basin margin faults and preexisting shear zones	**Early Eburnean Gold Deposits:** paleoplacer Au (**e.g.** Tarkwa, Damang (I)), orogenic Au (**e.g.** Obuasi (I), Bepkong, Mana (II)), intrusion-related Au (**e.g.** Morila (I))
			Clockwise *P-T* paths, up to 5–7 kbar and 700–800 °C for peak metamorphic conditions in southern Guinea	**Other Deposits:** Fe-(Au) skarn (Ity (II)), possible LCT pegmatites (**e.g.** Goulamina field, related to Morila intrusion?)
c. 2135–2120 Ma	Sedimentary series unconformably overlying earlier volcanic series, local evidence for conformable or disconformable basal contact	Emplacement of *syn*-tectonic felsic plutons and shallow intrusive rocks likely coeval to voluminous felsic volcanism	Post-tectono-thermal peak of the **Eoeburnean Tectonic Event**	No record available
	Peak deposition of shallow to deep water volcanoclastic and epiclastic sedimentary series in ~ 50–200 km wide depocentres in the eastern-central Baoulé-Mossi Domain	Spatial distribution and potential chemical heterogeneity poorly documented	Basin formation dominated by extensional/transtensional tectonics in the central-eastern Baoulé-Mossi Domain, and transpressional tectonics along the margins of north-eastern Burkina Faso, no clear deformation model	
	Development of slightly younger, narrow depocentres, hosting shallow water to subaerial sedimentary series		Evidence for exhumation of amphibolite-facies rocks from ~ 12 kbar to ~ 5 kbar at 700–800 °C and related migmatisation during local extension	
c. 2200–2135 Ma	Peak of the calc-alkaline bimodal volcanism between c. 2200–2175 Ma in the eastern-central Baoulé-Mossi Domain, significant intermediate to felsic magmatism between c. 2175 and 2135 Ma	Emplacement of calc-alkaline TTG-like plutons	**Eoeburnean Tectonic Event**: first major deformation in the Baoulé-Mossi Domain, started around c. 2175 Ma	**Eoeburnean Mineralising Event in the central-eastern part of the** Baoulé-Mossi Domain
	Reworking of felsic volcanic edifices: early deposition of volcanoclastic and epiclastic sedimentary rocks in depocentres, with diminishing volcanic input over time, commenced as early as 2150 Ma	Widespread across the Baoulé-Mossi Domain and the Kédougou-Kénieba Inlier	Expressed in the north-eastern Baoulé-Mossi Domain by ENE-striking fabrics and shear zones resulting from NNW-directed shortening, or NW-SE-directed progressive shortening	**Early Eoburnean (c. 2200–2170 Ma):** VMS (e.g. Perkoa, Tiébélé), porphyry-Cu-(Au-Mo) (e.g. Gaoua (I), Kourki), orogenic Au (e.g. Mana (I), Wassa (I))

(*continued on next page*)

Table 1 (*continued*)

	Stratigraphy	Plutonism	Tectonics: Deformation-Metamorphism	Metallogeny
	Subaerial setting, emerged volcanic centres	Emplacement during crust thickening, from a source dominated by material with a juvenile isotopic signature (mantle-derived?), except for the south-eastern Baoulé-Mossi Domain with evidence for local reworking of Archean crust	Significant crustal thickening and metamorphism ranging from upper greenschist to granulite facies (up to 12–14 kbar – 550–600 °C) at c. 2145–2120 Ma	**Late Eoburnean (c. 2140 Ma):** Au skarn (e.g. Tongon)
c. 2265–2200 Ma	Cessation of volcanism across the eastern-central Baoulé-Mossi Domain at c. 2135 Ma Emplacement of volcanic series overlying older tholeiitic units, with local basal unconformities Transitional to calc-alkaline bimodal volcanism, comprising basalt-andesite-dacite-rhyolite series associated with pyroclastic deposits and co-magmatic gabbro-pyroxenite complexes Subaqueous setting to emergence of volcanic centres Onset of calc-alkaline bimodal volcanism likely diachronous between the eastern and western Baoulé-Mossi Domain	Calc-alkaline felsic plutonism associated with the transitional to calc-alkaline bimodal volcanism Mostly reported in the eastern Baoulé-Mossi Domain, but some occurrences documented in the Kédougou-Kénieba Inlier Plutonism becomes more voluminous after 2200 Ma	**Initiation of the Eoeburnean Tectonic Event** at least ~ 25 Myr earlier than the current estimate? Early, cryptic phase of deformation before c. 2200 Ma in the eastern Baoulé-Mossi Domain, widely overprinted Expressed by *syn*-tectonic orthogneisses and foliated xenoliths in Ghana and north-eastern Burkina Faso	Identifying mineralisation older than c. 2200 Ma across the sWAC is challenging due to intense subsequent tectono-thermal overprints, limited robust geochronological constraints on multi-commodity ores, and the low preservation potential of certain mineral systems
c. 2350–2265 Ma	Emplacement of the basal part of greenstone belts Voluminous mafic volcanism expressed by tholeiitic massive and pillow basalts Subaqueous setting	No record available	No record available	No record available

along ductile shear zones on the eastern Kénéma-Man Domain margin dated at 2071 ± 2 Ma (U-Pb on titanite, Feybesse et al., 2000; Lerouge et al., 2004). Peak regional metamorphic conditions in south-eastern Ghana were also constrained at 4.5–6 kbar and 500–610 °C in the Kibi-Winneba greenstone belt (Klemd et al., 2002) and 5–6 kbar and 500–650 °C in the Ashanti greenstone belt (Oberthür et al., 1998; John et al., 1999; White et al., 2013). In the Kédougou-Kénieba Inlier, peak regional metamorphic conditions reached 6–7 kbar and 550–650 °C between c. 2095–2060 Ma (U-Pb on monazite and Sm-Nd on garnet; Koné, 2020; Fig. 4).

Although retrograde mineral assemblages were identified in several locations across the Baoulé-Mossi Domain after c. 2060 Ma, the eastern margin of the Kénéma-Man Domain recorded granulite-facies metamorphism from c. 2060 Ma down to c. 2030 Ma (U-Pb on monazite and zircon rims), possibly due to a combination of crustal thickening and heating by accretion of hot, juvenile Paleoproterozoic crust, and/or delamination (Chardon et al., 2020; Traoré et al., 2022), and/or metacratonisation processes (Wane et al., 2018). This late-orogenic, high-grade metamorphic event was best documented in western and south-western Côte d'Ivoire (Fig. 4) where peak metamorphic conditions ranged from 4 to 7 kbar at 600–650 °C to 7–9 kbar at 700–800 °C to 13–14 kbar at 850–1000 °C (Kouamélan et al., 1997; Triboulet and Feybesse, 1998; Pitra et al., 2010; Koffi et al., 2022, 2023).

3.6.5. *Metallogenic inventory*

This time slice marks an increase in the variety of mineral systems compared to the early Eburnean period (e.g. orogenic Au, intrusion-related Au, intrusion-hosted Ni-Cu-Platinum group elements (PGE), LCT-pegmatite). Across the Baoulé-Mossi Domain, deposits assigned to this "*late Eburnean gold stage*", as defined by Thébaud et al. (2020), formed predominantly under localised transpressional, wrench, or transtensional deformation along retrograde *P-T-t-d* paths (Goldfarb et al., 2017). The vast majority of orogenic Au occurrences across the Kédougou-Kénieba Inlier in western Mali and eastern Senegal (e.g. Massawa, Sabodala, Loulo, Sadiola-Yatela) had formed by c. 2060 Ma (Delor et al., 2010; Lawrence et al., 2013a,b; Hein et al., 2015; Treloar et al., 2015; Masurel et al., 2017a; Allibone et al., 2020). On one hand, the formation of these deposits can be protracted and involve several stages of gold introduction and refinement during the late Eburneam period (e.g. early tourmaline alteration stage and later orogenic Au event resulting into the economic ore at Loulo; Allibone et al., 2020). On the other hand, a late Eburnean increment of orogenic Au mineralisation overprinted an early Eburnean gold mineralisation in some other places. For instance, early Eburnean Au-(Sb-Bi-Te) intrusion-related mineralisation at Morila is overprinted by an orogenic Au event dated at 2074 ± 4 Ma (U-Pb on hydrothermal titanite, McFarlane et al., 2011). This pattern echoes with observations made at Bonikro in southcentral Côte d'Ivoire whereby an undated intrusion-related Au mineralisation stage is overprinted by a younger orogenic Au event at 2074 ± 16 Ma (U-Pb on hydrothermal molybdenite, Masurel et al., 2019). Such pattern was also recognised at Damang where an orogenic Au mineralisation locally overprints paleoplacer Au ores at 2063 ± 9 Ma (U-Pb on hydrothermal xenotime, Pigois et al., 2003). Although undated yet, the Tabakoto deposit, Kedougou-Kenieba Inlier, also illustrates this pattern, as hydrothermal mineralisation overprinted pre-existing intrusion-related Au mineralisation (Diallo et al., 2024).

Intrusion-hosted Ni-Cu-PGE mineralisation also occurred during this period, as exemplified by the Samapleu deposit. There, nickel mineralisation is constrained between 2091 ± 18 and 2080 ± 13 Ma and is genetically associated with the Samapleu-Yacouba layered igneous complex that intruded Archean granulite-gneisses (Gouedji et al., 2014).

LCT pegmatites and rare metal granites are the last significant class of deposits assigned to this period. The Kokobin pegmatite field (also referred to as the Akim Oda Nb-Ta rare metal granite complex) in south-eastern Ghana yielded ages between 2085 ± 1 and 2074 ± 8 Ma (Melcher et al., 2008, 2015), while the Winneba-Mankoadze pegmatite

field, located 100 km to the west, yielded ages between c. 2080 and 2060 Ma (based on unpublished data; Adams et al., 2023). In Burkina Faso's Mangodara district, pegmatites dated at 2094 ± 9 Ma and 2055 ± 20 Ma were interpreted to reflect progressive partial melting and crystallisation during the late Eburnean orogeny (Bonzi et al., 2021, 2023). Additionally, the Issia granitic complex in Côte d'Ivoire, part of the Férké multistage batholith, features LCT pegmatites dated at 2050 ± 3 Ma and interpreted to have formed by low-degree partial melting of the Issia granite > 30 million years after crystallisation of the latter (Brou et al., 2022). This timing is coeval with granulite-facies metamorphism recorded in western Côte d'Ivoire between 2055 and 2033 Ma (Kouamélan et al., 1997, 2018).

4. Summary-Synthesis

4.1. Tracking tectonic mode(s) in the sWAC between c. 2350–2060 Ma

Modern Earth's plate tectonics are defined by a globally interconnected, kinematically linked network of rigid lithospheric plates (e.g. Dewey, 1969; Korenaga, 2018). In contrast, the tectonic modes that may have operated in pre-Neoproterozoic times remain a subject of ongoing debate (e.g. stagnant lid, sluggish lid, active lid, Lenardic, 2018 and references therein). A direct implication is that establishing a coherent tectonic model for a given Precambrian region hinges on our ability to analyse and integrate multi-disciplinary geoscientific datasets. In this section, we use the sWAC as a case study and interpret the space–time-integrated patterns presented above to propose a revised tectonic model for its late Siderian to Rhyacian tectonic evolution. The section below is structured around two key time slices, representing the late Siderian and Rhyacian periods, respectively. These time slices provide critical insights into the potential tectonic modes that shaped the sWAC as it transitioned out of the Archean Era.

4.1.1. c. 2350–2265 Ma time slice

A critical aspect of the sWAC Paleoproterozoic geodynamic puzzle involves deciphering its cryptic Siderian geological evolution between c. 2500–2300 Ma. The main challenges consist in (i) unravelling the relative position of Archean blocks with respect to nascent Paleoproterozoic crust; (ii) deciphering the nature of the continental lithospheric mantle and lower to mid-crust beneath Siderian upper crust across the Baoulé-Mossi Domain; and (iii) framing a coherent and testable tectonic setting for the lowermost part of the stratigraphic record in the Baoulé-Mossi Domain through multi-data integration.

Large portions of the Archean Kénéma-Man Domain have been interpreted to represent a passive margin setting between c. 2615–2350 Ma, as supported by the presence of shallow marine siliciclastic sedimentary rocks, mafic igneous rocks, and banded iron formations (e.g. Simandou and Nimba series) that unconformably overlie > 2800 Ma higher-grade crystalline basement rocks (Billa et al., 1999; Thiéblemont et al., 2004). Yet, Feybesse et al. (1998) advocated for the break-up of an Archean craton with no ocean opening between c. 2515–2435 Ma, illustrating uncertainties about what happened during this period. Moreover, the paleogeographic positions of the Archean Kénéma-Man and Reguibat Domains remain unknown before Neoproterozoic times (Gong et al., 2021). Consequently, these two Archean blocks are conventionally treated as independent lithospheric entities, and existing data are insufficient to decipher whether they once formed part of a hypothesised Archean supercraton (i.e. Kenorland, Bleeker, 2003), remained close neighbours, or were far removed from each other by the dawn of the Paleoproterozoic.

Within the Baoulé-Mossi Domain, basal tholeiitic basalts recently dated by Hayman et al. (2023) at c. 2350 Ma extend the Paleoproterozoic magmatic history of the sWAC by c. 80 Myr beyond the accepted emergence of felsic igneous bodies previously constrained at c. 2265 Ma (Grenhölm et al., 2019a). Despite these recent advances, available data for this late Siderian period remain largely dominated by geochemical data, which alone do not allow for robust discrimination between mid-ocean ridge basalts (MORBs, Leube et al., 1990), oceanic flood basalts (OFBs, Lompo, 2009; Hayman et al., 2023), and intra-oceanic island arc basalts (IOABs, Salah et al., 1996). The non-diagnostic nature of geochemistry for discriminating between tectonic settings results from a demonstrated overlap and blurring of compositional differences, particularly evident for late Archean and Paleoproterozoic igneous rocks (Li et al., 2015; Barnes et al., 2021; Doucet et al., 2022). Thus, until additional, high-resolution geochronological data become available for the lowermost part of the stratigraphic record across the Baoulé-Mossi Domain, the unifying implication of these hypotheses is the prevalence of an oceanic realm by c. 2350 Ma. It is also important to note that these models are not necessarily mutually exclusive. For instance, one plausible scenario involves (i) the opening of an oceanic basin via thinning of Archean continental lithosphere, progressing to a full breakup and spreading stage (MORBs); followed by (ii) mantle upwelling impacting the newly formed oceanic lithosphere (OFBs); and, ultimately, (iii) plate reorganisation leading to convergence and the development of intra-oceanic subduction zones (IOABs). In this context, the interpreted geochemical signatures could reflect temporal evolution rather than conflicting spatial patterns.

4.1.2. c. 2265–2060 time slice

Rhyacian granitoids dated between c. 2265 and 2095 Ma across the sWAC are conventionally regarded as vestiges of a magmatic arc(s) constructed in an intra-oceanic subduction zone setting (Grenhölm et al., 2019a and references therein). However, calc-alkaline, arc-like compositions (i.e. LILE enrichment and negative Nb-Ti anomalies) in granitoids can be produced by a range of different processes, including: (i) subduction and water-fluxed melting (Klemme et al., 2005); (iii) sagduction (Bédard, 2018, 2024); (iii) dripping (Nebel et al., 2018; Mole et al., 2021); and/or (iv) derivation of parental magmas from previously metasomatised continental lithospheric mantle either by subduction processes or under a stagnant lid regime (Richards, 2009; Yang et al., 2014). Thus, the use of geochemical arguments alone is not able to robustly discriminate between different tectonic settings for the emplacement of pre-Neoproterozoic igneous rocks (Moyen and Laurent, 2018; Chelle-Michou et al., 2022).

In this study, we provide additional, multi-disciplinary lines of evidence that support the operation of subduction processes in the sWAC between c. 2265–2060 Ma, which are listed hereafter:

(i) the abundance of disparate U-Pb-Hf-O zircon evolutionary paths (i.e. εHf(t)-time and $\delta^{18}O$-time arrays, Roberts and Spencer, 2015; Spencer et al., 2019) documented in the sWAC (e.g. Parra-Avila et al., 2017; Thébaud et al., submitted). These patterns align with those observed in other Paleoproterozoic provinces and are consistent with tectonic models involving accretion and/or collisions between continental or microcontinental blocks and exotic terranes (e.g. Rio Apa Terrane in the Amazonian Craton between c. 2100–1720 Ma, Ribeiro et al., 2020; Minas-Bahia orogenic belt in the São Francisco Craton between c. 2500–2000 Ma, Bruno et al., 2021; North Tarim Orogen in the North China Craton between c. 1940–1850 Ma, Ge et al., 2015; Wopmay Orogen in north-west Laurentia between c. 2000–1890 Ma, Davis et al., 2015).

(ii) the Baoulé-Mossi Domain records a systematic and diachronous transition from tholeiitic mafic volcanism to voluminous and spatially extensive calc-alkaline bimodal volcanism between c. 2265–2175 Ma (e.g. Baratoux et al., 2011; Grenhölm et al., 2019a; Hayman et al., 2023; Labou et al., 2020; Ngom et al., 2010; Pouclet et al., 2006; Masurel et al., 2022).

(iii) the orogen-scale bimodal distribution of igneous zircon ages (Parra-Avila et al., 2017; Grenhölm et al., 2019a,b) is consistent with a model of prolonged seafloor subduction, leading to

multiple, diachronous collisions with Archean continental blocks (i.e. accretionary-collisional orogenesis);

(iv) the characterisation of low-temperature eclogite-facies, Paleoproterozoic oceanic crust ($P > 10$ kbar, $T < 450$ °C) such as the c. 2175–2135 Ma Fada N'Gourma eclogite in Burkina Faso (Ganne et al., 2012) provides further evidence. This suggests that the scarcity of Paleoproterozoic blueschist-facies rocks may stem from methodological challenges in reconstructing *P-T-t-d* paths (e.g. Palin et al., 2020) or overprinting by later metamorphic events (e.g. Brown et al., 2022), rather than a genuine absence.

(v) paleomagnetic indicate significant horizontal displacement since the initiation of Nuna's assembly at c. 2200 Ma (e.g. Mitchell et al., 2014; Meert and Santosh, 2017; Cawood et al., 2018).

A last, less conventional, and commonly overlooked line of evidence for unravelling potential tectonic modes lies in analysing the space–time-integrated metallogenic inventory of a region. Indeed, Huston et al. (2023) documented that paleo-convergent margins associated with several major metallogenic provinces exhibit a different metallogenic inventory at different stages of their respective evolutions. These authors coined the term "convergent margin metallogenic cycle" (CMMC) to define a unified metallogenic path from VMS and/or calc-alkaline porphyry Cu-(Au) → orogenic Au → alkalic porphyry Cu → granite-related rare metals and/or LCT pegmatites. Importantly, Huston et al. (2023) proposed the fundamental changes in duration and multiplicity of CMMC, as recorded in major metallogenic provinces of Archean to Phanerozoic age, to track secular changes in tectonic processes. Relying on the space–time-integrated metallogenic inventory of the Paleoproterozoic sWAC (Fig. 11; Electronic Supplementary Material 2; see compilations by Goldfarb et al., 2017; Grenholm et al., 2019a; Markwitz et al., 2016; Eglinger et al., 2022; Thébaud et al., 2020; Masurel et al., 2022), it appears that ore deposits developed over a ~155 Myr-long metallogenic cycle. This cycle was initiated by VMS and porphyry Cu-(Au) mineralisation along central Côte d'Ivoire and south-western Burkina Faso at c. 2190–2140 Ma (Masurel et al., 2022)and references therein). It ended with the emplacement of garnet-HREE-Ti-Y- and garnet-columbite (Li-Nb)-bearing pegmatites during the late collisional stage of the Eburnean orogeny to post-Eburnean period, as illustrated by the Mangodara district in Burkina Faso (c. 2035 Ma; Bonzi et al., 2021), and the Malian Bougini LCT-pegmatites (c. 2070–2000 Ma; Sanogo, 2022). Based on Huston et al. (2023), this ~155 Myr long metallogenic cycle is best regarded as "*transitional*" between consistently short-lived (~60–150 Myr), single CMMCs recorded in Late Mesoarchean to Neoarchean provinces (e.g. Slave, Superior, Yilgarn) and longer (~220–440

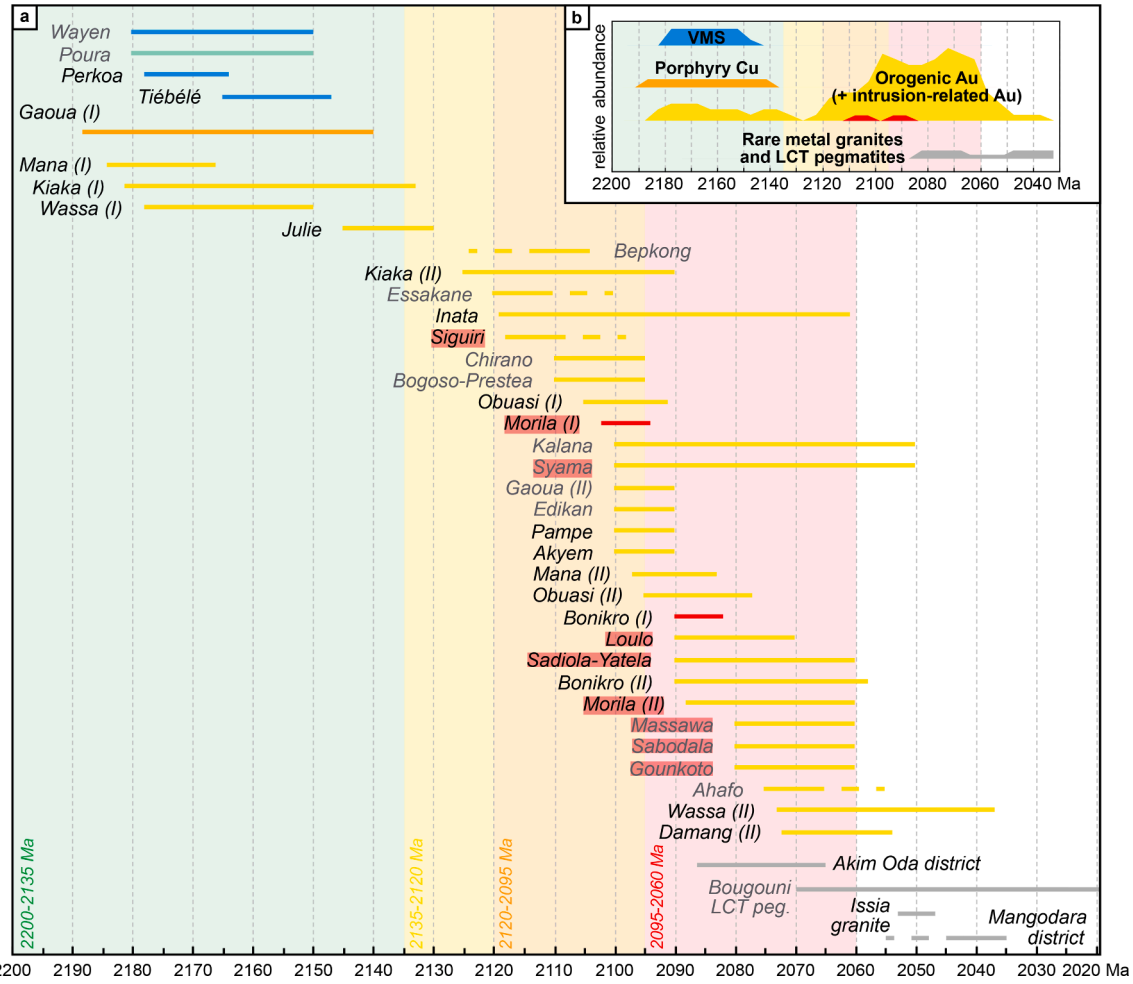

Fig. 11. The Metallogenic Cycle of the Paleoproterozoic sWAC. **a.** Timing of major types of ore deposits (using the same colour legend as in Figs. 5–10) illustrating the Baoulé-Mossi Domain Metallogenic Cycle. Only deposit types representative of a Convergent Margin Metallogenic Cycle (Huston et al., 2023) are included (refer to main text for details). Note that age bars are centred on obtained ages and represent age uncertainties; they do not indicate the duration of deposit emplacement. Dashed lines mark minimum and maximum age constraints. Deposits labelled in grey are somehow less constrained than the others. Those predominantly late with a red tag are situated in the western Baoulé-Mossi Domain. Background coloured intervals correspond to previously defined time slices, providing stratigraphic, tectonic, magmatic, and metamorphic context to the mineralisation. **b.** Relative abundance of the different types of ore deposits formed between 2200 and 2020 Ma (same colour legend as in panel **a**). Geochronological constraints and corresponding references are provided in Electronic Supplementary Material 2.

Myr), multiple CMMCs of Phanerozoic provinces (e.g. Appalachians, Tasmanides, Western Cordillera). This time-integrated pattern thus consolidates the idea that the transition from Archean enigmatic tectonic modes to modern-style plate tectonics was at play during Paleoproterozoic times in the sWAC.

This interpretation is in line with previous work by Grenhölm (2019), who proposed that the Eburnean Orogen formed in an equivalent tectonic setting as the Neoproterozoic East African-Antartica Orogen, with insights into secular changes in tectonic modes during the Proterozoic Eon. However, we emphasise that this transition was likely diachronous across the Earth and thus pieces of evidence mentioned above do not imply the existence of a global, interconnected network of plates by the Rhyacian period or that subduction zones looked exactly the same as their Phanerozoic counterparts. Indeed, Proterozoic mantle potential temperatures ~ 80–150 °C hotter than at present likely caused the hypothesised subduction zone(s) and orogen(s) to be associated with different geological attributes when compared to their Phanerozoic counterparts (Spencer et al., 2021). For instance, based on numerical modelling, several authors proposed that mid-Proterozoic (c. 1850–850 Ma) subduction zones were characterised by (i) extensive and rapid rollback of the subducting slab; (ii) greater width between back-arc and subduction trench; and (iii) voluminous decompression melting of asthenospheric mantle (Sizova et al., 2010, Fisher and Gerya, 2016, and Perchuk et al., 2019). These observations echo well with time-integrated global metamorphic data presented in Brown et al. (2020), who proposed that Paleoproterozoic high-pressure granulites and high-temperature eclogites indicate that subduction processes at that time operated under a higher geothermal gradient than that observed in Neoproterozoic to Phanerozoic subduction systems, which are characterised by blueschist-facies metamorphic rocks.

4.2. Knowledge gaps and future research avenues

Finally, we build on the review of available data and current knowledge on the Paleoproterozoic geological evolution of the sWAC, this subsection outlines key avenues for future research that could enhance our understanding of the tectonic evolution of the sWAC and its geodynamic driver(s).

4.2.1. Stratigraphic record, diachroneity in geological development, and tectonic significance of greenstone belts

While portions of the volcanosedimentary stratigraphic sequences are well described and associated with robust ages (Fig. 2), current data resolution does not allow for detailed craton-scale stratigraphic correlations, largely due to difficulties in dating lithologies such as basalts, andesites, shales, and conglomerates. In contrast, plutonic rocks clearly indicate diachronous geological development across the Baoulé-Mossi Domain through the Rhyacian. Additional, high-quality geochronological data on greenstone rock sequences are essential to improve available constraints on the diachroneity in geological development between the eastern and western Baoulé-Mossi Domain. Key knowledge gaps include (i) the age of the oldest stratigraphic unit across the Baoulé-Mossi Domain; (ii) the degree of geochemical variability and/or stratigraphic heterogeneity across greenstone belts of the Baoulé-Mossi Domain between c. 2350 and 2265 Ma; and (iii) the possibility to support the observed diachroneity in plutonism from ages on Rhyacian volcanic suites and sedimentary series across the Baoulé-Mossi Domain. Also, it is unclear whether these greenstone belts resulted from tectonically enhanced Rayleigh-Taylor instabilities, density-driven processes, or formed in rift, arc, or back-arc settings (Vidal, et al., 2009; Baratoux et al., 2011; Gapais et al., 2014; Hayman et al., 2023). There is therefore still room for further understanding of the tectonic significance of these Paleoproterozoic greenstone belts.

4.2.2. Lithospheric architecture

The possible presence of Archean subcontinental lithospheric mantle and/or lower-mid crust beneath Paleoproterozoic upper crust in the Baoulé-Mossi Domain remains debated. Outside of the exposed Archean Kénéma-Man and SASCA Domains, a concealed Archean lithospheric block of unknown extent was indirectly mapped in south-easternmost Ghana through U-Pb-Hf isotopes on felsic igneous zircon (Petersson et al., 2016, 2018; Amponsah et al., 2023). Yet, the vast majority of Nd (whole-rock) and Hf (zircon) isotopic data collected on igneous rocks across the Baoulé-Mossi Domain consistently yield suprachondritic, juvenile compositions (Thébaud et al., submitted). Furthermore, an oceanic realm also appears supported by geochemical signatures of c. 2350–2265 Ma igneous rocks (Hayman et al., 2023 and references therein).

The simplest explanation for the lack of Archean geochemical and isotopic signatures is the absence of Archean rocks to influence the chemical composition of igneous rocks and their xenocrystic zircon populations. Alternatively, some studies suggest these xenocrysts could derive from a zircon-poor mafic protolith (Parra-Avila et al., 2018; Petersson et al., 2018). The same authors emphasise the risk for Archean contribution in Rhyacian magmatism to be under-estimated. In their view, the term "*juvenile*" would apply on an isotopic point of view, when the *"isotopic signature is no where near the depleted mantle"* (Moyen et al., 2017), but not in a melt source point of view, when the crustal material is extracted *"from the mantle not long before its incorporation into the belts"* (Couzinié et al., 2020). Future work should focus on the nature and composition of the subcontinental lithospheric mantle beneath the Baoulé-Mossi Domain, such as Re-Os dating of mantle xenolith sulphides or mineralogical analysis of garnet xenocrysts (Griffin et al., 2009). Understanding the distribution of possible Archean lithosphere beneath Paleoproterozoic upper crust, not demonstrated yet, would be pivotal to elucidating its role in the formation and spatial distribution of Siderian to Rhyacian greenstone belts, and the tectonic processes involved.

4.2.3. Timing of deformation and metamorphism

Our ability to constrain the timing of deformation and metamorphic events in the sWAC is limited by the lack of studies integrating structural, metamorphic, and geochronological data (e.g. Block et al., 2016b; McFarlane et al., 2019). Comprehensive *P-T-t-d* paths across the Baoulé-Mossi Domain would illuminate the spatial and temporal succession of tectonic processes underlying the formation of the sWAC.

4.2.4. Global context and the place of the WAC during Nuna assembly

Space-time-integrated patterns in stratigraphic development, magmatism, deformation, metamorphism, and metallogeny of the Paleoproterozoic sWAC shall be compared to those of its northern counterpart (nWAC: Reguibat Archean Domain, Yetti and Eglab Paleoproterozoic terranes, Anti-Atlas Inliers). Such comparative analysis of their respective geological evolution would provide critical insights towards building a unified tectonic model for the Paleoproterozoic WAC. Looking beyond the WAC, our best chance to solve this Paleoproterozoic puzzle lies in improving our understanding of the geological evolution of the Guiana Shield during the c. 2250–2000 Ma Eburnean-Transamazonian Orogeny (Vanderhaeghe et al., 1998; Delor et al., 2003; Klein and Rodrigues, 2022). Interestingly, combined geological, geochronological, geochemical, isotopic, and geophysical evidence collectively indicate that the São Luis Cratonic Fragment and the basement of the Gurupi belt in northern Brazil were connected to the sWAC during Paleoproterozoic times (Klein and Moura, 2008). Other configurations also advocate for the connection between the Eburnean and the Transamazonian Orogens in the Paleoproterozoic (e.g. Nomade et al., 2003; Grenhölm et al., 2019b; Chardon et al., 2020). In the same line, similarities in the space–time patterns of the sedimentary, tectonic, metamorphic, and magmatic events between terrains of the West-Central Africa and Amazonia lead to consider they used to form a vast orogenic domain, comprising the West and Central African Orogens, the Transamazonian Orogen and multiple Archean blocks (e.g. Feybesse et al., 1998).

From a paleomagnetic perspective, there are no robust data for the WAC prior to c. 860 Ma (Antonio et al., 2021a) and thus, there is no consensus on the relative positions of the Amazon Craton and the WAC prior to Neoproterozoic times. This has left room for multiple Paleoproterozoic configurations of the Amazon Craton (AC), divided here into the Guiana Shield (GS) and the Central Brazil Shield (CBS), with respect to the West African Craton (WAC) to have been proposed, including (Fig. 12): (i) the AC south-west of WAC, unrotated from current orientation (Ledru et al., 1994); (ii) AC west of the WAC, unrotated (Davis, 2013); (iii) the AC south of the WAC, rotated 30° anti-clockwise (Chardon et al., 2020; Antonio et al., 2021b); (iv) the AC north-east of WAC, rotated 180° clockwise (Li et al., 2023); and finally (v) the AC north-west of WAC, rotated 90° clockwise (Cao et al., 2024). Some of these models (e.g., Ledru et al., 1994) are already discounted in the literature as they did not consider the Neoproterozoic relative displacement between the two cratons (e.g., Chardon et al., 2020). The Apparent Polar Wander paths proposed by Antonio et al (2021b) indicate that even if these two blocks ended up nearby each other at the end of the Eburnean, they were not particularly close for much, if not all, of the major period of crustal formation and reworking prior to 2000 Ma. This is in spite of the similar age spectra between 2500 and 2000 Ma for felsic magmatism in both blocs (Parra-Avila et al., 2018; Tedeschi et al. 2020). Furthermore, none of these reconstructions explain the lack of diachronism in the Guiana Shield, the lack of a younger Orocaima (1980 to 1960 Ma; Fraga et al., 2024) signature for magmatism in the WAC or Benino-Nigerian Shield (Caxito et al., 2020) nor the complex geometries of the greenstone belts in the Guiana Shield compared to the mostly linear belts seen in the WAC. It illustrates that systematic dating and robust paleomagnetic studies of mafic dyke swarms slightly younger than the craton-forming processes are needed to refine these models (e.g. Baratoux et al., 2019). Promising targets include the c. 1950 Ma Goboy mafic dyke in the Guiana Shield (Kroonenberg et al., 2022) and the c. 2040 Ma mafic dykes in the Anti-Atlas Inliers of Morocco, such as the Ierhourtane dolerite (2040 ± 6 Ma, Walsh et al., 2002) and the Ifzwane dolerite (2040 ± 2 Ma, Kouyaté et al., 2013).

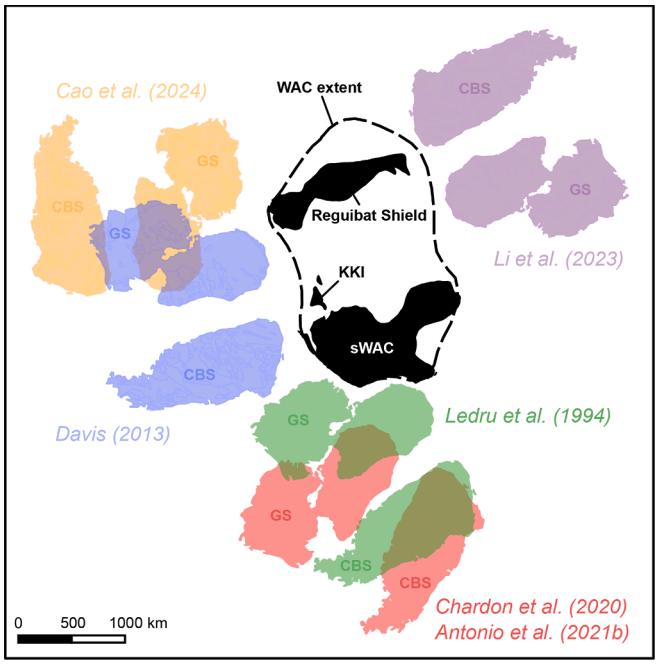

Fig. 12. Relative position and orientation of the West African Craton (WAC) with respect to the Amazonian Craton, which is divided into the Guiana Shield (GS) and the Central Brazil Shield (CBS), at the end of Nuna assembly as proposed by Ledru et al. (1994), Davis (2013), Antonio et al. (2021b), Li et al. (2023) and Cao et al. (2024). The Reguibat Shield, sWAC and Kédougou-Kénieba Inlier (KKI) extents are represented to make the variations in correlation between terrains of the WAC and sWAC more evident. The paleomagnetic study by Antonio et al. (2021a), which builds on the proposal by Chardon et al. (2020), represents the state of the art in terms of this type of data and suggest that the West African and Amazonian cratons only assembled near the end or even after the Eburnean Orogeny. The significant variability shown by these proposed models suggests further work still need to be done to position these two continental landmasses at c. 2000 Ma.

5. Funding sources

AMIRA Global, the industry sponsors, and sponsors in-kind are gratefully acknowledged for their support of the WAXI projects (P934) that enabled a large part of the more recent studies cited in this paper to be collected. This work was also partly supported by the Hammond and Nisbet fellowship at the University of Western Australia to Quentin Masurel. Additional funding was provided by the CNRS IRN FALCoL project.

CRediT authorship contribution statement

Julien Perret: Writing – original draft. **Mark W. Jessell:** Writing – original draft, Project administration, Funding acquisition, Data curation, Conceptualization. **Quentin Masurel:** Writing – original draft. **Patrick C. Hayman:** Writing – original draft. **Nicolas Thébaud:** Writing – original draft. **Lenka Baratoux:** Writing – original draft. **Alain Kouamélan:** Writing – review & editing. **Aurélien Eglinger:** Writing – review & editing. **Anne-Sylvie André-Mayer:** Writing – review & editing. **Augustin Y. Koffi:** Writing – review & editing. **Ibrahima Dia:** Writing – original draft. **Jacques Koné:** Writing – review & editing. **James Davis:** Writing – original draft. **Ousmane Wane:** Writing – review & editing. **Prince O. Amponsah:** Writing – review & editing. **Seta Naba:** Writing – review & editing. **Oliver Vanderhaeghe:** Writing – review & editing.

Declaration of competing interest

The authors declare the following financial interests/personal relationships which may be considered as potential competing interests: Alain Kouamelan reports financial support was provided by Amira International Ltd. Anne-Syvie Andre Mayer reports financial support was provided by Amira International Ltd. Aurelien Eglinger reports financial support was provided by AMIRA Global. Mark Jessell reports financial support was provided by AMIRA Global. Nicolas Thébaud reports financial support was provided by AMIRA Global. Patrick Hayman reports financial support was provided by Queensland University of Technology. Prince Ofori Amponsah reports financial support was provided by AMIRA Global. Quentin Masurel reports financial support was provided by Amira International Ltd. Seta Naba reports financial support was provided by AMIRA Global. Olivier Vanderhaeghe reports financial support was provided by AMIRA Global and the CNRS. If there are other authors, they declare that they have no known competing financial interests or personal relationships that could have appeared to influence the work reported in this paper.

Acknowledgements

This review is one of the key outcomes of collaborative research conducted during AMIRA Global P934 WAXI 1-3 and we wish to recognise our research colleagues from partner institutions worldwide (Electronic Supplementary Material 4). Additional funding was provided by the CNRS IRN FALCoL project. The authors also wish to acknowledge the foundational work undertaken by the West African, European and North American geological surveys and researchers for their fundamental observations and models that provided a solid basis for this geological endeavour. QM would like to acknowledge the Hammond and Nisbet trust for its support. J.-P. Liégeois and an

anonymous reviewer are warmly thanked for their comments that greatly help to focus the manuscript. We also thank V. Pease for editorial handling.

Appendix A. Supplementary data

Supplementary data to this article can be found online at https://doi.org/10.1016/j.precamres.2025.107707.

Data availability

Data will be made available on request.

References

Abouchami, W., Boher, M., Michard, A., Albarede, F., 1990. A major 2.1 Ga event of mafic magmatism in west Africa: An Early stage of crustal accretion. J. Geophys. Res. 95, 17605. https://doi.org/10.1029/JB095iB11p17605.

Adadey, K., Clarke, B., Théveniaut, H., Urien, P., Delor, C., Roig, J.Y., Feybesse, J.L., 2009. Geological map explanation—map sheet 0503 B (1: 100 000), CGS/BRGM/Geoman, Geological Survey Department of Ghana (GSD). No. MSSP/2005/GSD/5a.

Adams, S.J., Van Lichtervelde, M., Amponsah, P.O., Nude, P.M., Asiedu, D.K., Dampare, S.B., 2023. Characterisation and rare-metal potential of the Winneba-Mankoadze pegmatites, Southern Ghana: Evidence of two pegmatite fields. Journal of African Earth Sciences 207, 105049.

Adou, M., Delor, C., Siméon, Y., Zamblé, Z., Konan, G., Yao, B.D., Vidal, M., Diaby, I., Cautru, J.P., Chiron, J.C., Dommanget, A., Cocherie, A., 1995. Carte géologique de la Côte d'Ivoire 1:200 000 feuille Abengourou.

Allibone, A.H., McCuaig, T.C., Harris, D., Etheridge, M., Munroe, S., Byrne, D., Amanor, J., Gyapong, W., 2002a. Structural Controls on Gold Mineralization at the Ashanti Deposit, Obuasi, Ghana, in: Integrated Methods for Discovery - Global Exploration in the Twenty-First Century. Society of Economic Geologists. DOI: 10.5382/SP.09.04.

Allibone, A.H., Lawrence, D., Scott, J., Fanning, M., Lambert-Smith, J., Stenhouse, P., Harbidge, R., Vargas, C., Turnbull, R., Holliday, J., 2020. Chapter 7: Paleoproterozoic Gold Deposits of the Loulo District, Western Mali, in: Geology of the World's Major Gold Deposits and Provinces. Society of Economic Geologists, pp. 141–162. DOI: 10.5382/SP.23.07.

Almeida, G.M., Fuck, R.A., Dantas, E.L., Lima, S.S., 2022. Oblique collision and accretionary processes in the South Borborema Province: Insights from structural geology and geophysical data. Tectonophysics 844, 229607.

Amponsah, P.O., Salvi, S., Béziat, D., Baratoux, L., Siebenaller, L., Nude, P.M., Nyarko, R. S., Jessell, M.W., 2016. The Bepkong gold deposit, Northwestern Ghana. Ore Geology Reviews 78, 718–723. https://doi.org/10.1016/j.oregeorev.2015.06.022.

Amponsah, P.O., Kwayisi, D., Awunyo, E.K., Sapah, M.S., Sakyi, P.A., Su, B.-X., Lu, Y., Nude, P.M., 2023. New evidence for crustal reworking and juvenile arc-magmatism during the Palaeoproterozoic Eburnean events in the Suhum Basin, South-east Ghana. Geological Journal 58, 3734–3755.

Antonio, P.Y.J., Baratoux, L., Trindade, R., Rousse, S.A., Lana, C., Macouin, M., Adu, E., Sanchez, C., Silva, M., Firmin, P.A., Amponsah, P., Sakyi, P., 2021a. West Africa in Rodinia: High quality paleomagnetic pole from the~ 860 Ma Manso dyke swarm (Ghana). Gondwana Research. 94, 28–43.

Antonio, P.Y.J., D'Agrella-Filho, M.S., Nedelec, A., Poujol, M., Sanchez, C., Dantas, E.L., Dall'Agnol, R., Teixeira, M.F.B., Proietti, A., Dopico, C.M., 2021b. New constraints for paleogeographic reconstructions at ca. 1.88 Ga from geochronology and paleomagnetism of the Carajás dyke swarm (eastern Amazonia). Precambrian Research 353, 106039.

Anum, S., Sakyi, P.A., Su, B.-X., Nude, P.M., Nyame, F., Asiedu, D., Kwayisi, D., 2015. Geochemistry and geochronology of granitoids in the Kibi-Asamankese area of the Kibi-Winneba volcanic belt, southern Ghana. Journal of African Earth Sciences 102, 166–179.

Attoh, K., Evans, M.J., Bickford, M.E., 2006. Geochemistry of an ultramafic-rodingite rock association in the Paleoproterozoic Dixcove greenstone belt, southwestern Ghana. Journal of African Earth Sciences 45, 333–346.

Augustin, J., Gaboury, D., Crevier, M., 2017. Structural and gold mineralizing evolution of the world-class orogenic Mana district, Burkina Faso: Multiple mineralizing events over 150 million years. Ore Geology Reviews 91, 981–1012. https://doi.org/10.1016/j.oregeorev.2017.08.007.

Baratoux, L., Söderlund, U., Ernst, R.E., De Roever, E., Jessell, M.W., Kamo, S., Naba, S., Perrouty, S., Metelka, V., Yatte, D., 2019. New U–Pb baddeleyite ages of mafic dyke swarms of the West African and Amazonian cratons: implication for their configuration in supercontinents through time. Dyke swarms of the world: A modern perspective 263–314.

Baratoux, L., Jessell, M.W., Kouamélan, A.N. 2024. The West African Craton. In: Hamimi, Z., et al. The Geology of North Africa. Regional Geology Reviews. Springer, Cham. DOI: 10.1007/978-3-031-48299-1_3.

Baratoux, L., Metelka, V., Naba, S., Jessell, M.W., Grégoire, M., Ganne, J., 2011. Juvenile Paleoproterozoic crust evolution during the Eburnean orogeny (~2.2–2.0Ga), western Burkina Faso. Precambrian Research 191, 18–45. https://doi.org/10.1016/j.precamres.2011.08.010.

Barnes, S.J., Williams, M., Smithies, R.H., Hanski, E., Lowrey, J.R., 2021. Trace element contents of mantle-derived magmas through time. Journal of Petrology 62, egab024. https://doi.org/10.1093/petrology/egab024.

Bayer, R., Lesquer, A., 1978. Les anomalies gravimetriques de la bordure orientale du craton ouest-africain:geometrie d'une suture pan-africaine. Bull. Soc. Geol. Fr. 20 (6), 863–876.

Bédard, J.H., 2018. Stagnant lids and mantle overturns: Implications for Archaean tectonics, magmagenesis, crustal growth, mantle evolution, and the start of plate tectonics. Geoscience Frontiers 9, 19–49.

Bédard, J.H., 2024. A gradual Proterozoic transition from an Unstable Stagnant Lid to the modern Plate Tectonic system. Journal of the Geological Society. The Geological Society of London.

Bessoles, B., 1977. Géeologie de l'Afrique. Le craton Ouest Africain, Mémoire du BRGM.

Béziat, D., Bourges, F., Debat, P., Lompo, M., Martin, F., Tollon, F., 2000. A Paleoproterozoic ultramafic-mafic assemblage and associated volcanic rocks of the Boromo greenstone belt: fractionates originating from island-arc volcanic activity in the West African craton. Precambrian Research 101, 25–47.

Béziat, D., Siebenaller, L., Salvi, S., Chevalier, P., 2016. A weathered skarn-type mineralization in Ivory Coast: The Ity gold deposit. Ore Geology Reviews 78, 724–730. https://doi.org/10.1016/j.oregeorev.2015.07.011.

Billa, M., Feybesse, J.-L., Bronner, G., Lerouge, C., Milési, J.-P., Traoré, S., Diaby, S., 1999. Les formations à quartzites rubanés ferrugineux des Monts Nimba et du Simandou: des unités empilées tectoniquement, sur un «soubassementplutonique Archéen (craton de Kénéma-Man), lors de l'orogène Éburnéen. Comptes Rendus De L'académie Des Sciences-Series IIA-Earth and Planetary Science 329, 287–294.

Bindeman, I.N., Zakharov, D.O., Palandri, J., Greber, N.D., Dauphas, N., Retallack, G.J., Hofmann, A., Lackey, J.S., Bekker, A., 2018. Rapid emergence of subaerial landmasses and onset of a modern hydrologic cycle 2.5 billion years ago. Nature 557, 545–548.

Bleeker, W., 2003. The late Archean record: a puzzle in ca. 35 pieces. Lithos 71, 99–134.

Block, S., Ganne, J., Baratoux, L., Zeh, A., Parra-Avila, L.A., Jessell, M., Ailleres, L., Siebenaller, L., 2015. Petrological and geochronological constraints on lower crust exhumation during Paleoproterozoic (Eburnean) orogeny, NW Ghana, West African Craton. Journal Metamorphic Geology 33, 463–494. https://doi.org/10.1111/jmg.12129.

Block, S., Baratoux, L., Zeh, A., Laurent, O., Bruguier, O., Jessell, M., Ailleres, L., Sagna, R., Parra-Avila, L.A., Bosch, D., 2016a. Paleoproterozoic juvenile crust formation and stabilisation in the south-eastern West African Craton (Ghana); New insights from U-Pb-Hf zircon data and geochemistry. Precambrian Research 287, 1–30. https://doi.org/10.1016/j.precamres.2016.10.011.

Block, S., Jessell, M., Aillères, L., Baratoux, L., Bruguier, O., Zeh, A., Bosch, D., Caby, R., Mensah, E., 2016b. Lower crust exhumation during Paleoproterozoic (Eburnean) orogeny, NW Ghana, West African Craton: Interplay of coeval contractional deformation and extensional gravitational collapse. Precambrian Research 274, 82–109. https://doi.org/10.1016/j.precamres.2015.10.014.

Bogdanova, S.V., Bingen, B., Gorbatschev, R., Kheraskova, T.N., Kozlov, V.I., Puchkov, V. N., Volozh, Y.A.. The East European Craton (Baltica) before and during the assembly of Rodinia. Precambrian Research 160, 23–45.

Boher, M., Abouchami, W., Michard, A., Albarede, F., Arndt, N.T., 1992. Crustal growth in West Africa at 2.1 Ga. J. Geophys. Res. 97, 345. https://doi.org/10.1029/91JB01640.

Bonhomme, M., 1962. Contribution à l'étude géochronologique de la plate-forme de l'Ouest Africain, Annals de la Faculté des Sciences de Université de Clermont-Ferrand Géol. Minéral.

Bonzi, W., Van Lichtervelde, M., Vanderhaeghe, O., André-Mayer, A.-S., Salvi, S., Wenmenga, U., 2023. Insights from mineral trace chemistry on the origin of NYF and mixed LCT + NYF pegmatites and their mineralization at Mangodara, SW Burkina Faso. Mineralium Deposita. https://doi.org/10.1007/s00126-022-01127-x.

Bonzi, W.-M.-E., Vanderhaeghe, O., Van Lichtervelde, M., Wenmenga, U., André-Mayer, A.-S., Salvi, S., Poujol, M., 2021. Petrogenetic links between rare metal-bearing pegmatites and TTG gneisses in the West African Craton: The Mangodara district of SW Burkina Faso. Precambrian Research 364, 106359. https://doi.org/10.1016/j.precamres.2021.106359.

Bossière, G., Bonkoungou, I., Peucat, J.-J., Pupin, J.-P., 1996. Origin and age of Paleoproterozoic conglomerates and sandstones of the Tarkwaian Group in Burkina Faso, West Africa. Precambrian Research 80, 153–172.

Brou, J.K., Van Lichtervelde, M., Kouamélan, N.A., Baratoux, D., Thébaud, N., 2022. Petrogenetic relationships between peraluminous granites and Li-Cs-Ta rich pegmatites in south Issia zone (Central-West of Côte d'Ivoire): Petrography, Mineralogy, Geochemistry and zircon U–Pb Geochronology. Mineralogy and Petrology 116, 443–471.

Brown, M., Johnson, T., Gardiner, N.J., 2020. Plate Tectonics and the Archean Earth. Annual Review of Earth and Planetary Sciences 48, 291–320. https://doi.org/10.1146/annurev-earth-081619-052705.

Brown, M., Johnson, T., Spencer, C.J., 2022. Secular changes in metamorphism and metamorphic cooling rates track the evolving plate-tectonic regime on Earth. jgs2022-050 JGS 179. https://doi.org/10.1144/jgs2022-050.

Bruno, H., Elizeu, V., Heilbron, M., de Morisson Valeriano, C., Strachan, R., Fowler, M., Bersan, S., Moreira, H., Dussin, I., do Eirado Silva, L.G., 2020. Neoarchean and Rhyacian TTG-Sanukitoid suites in the southern São Francisco Paleocontinent, Brazil: evidence for diachronous change towards modern tectonics. Geoscience Frontiers 11, 1763–1787.

Bruno, H., Heilbron, M., Strachan, R., Fowler, M., de Morisson Valeriano, C., Bersan, S., Moreira, H., Cutts, K., Dunlop, J., Almeida, R., 2021. Earth's new tectonic regime at the dawn of the Paleoproterozoic: Hf isotope evidence for efficient crustal growth and reworking in the São Francisco craton, Brazil. Geology 49, 1214–1219.

Burke, K., Whiteman, A.J., 1973. In: Tarling, D.H., Runcorn, S.K. (Eds.), Uplift, Rifting and the Breakup of Africa. In Implications of Continental Drift to the Earth Sciences, 2. Academic, London, pp. 735e745. In: Burke, K. 2011. Plate Tectonics, the Wilson

Cycle, and Mantle Plumes: Geodynamics from the Top. Annual Review of Earth and Planetary Sciences, Vol. 39, pp. 1e29. doi:10.1146/annurev-earth-040809-152521.
Caby, R., Delor, C., Agoh, O., 2000. Lithology, structure and metamorphism of the Birimian formations in the Odienné area (Ivory Coast): the major role played by plutonic diapirism and strike-slip faulting at the border of the Man Craton. Journal of African Earth Sciences 30, 351–374.
Camil, J., Tempier, P., Pin, C., 1983. Age libérien des quartzites à magnétite de la région de Man (Côte d'Ivoire) et leur place dans l'orogène libérien. Comptes Rendus De L'academie Des Sciences 296, 149–151.
Cao, X., Collins, A., Pisarevsky, S., Flament, N., Li, S., Hasterok, D., Müller, R., 2024. Earth's tectonic and plate boundary evolution over 1.8 billion years (preprint). In: Physical Sciences and Mathematics. https://doi.org/10.31223/X5CW96.
Castaing, C., Billa, M., Milési, J.P., Thiéblemont, D., Le Metour, J., Egal, E., Donzeau, M., Guerrot, C., Cocherie, A., Chèvremont, P., Tegyey, M., Itard, Y., Zida, B., Ouedraogo, I., Kote, S., Kabore, B.E., Ouedraogo, C., Ki, J.C., Zunino, C., 2003. Notice explicative de la carte géologique et minière du Burkina Faso à 1/1,000,000.
Cawood, P.A., Hawkesworth, C.J., Pisarevsky, S.A., Dhuime, B., Capitanio, F.A., Nebel, O., 2018. Geological archive of the onset of plate tectonics. Phil. Trans. r. Soc. a. 376, 20170405. https://doi.org/10.1098/rsta.2017.0405.
Cawood, P.A., Chowdhury, P., Mulder, J.A., Hawkesworth, C.J., Capitanio, F.A., Gunawardana, P.M., Nebel, O., 2022. Secular evolution of continents and the Earth system. Reviews of Geophysics 60, e2022RG000789.
Caxito, F.A., Santos, L.C.M.L., Ganade, C.E., Bendaoud, A., Fettous, E.-H., Bouyo, M.H., 2020. Toward an integrated model of geological evolution for NE Brazil-NW Africa: The Borborema Province and its connections to the Trans-Saharan (Benino-Nigerian and Tuareg shields) and Central African orogens. Brazilian Journal of Geology. 50, 02. https://doi.org/10.1590/2317-4889202020190122.
Chardon, D., Bamba, O., Traoré, K., 2020. Eburnean deformation pattern of Burkina Faso and the tectonic significance of shear zones in the West African craton. Bulletin De La Société Géologique De France 191, 2. https://doi.org/10.1051/bsgf/2020001.
Chardon, D., Berger, J., Martellozzo, F., 2024. Archean craton assembly and Paleoproterozoic accretion-collision tectonics in the Reguibat Shield, West African Craton. Precambrian Research 413, 107570. https://doi.org/10.1016/j.precamres.2024.107570.
Chelle-Michou, C., McCarthy, A., Moyen, J.-F., Cawood, P.A., Capitanio, F.A., 2022. Make subductions diverse again. Earth-Science Reviews 226, 103966.
Condie, K.C., 2018. A planet in transition: The onset of plate tectonics on Earth between 3 and 2 Ga? Geoscience Frontiers 9, 51–60.
Condie, K.C., Puetz, S.J., Spencer, C.J., Roberts, N.M., 2024. Four billion years of secular compositional change in granitoids. Chemical Geology 644, 121868.
Couzinié, S., Ménot, R.-P., Doumnang, J.-C., Paquette, J.L., Rochette, P., Quesnel, Y., Deschamps, P., Ménot, G., 2020. Crystalline inliers near Lake Iro (SE Chad): Postcollisional Ediacaran A2-type granitic magmatism at the southern margin of the Saharan Metacraton. Journal of African Earth Sciences 172, 103960.
D'Agrella-Filho, M.S., Antonio, P.Y., Trindade, R.I., Teixeira, W., Bispo-Santos, F., 2021. The Precambrian drift history and paleogeography of Amazonia, in: Ancient Supercontinents and the Paleogeography of Earth. Elsevier, pp. 207–241.
Dabo, M., Aïfa, T., Gning, I., Faye, M., Ba, M.F., Ngom, P.M., 2017. Lithological architecture and petrography of the Mako Birimian greenstone belt, Kédougou-Kénièba Inlier, eastern Senegal. Journal of African Earth Sciences 131, 128–144. https://doi.org/10.1016/j.jafrearsci.2017.04.005.
Dampare, S.B., Shibata, T., Asiedu, D.K., Osae, S., Banoeng-Yakubo, B., 2008. Geochemistry of Paleoproterozoic metavolcanic rocks from the southern Ashanti volcanic belt, Ghana: Petrogenetic and tectonic setting implications. Precambrian Research 162, 403–423.
Davis, A., 2013. Global evolution between 2100 and 1350 Ma; an Australian focus. University of Sydney, p. 110. Unpublished Honours Thesis.
Davis, W.J., Ootes, L., Newton, L., Jackson, V., Stern, R.A., 2015. Characterization of the Paleoproterozoic Hottah terrane, Wopmay Orogen using multi-isotopic (U-Pb, Hf and O) detrital zircon analyses: An evaluation of linkages to northwest Laurentian Paleoproterozoic domains. Precambrian Research 269, 296–310. https://doi.org/10.1016/j.precamres.2015.08.012.
De Kock, G.S., Armstrong, R.A., Siegfried, H.P., Thomas, E., 2011. Geochronology of the Birim Supergroup of the West African craton in the Wa-Bolé region of west-central Ghana: Implications for the stratigraphic framework. Journal of African Earth Sciences 59, 1–40. https://doi.org/10.1016/j.jafrearsci.2010.08.001.
De Kock, G.S., Théveniaut, H., Botha, P.M.W., Gyapong, W., 2012. Timing the structural events in the Palaeoproterozoic Bolé–Nangodi belt terrane and adjacent Maluwe basin, West African craton, in central-west Ghana. Journal of African Earth Sciences 65, 1–24. https://doi.org/10.1016/j.jafrearsci.2011.11.007.
de Lira Santos, L.C.M., Caxito, F.A., Bouyo, M.H., Ouadahi, S., Araïbia, K., Lages, G.A., Santos, G.L., Pitombeira, J.P.A., Cawood, P.A., 2023. Relics of ophiolite-bearing accretionary wedges in NE Brazil and NW Africa: connecting threads of western Gondwaná s ocean during Neoproterozoic times. Geosystems and Geoenvironment 2, 100148.
Debat, P., Nikiéma, S., Mercier, A., Lompo, M., Béziat, D., Bourges, F., Roddaz, M., Salvi, S., Tollon, F., Wenmenga, U., 2003. A new metamorphic constraint for the Eburnean orogeny from Paleoproterozoic formations of the Man shield (Aribinda and Tampelga countries, Burkina Faso). Precambrian Research 123, 47–65. https://doi.org/10.1016/S0301-9268(03)00046-9.
Delor, C., Lahondère, D., Egal, E., Lafon, J.M., Cocherie, A., Guerrot, C., Rossi, P., Truffert, C., Théveniaut, H., Phillips, D., de Avelar, V.G., 2003. Transamazonian crustal growth and reworking as revealed by the 1:500,000-scale geological map of French Guiana (2nd edition) (No. 2-3–4), Géologie de la France. BRGM.
Delor, C., Couëffé, R., Goujou, J.C., Diallo, D.P., Théveniaut, H., Fullgraf, T., Ndiaye, P. M., Dioh, E., Blein, O., Barry, T.M.M., Le Métour, J., Martelet, G., Sergeev, S., Wemmer, K., 2010. Notice explicative de la carte géologique à 1/200 000 du Sénégal, feuille Saraya-Kédougou Est.
Dewey, J.F., 1969. Evolution of the Appalachian/Caledonian orogen. Nature 222, 124–129.
Dia, A., Van Schmus, W.R., Kröner, A., 1997. Isotopic constraints on the age and formation of a Palaeoproterozoic volcanic arc complex in the Kedougou Inlier, eastern Senegal, West Africa. Journal of African Earth Sciences 24, 197–213.
Diallo, M., Baratoux, L., Dufréchou, G., Jessell, M.W., Vanderhaeghe, O., Ly, S., Baratoux, D., 2020. Structure of the Paleoproterozoic Kédougou-Kénièba Inlier (Senegal-Mali) deduced from gravity and aeromagnetic data. Journal of African Earth Sciences 162. https://doi.org/10.1016/j.jafrearsci.2019.103732.
Diallo, M., Salvi, S., Baratoux, L., Béziat, D., Vanderhaeghe, O., Labou, I., Baratoux, D., Ly, S., 2024. Geology of the Tabakoto gold deposit, Kédougou-Kénièba Inlier, West African Craton, Mali. BSGF-Earth Sciences Bulletin 195 (1), 24. https://doi.org/10.1051/bsgf/2024024.
Doucet, L.S., Tetley, M.G., Li, Z.-X., Liu, Y., Gamaleldien, H., 2022. Geochemical fingerprinting of continental and oceanic basalts: A machine learning approach. Earth-Science Reviews 233, 104192. https://doi.org/10.1016/j.earscirev.2022.104192.
Doumbia, S., Pouclet, A., Kouamélan, A., Peucat, J.J., Vidal, M., Delor, C., 1998. Petrogenesis of juvenile-type Birimian (Paleoproterozoic) granitoids in Central Côte-d'Ivoire, West Africa: geochemistry and geochronology. Precambrian Research 87, 33–63. https://doi.org/10.1016/S0301-9268(97)00201-5.
Egal, E., Thiéblemont, D., Lahondère, D., Guerrot, C., Costea, C.A., Iliescu, D., Delor, C., Goujou, J.-C., Lafon, J.M., Tegyey, M., Diaby, S., Kolié, P., 2002. Late Eburnean granitization and tectonics along the western and northwestern margin of the Archean Kénéma–Man domain (Guinea, West African Craton). Precambrian Research 117, 57–84. https://doi.org/10.1016/S0301-9268(02)00060-8.
Eglinger, A., André-Mayer, A.-S., Thébaud, N., Masurel, Q., 2022. La province métallogénique du craton de Leo-Man en Afrique de l'Ouest, in: Ressources Métalliques 2 - Cadre Géodynamique et Exemples Remarquables Dans Le Monde, Géosciences - Ressources Naturelles : La Recherche Fondamentale Appliquée. pp. 257–298.
Eglinger, A., Thébaud, N., Zeh, A., Davis, J., Miller, J., Parra-Avila, L.A., Loucks, R., McCuaig, C., Belousova, E., 2017. New insights into the crustal growth of the Paleoproterozoic margin of the Archean Kéména-Man domain, West African craton (Guinea): Implications for gold mineral system. Precambrian Research 292, 258–289. https://doi.org/10.1016/j.precamres.2016.11.012.
Ennih, N., Liégeois, J.-P. (Eds.), 2008a. The Boundaries of the West African Craton (IGCP485), Geological Society of London Special Publication 297, p. 534.
Ernst, W.G., Liou, J.G., 2008. High- and ultrahigh-pressure metamorphism: Past results and future prospects. American Mineralogist 93, 1771–1786. https://doi.org/10.2138/am.2008.2940.
Feybesse, J.-L., Billa, M., Guerrot, C., Duguey, E., Lescuyer, J.-L., Milesi, J.-P., Bouchot, V., 2006. The paleoproterozoic Ghanaian province: Geodynamic model and ore controls, including regional stress modeling. Precambrian Research 149, 149–196.
Feybesse, J.-L., Bangoura, A., Billa, M., Costea, A.C., Diabate, B., Diaby, S., Diallo, A., Diallo, S., Diallo, A.B., Egal, E., Freyssinet, P., Gaye, F., Guerrot, C., Iliescu, D., Lacomme, A., Lahondère, D., Le Berre, P., Milési, J.P., Minthe, D., Soumah, D., 1999. Notice explicative de la Carte géologique de la Guinée à 1/200 000, Feuille no. 19, Kankan.
Feybesse, J.L., Billa, M., Milesi, J.P., Lerouge, C., Le Goff, E., 2000. Relationships between metamorphism-deformation-plutonism in the Archean-Paleoproterozoic contact zone of West Africa, in: 31st International Geological Congress, Rio, CD-ROM Abstract.
Feybesse, J.L., Johan, V., Triboulet, C., Guerrot, C., Mayaga-Mikolo, F., Bouchot, V., Eko N'dong, J., 1998. The West Central African belt: a model of 2.5–2.0Ga accretion and two-phase orogenic evolution. Precambrian Research 87, 161–216. https://doi.org/10.1016/S0301-9268(97)00053-3.
Feybesse, J.-L., Milési, J.-P., Johan, V., Dommanget, A., Calvez, J.-Y., Boher, M., 1989. La limite Archéen/Protérozoïque inférieur d'Afrique de l'Ouest: une zone de chevauchement majeure antérieure à l'accident de Sassandra; l'exemple des régions d'Odiénné et de Touba (Côte-d'Ivoire). Comptes rendus de l'Académie des sciences. Série 2. Mécanique, Physique, Chimie, Sciences De L'univers, Sciences De La Terre 309, 1847–1853.
Feybesse, J.-L., Milési, J.-P., 1994. The Archaean/Proterozoic contact zone in West Africa: a mountain belt of décollement thrusting and folding on a continental margin related to 2.1 Ga convergence of Archaean cratons? Precambrian Research 69, 199–227. https://doi.org/10.1016/0301-9268(94)90087-6.
Fisher, R., Gerya, T., 2016. Early Earth plume-lid tectonics: a high-resolution 3D numerical modeling approach. J. Geodyn. 100, 198–214.
Fontaine, A., Eglinger, A., Ada, K., André-Mayer, A.-S., Reisberg, L., Siebenaller, L., Le Mignot, E., Ganne, J., Poujol, M., 2017. Geology of the world-class Kiaka polyphase gold deposit, West African Craton, Burkina Faso. Journal of African Earth Sciences 126, 96–122. https://doi.org/10.1016/j.jafrearsci.2016.11.017.
Fougerouse, D., Micklethwaite, S., Ulrich, S., Miller, J., Godel, B., Adams, D.T., McCuaig, T.C., 2017. Evidence for two stages of mineralization in West Africa's largest gold deposit: Obuasi, Ghana. Economic Geology 112, 3–22. https://doi.org/10.2113/econgeo.112.1.3.
Fraga, L.M., Cordani, U., Dreher, A.M., Sato, K., Reis, N.J., Nadeau, S., De Roever, E., Kroonenberg, S., Maurer, V.C., 2024. Early Orosirian belts of the central Guiana Shield, northern Amazonian Craton: U-Pb geochronology and tectonic implications. Precambrian Research 407, 107362. https://doi.org/10.1016/j.precamres.2024.107362.

Galipp, K., Klemd, R., Hirdes, W., 2003. Metamorphism and geochemistry of the Paleoproterozoic Birimian Sefwi volcanic belt (Ghana, West Africa). Geologisches Jahrbuch D111, 151–191.
Ganne, J., De Andrade, V., Weinberg, R.F., Vidal, O., Dubacq, B., Kagambega, N., Naba, S., Baratoux, L., Jessell, M., Allibon, J., 2012. Modern-style plate subduction preserved in the Palaeoproterozoic West African craton. Nature Geosci 5, 60–65. https://doi.org/10.1038/ngeo1321.
Ganne, J., Gerbault, M., Block, S., 2014. Thermo-mechanical modeling of lower crust exhumation—Constraints from the metamorphic record of the Palaeoproterozoic Eburnean orogeny, West African Craton. Precambrian Research 243, 88–109. https://doi.org/10.1016/j.precamres.2013.12.016.
Gapais, D., Jaguin, J., Cagnard, F., Boulvais, P., 2014. Pop-down tectonics, fluid channelling and ore deposits within ancient hot orogens. Tectoophysics 618, 102–106. https://doi.org/10.1016/j.tecto.2014.01.027.
Gasquet, D., Barbey, P., Adou, M., Paquette, J.L., 2003. Structure, Sr–Nd isotope geochemistry and zircon U–Pb geochronology of the granitoids of the Dabakala area (Côte d'Ivoire): evidence for a 2.3 Ga crustal growth event in the Palaeoproterozoic of West Africa? Precambrian Research 127, 329–354. https://doi.org/10.1016/S0301-9268(03)00209-2.
Ge, R., Zhu, W., Wilde, S.A., He, J., Cui, X., 2015. Synchronous crustal growth and reworking recorded in late Paleoproterozoic granitoids in the northern Tarim craton: In situ zircon U-Pb-Hf-O isotopic and geochemical constraints and tectonic implications. Geological Society of America Bulletin 127, 781–803. https://doi.org/10.1130/B31050.1.
Goldfarb, R.J., André-Mayer, A.-S., Jowitt, S.M., Mudd, G.M., 2017. West Africa: The World's Premier Paleoproterozoic Gold Province. Economic Geology 112, 123–143. https://doi.org/10.2113/econgeo.112.1.123.
Gong, Z., Evans, D.A., Youbi, N., Lahna, A.A., Söderlund, U., Malek, M.A., Wen, B., Jing, X., Ding, J., Boumehdi, M.A., 2021. Reorienting the West African craton in Paleoproterozoic–Mesoproterozoic supercontinent Nuna. Geology 49, 1171–1176.
Gouedji, F., Picard, C., Coulibaly, Y., Audet, M.-A., Auge, T., Goncalves, P., Paquette, J.-L., Ouattara, N., 2014. The Samapleu mafic-ultramafic intrusion and its Ni-Cu-PGE mineralization: an Eburnean (2.09 Ga) feeder dyke to the Yacouba layered complex (Man Archean craton, western Ivory Coast). Bulletin De La Société Géologique De France 185, 393–411. https://doi.org/10.2113/gssgfbull.185.6.393.
Grenhölm, M., 2019. The global tectonic context of the ca. 2.27-1.96 Ga Birimian Orogen – Insights from comparative studies, with implications for supercontinent cycles. Earth-Science Reviews 193, 260–298. https://doi.org/10.1016/j.earscirev.2019.04.017.
Grenhölm, M., Jessell, M., Thébaud, N., 2019a. Paleoproterozoic volcano-sedimentary series in the ca. 2.27–1.96 Ga Birimian Orogen of the southeastern West African Craton. Precambrian Research 328, 161–192. https://doi.org/10.1016/j.precamres.2019.04.005.
Grenhölm, M., Jessell, M., Thébaud, N., 2019b. A geodynamic model for the Paleoproterozoic (ca. 2.27–1.96 Ga) Birimian Orogen of the southern West African Craton – Insights into an evolving accretionary-collisional orogenic system. Earth-Science Reviews 192, 138–193. https://doi.org/10.1016/j.earscirev.2019.02.006.
Griffin, W.L., O'Reilly, S.Y., Afonso, J.C., Begg, G.C., 2009. The composition and evolution of lithospheric mantle: a re-evaluation and its tectonic implications. Journal of Petrology 50, 1185–1204.
Gueye, M., Siegesmund, S., Wemmer, K., Pawlig, S., Drobe, M., Nolte, N., Layer, P., 2007. New evidences for an early Birimian evolution in the West African Craton: An example from the Kedougou-Kenieba inlier, southeast Senegal. South African Journal of Geology 110, 511–534. https://doi.org/10.2113/gssajg.110.4.511.
Guillot, S., Hattori, K., Agard, P., Schwartz, S., Vidal, O., 2009. Exhumation Processes in Oceanic and Continental Subduction Contexts: A Review. In: Lallemand, S., Funiciello, F. (Eds.), Subduction Zone Geodynamics. Springer, Berlin Heidelberg, Berlin, Heidelberg, pp. 175–205. https://doi.org/10.1007/978-3-540-87974-9_10.
Hallarou, M.M., Konaté, M., Olatunji, A.S., Ahmed, Y., 2021. The Paleoproterozoic porphyry copper–molybdenum deposit of Kourki (Liptako Province, western Niger). SP 502, 97–119.
Hawkesworth, C., Cawood, P.A., Dhuime, B., Kemp, T., 2024. Tectonic processes and the evolution of the continental crust. Journal of the Geological Society. The Geological Society of London.
Hayman, P.C., Bolz, P., Senyah, G., Tegan, E., Denyszyn, S., Murphy, D.T., Jessell, M.W., 2023. Physical and geochemical reconstruction of a 2.35–2.1 Ga volcanic arc (Toumodi Greenstone Belt, Ivory Coast, West Africa). Precambrian Research 389, 107029. https://doi.org/10.1016/j.precamres.2023.107029.
Hein, K.A.A., 2010. Succession of structural events in the Goren greenstone belt (Burkina Faso): implications for West African tectonics. Journal of African Earth Sciences 56, 83–94. https://doi.org/10.1016/j.jafrearsci.2009.06.002.
Hein, K.A.A., Matsheka, I.R., Bruguier, O., Masurel, Q., Bosch, D., Caby, R., Monié, P., 2015. The Yatela gold deposit: 2 billion years in the making. Journal of African Earth Sciences 112, 548–569. https://doi.org/10.1016/j.jafrearsci.2015.07.017.
Hirdes, W., Davis, D.W., 1998. First U-Pb zircon age of extrusive volcanism in the Birimian supergroup of Ghana/West Africa. Journal of African Earth Sciences 27, 291–294. https://doi.org/10.1016/S0899-5362(98)00062-1.
Hirdes, W., Davis, D.W., 2002. U–Pb Geochronology of Paleoproterozoic Rocks in the Southern Part of the Kedougou-Kéniéba Inlier, Senegal, West Africa: Evidence for Diachronous Accretionary Development of the Eburnean Province. Precambrian Research 118, 83–99. https://doi.org/10.1016/S0301-9268(02)00080-3.
Hirdes, W., Davis, D.W., Eisenlohr, B.N., 1992. Reassessment of Proterozoic granitoid ages in Ghana on the basis of U/Pb zircon and monazite dating. Precambrian Research 56, 89–96. https://doi.org/10.1016/0301-9268(92)90085-3.
Hirdes, W., Davis, D.W., Lüdtke, G., Konan, G., 1996. Two generations of Birimian (Paleoproterozoic) volcanic belts in northeastern Côte d'Ivoire (West Africa): consequences for the 'Birimian controversy. Precambrian Research 80, 173–191. https://doi.org/10.1016/S0301-9268(96)00011-3.
Hirdes, W., Senger, R., Adjei, J., Efa, E., Loh, G., Tettey, A., 1993. Explanatory notes for the geological map of Southwest Ghana 1: 100,000: sheets Wiawso (0603D), Asafo (0603C), Kukuom (0603B), Goaso (0603A), Sunyani (0703D) and Berekum (0703C); with 18 tables. Schweizerbart.
Hirdes, W., Konan, K.G., N'Da, D., Okou, A., Sea, P., Zamble, Z.B., Davis, D.W., 2007. Geology of the northern portion of the Oboisso Area, Côte d'Ivoire. Sheets 4A B 4.
Hirdes, W., Toloczyki, M., Davis, D.W., Agyei Duodu, J., Loh, G.K., Boamah, K., Baba, M., 2009. Geological Map of Ghana, 1: 1,000,000. Geological Survey Department, Accra, Ghana (GSD) and Bundesanstalt für Geowissenschaften und Rohstoffe, Hannover, Germany (BGR). BGR Library.
Hirdes, W., Nunoo, B., 1994. The Proterozoic paleoplacers at Tarkwa gold mine, SW Ghana: sedimentology, mineralogy, and precise age dating of the Main Reef and West Reef, and bearing of the investigations on source area aspects. Geologisches Jahrbuch D 100, 247–311.
Huang, B., Liu, M., Kusky, T.M., Johnson, T.E., Wilde, S.A., Fu, D., Deng, H., Qian, Q., 2023. Changes in orogenic style and surface environment recorded in Paleoproterozoic foreland successions. Nature Communications 14, 7997.
Huang, G., Mitchell, R.N., Palin, R.M., Spencer, C.J., Guo, J., 2022. Barium content of Archaean continental crust reveals the onset of subduction was not global. Nature Communications 13, 6553.
Huston, D.L., Doublier, M.P., Eglington, B., Pehrsson, S., Piercey, S., Mercier-Langevin, P., 2023. Convergent margin metallogenic cycles: A window to secular changes in Earth's tectonic evolution. Earth-Science Reviews 245, 104551. https://doi.org/10.1016/j.earscirev.2023.104551.
Ilboudo, H., Lompo, M., Wenmenga, U., Napon, S., Naba, S., Ngom, P.M., 2017. Evidence of a Volcanogenic Massive Sulfide (Zn Pb Cu Ag) district within the Tiébélé Birimian (Paleoproterozoic) Greenstone Belts, Southern Burkina Faso (West – Africa). Journal of African Earth Sciences 129, 792–813. https://doi.org/10.1016/j.jafrearsci.2017.01.020.
Jessell, M.W., Amponsah, P.O., Baratoux, L., Asiedu, D.K., Loh, G.K., Ganne, J., 2012. Crustal-scale transcurrent shearing in the Paleoproterozoic Sefwi-Sunyani-Comoé region, West Africa. Precambrian Research 212–213, 155–168. https://doi.org/10.1016/j.precamres.2012.04.015.
Jessell, M.W., Begg, G.C., Miller, M.S., 2016. The geophysical signatures of the West African Craton. Precambrian Research 274, 3–24. https://doi.org/10.1016/j.precamres.2015.08.010.
John, T., Klemd, R., Hirdes, W., Loh, G., 1999. The metamorphic evolution of the Paleoproterozoic (Birimian) volcanic Ashanti belt (Ghana, West Africa). Precambrian Research 98, 11–30. https://doi.org/10.1016/S0301-9268(99)00024-8.
Kennedy, Q.W., 1964. The Structural Differentiation of African in the Pan-African (± 500 my) Tectonic Episode. Annual Report, Leeds University, Institute of African Geology, Leeds 8, 48–49.
Kiessling, R., Treder, H.W., Zitzmann, A., 1997. Mineral occurrences, geochemical investigation and gold potential in the Bui Belt Area in Ghana. Geologisches Jahrbuch Reihe B 207–269.
Kitson, A.E., 1918. Ann. Report, Gold Coast Geol. Surv., 1916/1917 (Annual Report). Gold Coast Geological Survey, Accra, Ghana.
Klein, E.L., Moura, C.A.V., 2008. São Luís craton and Gurupi Belt (Brazil): possible links with the West African craton and surrounding Pan-African belts. Geological Society, London, Special Publications 294, 137–151.
Klein, E.L., Rodrigues, J.B., Lopes, E.C., de Oliveira, R.G., Souza-Gaia, S.M., de Oliveira, L.B.T., 2020. Age, provenance and tectonic setting of metasedimentary sequences of the Gurupi Belt and São Luís cratonic fragment, northern Brazil: broadening the understanding of the Proterozoic-Early Cambrian tectonic evolution. Precambrian Research 351, 105950.
Klein, E.L., Rodrigues, J.B., 2022. Lu–Hf constraints on pre-, syn, and post-collision associations of the Gurupi Belt, Brazil: Insights on the Rhyacian crustal evolution. Geoscience Frontiers 13, 101199.
Kleinschrot, D., Klemd, R., Bröcker, M., Okrusch, M., Frantz, L., Schmidt, K., 1994. Protores and country rocks of the Nsuta manganese deposit (Ghana). Neues Jahrbuch Für Mineralogie-Abhandlungen 1, 67–108.
Klemd, R., Hirdes, W., Olesch, M., Oberthür, T., 1993. Fluid inclusions in quartz-pebbles of the gold-bearing Tarkwaian conglomerates of Ghana as guides to their provenance area. Mineralium Deposita 28, 334–343.
Klemd, R., Hünken, U., Olesch, M., 2002. Metamorphism of the country rocks hosting gold–sulfide-bearing quartz veins in the Paleoproterozoic southern Kibi-Winneba belt (SE-Ghana). Journal of African Earth Sciences 35, 199–211. https://doi.org/10.1016/S0899-5362(02)00122-7.
Klemd, R., Oberthür, T., Ouedraogo, A., 1997. Gold-telluride mineralisation in the Birimian at Diabatou, Burkina Faso: the role of CO2N2 fluids. J. Afr. Earth Sc. 24, 227–239. https://doi.org/10.1016/S0899-5362(97)00040-7.
Klemme, S., Prowatke, S., Hametner, K., Günther, D., 2005. Partitioning of trace elements between rutile and silicate melts: implications for subduction zones. Geochimica et Cosmochimica Acta 69, 2361–2371.
Koffi, A.Y., Thébaud, N., Kouamélan, A.N., Baratoux, L., Bruguier, O., Vanderhaeghe, O., Pitra, P., Kemp, A.I.S., Evans, N.J., 2022. Archean to Paleoproterozoic crustal evolution in the Sassandra-Cavally domain (Côte d'Ivoire, West Africa): Insights from Hf and U-Pb zircon analyses. Precambrian Research 382, 106875. https://doi.org/10.1016/j.precamres.2022.106875.
Koffi, A.Y., Baratoux, L., Pitra, P., Kouamélan, A.N., Vanderhaeghe, O., Thébaud, N., Bruguier, O., Block, S., Fossou Kouadio, H.-J.-L., Kone, J., 2023. A tectonic model for the juxtaposition of granulite- and amphibolite-facies rocks in the Eburnean orogenic

belt (Sassandra-Cavally domain, Côte d'Ivoire). Bulletin De La Société Géologique De France 194, 11. https://doi.org/10.1051/bsgf/2023007.
Koffi, G.-R.-S., Kouamélan, A.N., Allialy, M.E., Coulibaly, Y., Peucat, J.-J., 2020. Re-evaluation of Leonian and Liberian events in the geodynamical evolution of the Man-Leo Shield (West African Craton). Precambrian Research 338, 105582. https://doi.org/10.1016/j.precamres.2019.105582.
Koné, J., 2020. Structure et métamorphisme de la ceinture eburnéenne au Sénegal oriental. Signification en termes du contexte tectonique et de l'évolution thermomécanique de la croûte eburnéenne (Unpublished. University of Toulouse III, UCAD, Toulouse, France, Dakar, Senegal. PhD thesis.
Korenaga, J., 2018. Crustal evolution and mantle dynamics through Earth history. Philosophical Transactions of the Royal Society a: Mathematical, Physical and Engineering Sciences 376, 20170408.
Kouamélan, A.N., Delor, C., Peucat, J.-J., 1997. Geochronological evidence for reworking of Archean terrains during the Early Proterozoic (2.1 Ga) in the western Cote d'Ivoire (Man Rise-West African Craton). Precambrian Research 86, 177–199. https://doi.org/10.1016/S0301-9268(97)00043-0.
Kouamélan, A.N., Djro, S.C., Allialy, M.E., Paquette, J.-L., Peucat, J.-J., 2015. The oldest rock of Ivory Coast. Journal of African Earth Sciences 103, 65–70. https://doi.org/10.1016/j.jafrearsci.2014.12.004.
Kouamélan, A.N., Kra, K.S.A., Djro, S.C., Paquette, J.-L., Peucat, J.-J., 2018. The Logoualé band: a large Archean crustal block in the Kenema-Man domain (Man-Leo rise, West African craton) remobilized during Eburnean orogeny (2.05 Ga). Journal of African Earth Sciences 148, 6–13.
Kouyaté, D., Söderlund, U., Youbi, N., Ernst, R., Hafid, A., Ikenne, M., Soulaimani, A., Bertrand, H., El Janati, M., R'kha Chaham, K., 2013. U–Pb baddeleyite and zircon ages of 2040 Ma, 1650 Ma and 885 Ma on dolerites in the West African Craton (Anti-Atlas inliers): Possible links to break-up of Precambrian supercontinents. Lithos 174, 71–84. https://doi.org/10.1016/j.lithos.2012.04.028.
Kroonenberg, S., Ramlal, S., Tjin-Asjoe, X., Mason, P., Kamo, S., Denyszyn, S., Ernst, R., Ibáñez-Mejía, M.. 2022. The 1.98 Ga Goboy dolerite: a new dyke swarm in northern Suriname. 82-85. In Jessell, 2022, The 12th Inter-Guiana Geological Conference Extended Abstract Volume. 161pp. http://www.tectonique.net/saxi/wp-content/uploads/2023/02/IGGC12_Abstract_Volume_final_.pdf.
Kusky, T.M., Polat, A., Windley, B.F., Burke, K.C., Dewey, J.F., Kidd, W.S.F., Maruyama, S., Wang, J.P., Deng, H., Wang, Z.S., 2016. Insights into the tectonic evolution of the North China Craton through comparative tectonic analysis: A record of outward growth of Precambrian continents. Earth-Science Reviews 162, 387–432.
Labou, I., Benoit, M., Baratoux, L., Grégoire, M., Ndiaye, P.M., Thebaud, N., Béziat, D., Debat, P., 2020. Petrological and geochemical study of Birimian ultramafic rocks within the West African Craton: Insights from Mako (Senegal) and Loraboué (Burkina Faso) lherzolite/harzburgite/wehrlite associations. Journal of African Earth Sciences 162, 103677. https://doi.org/10.1016/j.jafrearsci.2019.103677.
Lahondère, D., Thiéblemont, D., Tegyey, M., Guerrot, C., Diabate, B., 2002. First evidence of early Birimian (2.21 Ga) volcanic activity in Upper Guinea: the volcanics and associated rocks of the Niani suite. Journal of African Earth Sciences 35, 417–431. https://doi.org/10.1016/S0899-5362(02)00145-8.
Lambert-Smith, J.S., Lawrence, D.M., Müller, W., Treloar, P.J., 2016a. Palaeotectonic setting of the south-eastern Kédougou-Kénièba Inlier, West Africa: New insights from igneous trace element geochemistry and U-Pb zircon ages. Precambrian Research 274, 110–135. https://doi.org/10.1016/j.precamres.2015.10.013.
Lawrence, D.M., Treloar, P.J., Rankin, A.H., Boyce, A., Harbidge, P., 2013a. A fluid inclusion and stable isotope study at the Loulo mining district, Mali, West Africa: Implications for multifluid sources in the generation of orogenic gold deposits. Economic Geology 108, 229–257.
Lawrence, D.M., Treloar, P.J., Rankin, A.H., Harbidge, P., Holliday, J., 2013b. The geology and mineralogy of the Loulo mining district, Mali, West Africa: Evidence for two distinct styles of orogenic gold mineralization. Economic Geology 108, 199–227.
Lawrence, D.M., Allibone, A.H., Chang, Z., Meffre, S., Lambert-Smith, J.S., Treloar, P.J., 2017. The Tongon Au Deposit, Northern Côte d'Ivoire: An Example of Paleoproterozoic Au Skarn Mineralization. Economic Geology 112, 1571–1593. https://doi.org/10.5382/econgeo.2017.4522.
Le Métour, J., Chevremont, P., Donzeau, M.E., Thiéblemont, E., Tegey, D., Guerrot, M.C. M., Itard, B., Castaing, Y., Delpont, C., Ki, G., Zunino, J.C.C., 2003. Notice explicative de la carte géologique du Burkina Faso à 1:200 000, feuille Houndé.
Le Mignot, E., Reisberg, L., André-Mayer, A.-S., Bourassa, Y., Fontaine, A., Miller, J., 2017a. Re-Os Geochronological Evidence for Multiple Paleoproterozoic Gold Events at the Scale of the West African Craton. Economic Geology 112, 145–168. https://doi.org/10.2113/econgeo.112.1.145.
Le Mignot, E., Siebenaller, L., Béziat, D., André-Mayer, A.-S., Reisberg, L., Salvi, S., Velasquez, G., Zimmermann, C., Naré, A., Franceschi, G., 2017b. The paleoproterozoic copper-gold deposits of the Gaoua District, Burkina Faso: superposition of orogenic gold on a porphyry copper occurrence? Economic Geology 112, 99–122. https://doi.org/10.2113/econgeo.112.1.99.
Lebrun, E., Thébaud, N., Miller, J., Ulrich, S., Bourget, J., Terblanche, O., 2016. Geochronology and lithostratigraphy of the Siguiri district: Implications for gold mineralisation in the Siguiri Basin (Guinea, West Africa). Precambrian Research 274, 136–160. https://doi.org/10.1016/j.precamres.2015.10.011.
Ledru, P., Johan, V., Milési, J.P., Tegyey, M., 1994. Markers of the last stages of the Palaeoproterozoic collision: evidence for a 2 Ga continent involving circum-South Atlantic provinces. Precambrian Research 69, 169–191. https://doi.org/10.1016/0301-9268(94)90085-X.
Léger, J.-M., Liégeois, J.-P., Pouclet, A., Vicat, J.-P., 1992. Occurrence of syntectonic alkali pyroxene-bearing granites of Eburnean Age (2.1 Ga) in Western Niger. Réunion Annuelle Des Sciences De La Terre.
Lenardic, A., 2018. The diversity of tectonic modes and thoughts about transitions between them. Philosophical Transactions of the Royal Society a: Mathematical, Physical and Engineering Sciences 376, 20170416.
Lerouge, C., Feybesse, J.L., Guerrot, C., Billa, M., Diaby, S., 2004. Reaction textures in Proterozoic calcsilicates from northern Guinea: a record of the fluid evolution. Journal of African Earth Sciences 39, 105–113. https://doi.org/10.1016/j.jafrearsci.2004.07.058.
Leube, A., Hirdes, W., Mauer, R., Kesse, G.O., 1990. The early Proterozoic Birimian Supergroup of Ghana and some aspects of its associated gold mineralization. Precambrian Research 46, 139–165.
Li, C., Arndt, N.T., Tang, Q., Ripley, E.M., 2015. Trace element indiscrimination diagrams. Lithos 232, 76–83. https://doi.org/10.1016/j.lithos.2015.06.022.
Li, Z.-X., Liu, Y., Ernst, R., 2023. A dynamic 2000—540 Ma Earth history: From cratonic amalgamation to the age of supercontinent cycle. Earth-Science Reviews 238, 104336. https://doi.org/10.1016/j.earscirev.2023.104336.
Liégeois, J.-P., De Waele, B., 2005. Datation géochronologique de deux échantillons de roches prélevés sur le territoire des feuilles de Tienko et de Tingréla. Projet de cartographie du Birimien malien, BRGM, 6p.
Liou, J.G., Zhang, R.Y., Ernst, W.G., Rumble, D., Maruyama, S., 1998. High pressure minerals from deeply subducted metamorphic rocks, in: Hemley, R.J. (Ed.), Ultrahigh Pressure Mineralogy. De Gruyter, pp. 33–96. DOI: 10.1515/9781501509179-004.
Liu, H., Sun, W., Zartman, R., Tang, M., 2019. Continuous plate subduction marked by the rise of alkali magmatism 2.1 billion years ago. Nature Communications 10, 3408.
Loh, G., Hirdes, W., 1999. Explanatory notes for the geological map of southwest Ghana 1: 100 000 sheets Axim (0403B) and Sekondi (0402A). Ghana Geological Survey Bulletin 49–63.
Lompo, M., 2009. Geodynamic evolution of the 2.25-2.0 Ga Palaeoproterozoic magmatic rocks in the Man-Leo Shield of the West African Craton. A model of subsidence of an oceanic plateau. Geological Society, London, Special Publications 323, 231–254. https://doi.org/10.1144/SP323.11.
Lompo, M., 2010. Paleoproterozoic structural evolution of the Man-Leo Shield (West Africa). Key structures for vertical to transcurrent tectonics. Journal of African Earth Sciences 58, 19–36. https://doi.org/10.1016/j.jafrearsci.2010.01.005.
Lüdtke, G., Hirdes, W., Konan, G., Kone, Y., Yao, C., Diarra, S., Zamble, Z., de la Géologie, D., 1999. Géologie de la Région Haute Comoe Nord= Geology of the-Haute Comoe North Area. Avec Carte Geologique 1/100000=-with geological map 1: 100000.
Markwitz, V., Hein, K.A.A., Miller, J., 2016. Compilation of West African mineral deposits: Spatial distribution and mineral endowment. Precambrian Research 274, 61–81. https://doi.org/10.1016/j.precamres.2015.05.028.
Masurel, Q., Thébaud, N., Miller, J., Ulrich, S., 2017a. The tectono-magmatic framework to gold mineralisation in the Sadiola-Yatela gold camp and implications for the paleotectonic setting of the Kédougou-Kénieba inlier, West Africa. Precambrian Research 292, 35–56. https://doi.org/10.1016/j.precamres.2017.01.017.
Masurel, Q., Thébaud, N., Allibone, A., André-Mayer, A.-S., Hein, K.A.A., Reisberg, L., Bruguier, O., Eglinger, A., Miller, J., 2019. Intrusion-related affinity and orogenic gold overprint at the Paleoproterozoic Bonikro Au–(Mo) deposit (Côte d'Ivoire, West African Craton). Mineralium Deposita 1–24. https://doi.org/10.1007/s00126-019-00888-2.
Masurel, Q., Eglinger, A., Thébaud, N., Allibone, A., André-Mayer, A.-S., McFarlane, H., Miller, J., Jessell, M., Aillères, L., Vanderhaeghe, O., Salvi, S., Baratoux, L., Perrouty, S., Begg, G., Fougerouse, D., Hayman, P., Wane, O., Tschibududze, A., Parra-Avila, L., Kouamelan, A., Amponsah, P.O., 2022. Gold metallogeny of the West African Craton: capturing pulses within a Paleoproterozoic orogenic cycle. Mineralium Deposita. https://doi.org/10.1007/s00126-021-01052-5.
McCuaig, T.C., Fougerouse, D., Salvi, S., Siebenaller, L., Parra-Avila, L.A., Seed, R., Béziat, D., André-Mayer, A.-S., 2016. The Inata deposit, Belahouro District, northern Burkina Faso. Ore Geology Reviews 78, 639–644. https://doi.org/10.1016/j.oregeorev.2015.11.014.
McFarlane, H.B., 2018. The geodynamic and tectonic evolution of the Palaeoproterozoic Sefwi Greenstone Belt, West African Craton (Unpublished. Monash University, University of Toulouse III, Melbourne, Australia, Toulouse, France. PhD thesis.
McFarlane, H.B., Ailleres, L., Betts, P., Ganne, J., Baratoux, L., Jessell, M.W., Block, S., 2019. Episodic collisional orogenesis and lower crust exhumation during the Palaeoproterozoic Eburnean Orogeny: Evidence from the Sefwi Greenstone Belt, West African Craton. Precambrian Research 325, 88–110. https://doi.org/10.1016/j.precamres.2019.02.012.
McFarlane, C.R.M., Mavrogenes, J., Lentz, D., King, K., Allibone, A., Holcombe, R., 2011. Geology and intrusion-related affinity of the morila gold mine, Southeast Mali. Economic Geology 106, 727–750. https://doi.org/10.2113/econgeo.106.5.727.
Meert, J.G., Santosh, M., 2017. The Columbia supercontinent revisited. Gondwana Research 50, 67–83. https://doi.org/10.1016/j.gr.2017.04.011.
Melcher, F., Graupner, T., Henjes-Kunst, F., Oberthür, T., Sitnikova, M., Gäbler, E., Gerdes, A., Brätz, H., Davis, D., Dewaele, S., 2008. Analytical Fingerprint of Columbite-Tantalite (Coltan) Mineralisation in Pegmatites – Focus on Africa. Presented at the Ninth International Congress for Applied Mineralogy, Brisbane, Australia.
Melcher, F., Graupner, T., Gäbler, H.-E., Sitnikova, M., Henjes-Kunst, F., Oberthür, T., Gerdes, A., Dewaele, S., 2015. Tantalum–(niobium–tin) mineralisation in African pegmatites and rare metal granites: Constraints from Ta–Nb oxide mineralogy, geochemistry and U–Pb geochronology. Ore Geology Reviews 64, 667–719. https://doi.org/10.1016/j.oregeorev.2013.09.003.
Mériaud, N., Thébaud, N., Masurel, Q., Hayman, P., Jessell, M., Kemp, A., Evans, N.J., Fisher, C.M., Scott, P.M., 2020. Lithostratigraphic evolution of the Bandamian Volcanic Cycle in central Côte d'Ivoire: Insights into the late Eburnean magmatic

resurgence and its geodynamic implications. Precambrian Research 347, 105847. https://doi.org/10.1016/j.precamres.2020.105847.
Milési, J.P., Frizon de Lamotte, D., De Kock, F., Toteu, F., 2010. Tectonic Map of Africa at 1:10,000,000 scale. Commission for the Geological Map of the World.
Milési, J.-P., Ledru, P., Feybesse, J.-L., Dommanget, A., Marcoux, E., 1992. Early proterozoic ore deposits and tectonics of the Birimian orogenic belt, West Africa. Precambrian Research 58, 305–344. https://doi.org/10.1016/0301-9268(92)90123-6.
Mitchell, R.N., Bleeker, W., Van Breemen, O., Lecheminant, T.N., Peng, P., Nilsson, M.K., Evans, D.A., 2014. Plate tectonics before 2.0 Ga: Evidence from paleomagnetism of cratons within supercontinent Nuna. American Journal of Science 314, 878–894.
Mole, D.R., Thurston, P.C., Marsh, J.H., Stern, R.A., Ayer, J.A., Martin, L.A.J., Lu, Y.J., 2021. The formation of Neoarchean continental crust in the south-east Superior Craton by two distinct geodynamic processes. Precambrian Research 356, 106104.
Moyen, J.-F., Laurent, O., 2018. Archaean tectonic systems: A view from igneous rocks. Lithos 302, 99–125.
Moyen, J.-F., Martin, H., 2012. Forty years of TTG research. Lithos 148, 312–336. https://doi.org/10.1016/j.lithos.2012.06.010.
Moyen, J.-F., Laurent, O., Chelle-Michou, C., Couzinié, S., Vanderhaeghe, O., Zeh, A., Villaros, A., Gardien, V., 2017. Collision vs. subduction-related magmatism: Two contrasting ways of granite formation and implications for crustal growth. Lithos 277, 154–177.
Mumin, A.H., Fleet, M.E., Longstaffe, F.J., 1996. Evolution of hydrothermal fluids in the Ashanti gold belt, Ghana; stable isotope geochemistry of carbonates, graphite, and quartz. Economic Geology 91, 135–148. https://doi.org/10.2113/gsecongeo.91.1.135.
Naba, S., Lompo, M., Debat, P., Bouchez, J.L., Béziat, D., 2004. Structure and emplacement model for late-orogenic Paleoproterozoic granitoids: the Tenkodogo–Yamba elongate pluton (Eastern Burkina Faso). Journal of African Earth Sciences 38, 41–57.
Nebel, O., Capitanio, F.A., Moyen, J.-F., Weinberg, R.F., Clos, F., Nebel-Jacobsen, Y.J., Cawood, P.A., 2018. When crust comes of age: on the chemical evolution of Archaean, felsic continental crust by crustal drip tectonics. Philosophical Transactions of the Royal Society a: Mathematical, Physical and Engineering Sciences 376, 20180103.
Neto, J.M.M., Lafon, J.-M., 2020. Crustal growth and reworking of Archean crust within the Rhyacian domains of the southeastern Guiana Shield, Brazil: Evidence from zircon U–Pb–Hf and whole-rock Sm–Nd geochronology. Journal of South American Earth Sciences 103, 102740.
Ngom, P.M., Cordani, U.G., Teixeira, W., de Janasi, V., A.,, 2010. Sr and Nd isotopic geochemistry of the early ultramafic–mafic rocks of the Mako bimodal volcanic belt of the Kedougou–Kenieba inlier (Senegal). Arabian Journal of Geosciences 3, 49–57.
Nomade, S., Chen, Y., Pouclet, A., Féraud, G., Théveniaut, H., Daouda, B.Y., Vidal, M., Rigolet, C., 2003. The Guiana and the West African Shield Palaeoproterozoic grouping: new palaeomagnetic data for French Guiana and the Ivory Coast. Geophysical Journal International 154, 677–694. https://doi.org/10.1046/j.1365-246X.2003.01972.x.
Nunoo, S., Hofmann, A., Kramers, J., 2022. Geology, zircon U–Pb dating and εHf data for the Julie greenstone belt and associated rocks in NW Ghana: Implications for Birimian-to-Tarkwaian correlation and crustal evolution. Journal of African Earth Sciences 186, 104444.
Oberthür, T., Mumm, A.S., Vetter, U., Simon, K., Amanor, J.A., 1996. Gold mineralization in the Ashanti Belt of Ghana; genetic constraints of the stable isotope geochemistry. Economic Geology 91, 289–301. https://doi.org/10.2113/gsecongeo.91.2.289.
Oberthür, T., Vetter, U., Davis, W.D., Amanor, J.A., 1998. Age constraints on gold mineralization and Paleoproterozoic crustal evolution in the Ashanti belt of southern Ghana. Precambrian Research 89, 129–143. https://doi.org/10.1016/S0301-9268(97)00075-2.
Oliver, N.H.S., Allibone, A., Nugus, M.J., Vargas, C., Jongens, R., Peattie, R., Chamberlain, V.A., 2020. Chapter 6: The Supergiant, High-Grade, Paleoproterozoic Metasedimentary Rock- and Shear Vein-Hosted Obuasi (Ashanti) Gold Deposit, Ghana, West Africa, in: Geology of the World's Major Gold Deposits and Provinces. Society of Economic Geologists, pp. 121–140. DOI: 10.5382/SP.23.06.
Opare-Addo, E., Browning, P., John, B.E., 1993. Pressure-temperature constraints on the evolution of an Early proterozoic plutonic suite in southern Ghana, West Africa. Journal of African Earth Sciences (and the Middle East) 17, 13–22. https://doi.org/10.1016/0899-5362(93)90018-L.
Palin, R.M., Santosh, M., Cao, W., Li, S.-S., Hernández-Uribe, D., Parsons, A., 2020. Secular change and the onset of plate tectonics on Earth. Earth-Science Reviews 207, 103172. https://doi.org/10.1016/j.earscirev.2020.103172.
Parra-Avila, L.A., Bourassa, Y., Miller, J., Perrouty, S., Fiorentini, M.L., Campbell McCuaig, T., 2015. Age constraints of the Wassa and Benso mesothermal gold deposits, Ashanti Belt, Ghana, West Africa. Journal of African Earth Sciences 112, 524–535. https://doi.org/10.1016/j.jafrearsci.2015.05.017.
Parra-Avila, L.A., Kemp, A.I.S., Fiorentini, M.L., Belousova, E., Baratoux, L., Block, S., Jessell, M., Bruguier, O., Begg, G.C., Miller, J., Davis, J., McCuaig, T.C., 2017. The geochronological evolution of the Paleoproterozoic Baoulé-Mossi domain of the Southern West African Craton. Precambrian Research 300, 1–27. https://doi.org/10.1016/j.precamres.2017.07.036.
Parra-Avila, L.A., Belousova, E., Fiorentini, M.L., Eglinger, A., Block, S., Miller, J., 2018. Zircon Hf and O-isotope constraints on the evolution of the Paleoproterozoic Baoulé-Mossi domain of the southern West African Craton. Precambrian Research 306, 174–188. https://doi.org/10.1016/j.precamres.2017.12.044.
Parra-Avila, L.A., Baratoux, L., Eglinger, A., Fiorentini, M.L., Block, S., 2019. The Eburnean magmatic evolution across the Baoulé-Mossi domain: Geodynamic implications for the West African Craton. Precambrian Research 332, 105392.
Pawlig, S., Gueye, M., Klischies, R., Schwarz, S., Wemmer, K., Siegesmund, S., 2006. Geochemical and Sr-Nd isotopic data on the Birimian of the Kedougou-Kenieba inlier (eastern Senegal): Implications on the Palaeoproterozoic evolution of the West African craton. South African Journal of Geology 109, 411–427.
Perchuk, A.L., Zakharov, V.S., Gerya, T.V., Brown, M., 2019. Hotter mantle but colder subduction in the Precambrian: What are the implications? Precambrian Research 330, 20–34. https://doi.org/10.1016/j.precamres.2019.04.023.
Perrouty, S., Aillères, L., Jessell, M.W., Baratoux, L., Bourassa, Y., Crawford, B., 2012. Revised Eburnean geodynamic evolution of the gold-rich southern Ashanti Belt, Ghana, with new field and geophysical evidence of pre-Tarkwaian deformations. Precambrian Research 204–205, 12–39. https://doi.org/10.1016/j.precamres.2012.01.003.
Petersson, A., Scherstén, A., Kemp, A.I.S., Kristinsdóttir, B., Kalvig, P., Anum, S., 2016. Zircon U–Pb–Hf evidence for subduction related crustal growth and reworking of Archaean crust within the Palaeoproterozoic Birimian terrane, West African Craton, SE Ghana. Precambrian Research 275, 286–309. https://doi.org/10.1016/j.precamres.2016.01.006.
Petersson, A., Scherstén, A., Gerdes, A., 2018. Extensive reworking of Archaean crust within the Birimian terrane in Ghana as revealed by combined zircon U-Pb and Lu-Hf isotopes. Geoscience Frontiers, Lid Tectonics 9, 173–189. https://doi.org/10.1016/j.gsf.2017.02.006.
Pigois, J.-P., Groves, D.I., Fletcher, I.R., McNaughton, N.J., Snee, L.W., 2003. Age constraints on Tarkwaian palaeoplacer and lode-gold formation in the Tarkwa-Damang district, SW Ghana. Miner Deposita 38, 695–714. https://doi.org/10.1007/s00126-003-0360-5.
Pinto, J.A.E., Lafon, J.M., Neto, J.M.M., 2024. Neoarchean magmatism and Rhyacian reworking in the northeast of the Amapá Block, southeastern Guiana Shield, Brazil: Geochemistry, U–Pb geochronology, and Hf–Nd isotopes. Journal of South American Earth Sciences 138, 104859.
Pitra, P., Kouamélan, A.N., Ballèvre, M., Peucat, J.-J., 2010. Palaeoproterozoic high-pressure granulite overprint of the Archean continental crust: evidence for homogeneous crustal thickening (Man Rise, Ivory Coast). Journal of Metamorphic Geology 28, 41–58. https://doi.org/10.1111/j.1525-1314.2009.00852.x.
Pouclet, A., Doumbia, S., Vidal, M., 2006. Geodynamic setting of the Birimian volcanism in central Ivory Coast (western Africa) and its place in the Palaeoproterozoic evolution of the Man Shield. Bulletin De La Société Géologique De France 177, 105–121. https://doi.org/10.2113/gssgfbull.177.2.105.
Ribeiro, B.V., Cawood, P.A., Faleiros, F.M., Mulder, J.A., Martin, E., Finch, M.A., Raveggi, M., Teixeira, W., Cordani, U.G., Pavan, M., 2020. A long-lived active margin revealed by zircon U–Pb–Hf data from the Rio Apa Terrane (Brazil): New insights into the Paleoproterozoic evolution of the Amazonian Craton. Precambrian Research 350, 105919. https://doi.org/10.1016/j.precamres.2020.105919.
Richards, J.P., 2009. Postsubduction porphyry Cu-Au and epithermal Au deposits: Products of remelting of subduction-modified lithosphere. Geology 37, 247–250.
Roberts, N.M., Spencer, C.J., 2015. The zircon archive of continent formation through time. The Geological Society of London, London.
Rollinson, H., 2016. Archaean crustal evolution in West Africa: A new synthesis of the Archaean geology in Sierra Leone, Liberia, Guinea and Ivory Coast. Precambrian Research 281, 1–12. https://doi.org/10.1016/j.precamres.2016.05.005.
Sakyi, P.A., Su, B.-X., Manu, J., Kwayisi, D., Anani, C.Y., Alemayehu, M., Malaviarachchi, S.P., Nude, P.M., Su, B.-C., 2020. Origin and tectonic significance of the metavolcanic rocks and mafic enclaves from the Palaeoproterozoic Birimian Terrane, SE West African Craton, Ghana. Geological Magazine 157, 1349–1366.
Salah, I.A., Liegeois, J.-P., Pouclet, A., 1996. Evolution d'un arc insulaire océanique birimien précoce au Liptako nigérien (Sirba): géologie, géochronologie et géochimie. Journal of African Earth Sciences 22, 235–254. https://doi.org/10.1016/0899-5362(96)00016-4.
Sanogo, S., 2022. Pegmatites lithinifères (Li-Cs-Ta) et roches plutoniques de Bougouni (Sud du Mali, Craton Ouest Africain) : approches pétrographiques, structurales, géochimiques et géochronologiques (PhD Thesis).
Schwartz, M.O., Melcher, F., 2004. The Falémé iron district, Senegal. Economic Geology 99, 917–939.
Senyah, G.A.A., 2021. Volcanic architecture of the Houndé and Boromo greenstone belts: Implications for Terrane Evolution. Queensland University of Technology, West-Africa.
Shields, G.A., Strachan, R.A., Porter, S.M., Halverson, G.P., Macdonald, F.A., Plumb, K.A., De Alvarenga, C.J., Banerjee, D.M., Bekker, A., Bleeker, W., 2022. A template for an improved rock-based subdivision of the pre-Cryogenian timescale. Journal of the Geological Society. The Geological Society of London.
Siegfried, P., Aggenbach, A., Clarke, B., Delor, C., Roig, J.F., 2009. Geological Map Explanation, Map Sheet 0903D (1:100 000). CGS/BRGM/Geoman.
Sizova, E., Gerya, T., Brown, M., Perchuk, L.L., 2010. Subduction styles in the Precambrian: Insight from numerical experiments. Lithos 116, 209–229. https://doi.org/10.1016/j.lithos.2009.05.028.
Soumaila, A., Garba, Z., 2006. Le métamorphisme des formations de la ceinture de roches vertes birimienne (paléoprotérozoïque) de Diagorou-Darbani (Liptako, Niger, Afrique de l'Ouest). Africa Geoscience Review 13, 107–128.
Soumaila, A., Henry, P., Garba, Z., Rossi, M., 2008. REE patterns, Nd-Sm and U-Pb ages of the metamorphic rocks of the Diagorou-Darbani greenstone belt (Liptako, SW Niger): implication for Birimian (Palaeoproterozoic) crustal genesis. Geological Society, London, Special Publications 297, 19–32. https://doi.org/10.1144/SP297.2.

Spencer, C.J., Partin, C.A., Kirkland, C.L., Raub, T.D., Liebmann, J., Stern, R.A., 2019. Paleoproterozoic increase in zircon δ18O driven by rapid emergence of continental crust. Geochimica et Cosmochimica Acta 257, 16–25.
Spencer, C.J., Mitchell, R.N., Brown, M., 2021. Enigmatic mid-proterozoic orogens: hot, thin, and low. Geophysical Research Letters 48, e2021GL093312. https://doi.org/10.1029/2021GL093312.
Stern, R.J., 2023. The Orosirian (1800–2050 Ma) plate tectonic episode: Key for reconstructing the Proterozoic tectonic record. Geoscience Frontiers 14, 101553. https://doi.org/10.1016/j.gsf.2023.101553.
Tapsoba, B., Lo, C.-H., Jahn, B.-M., Chung, S.-L., Wenmenga, U., Iizuka, Y., 2013. Chemical and Sr–Nd isotopic compositions and zircon U–Pb ages of the Birimian granitoids from NE Burkina Faso, West African Craton: Implications on the geodynamic setting and crustal evolution. Precambrian Research 224, 364–396. https://doi.org/10.1016/j.precamres.2012.09.013.
Tedeschi, M.T., Hagemann, S.G., Kemp, A.I.S., Kirkland, C.L., Ireland, T.R., 2020. Geochronological constrains on the timing of magmatism, deformation and mineralization at the Karouni orogenic gold deposit: Guyana, South America. Precambrian Research 337, 105329. https://doi.org/10.1016/j.precamres.2019.04.015.
Terentiev, R.A., Santosh, M., 2020. Baltica (East European Craton) and Atlantica (Amazonian and West African Cratons) in the Proterozoic: The pre-Columbia connection. Earth-Science Reviews 210, 103378.
Thébaud, N., Allibone, A., Masurel, Q., Eglinger, A., Davis, J., André-Mayer, A.-S., Miller, J., François Ouedrago, M., Jessell, M., 2020. The Paleoproterozoic (Rhyacian) Gold Deposits of West Africa, in: Geology of the World's Major Gold Deposits and Provinces. Society of Economic Geologists, pp. 735–752. DOI: 10.5382/SP.23.34.
Thiéblemont, D., 1989. Géochimie des Chaînons Volcaniques de Niandian et Kéniéro (Birimien de Guinée) Comparaison avec le Magmatisme Birimien de Côte d'Ivoire et du Sénégal. Implications Géodynamiques. Notes BRGM DAM/DEX No, MII.
Thiéblemont, D., Goujou, J.C., Egal, E., Cocherie, A., Delor, C., Lafon, J.M., Fanning, C. M., 2004. Archean evolution of the Leo Rise and its Eburnean reworking. Journal of African Earth Sciences 39, 97–104.
Traoré, K., Chardon, D., Naba, S., Wane, O., Bouaré, M.L., 2022. Paleoproterozoic collision tectonics in West Africa: Insights into the geodynamics of continental growth. Precambrian Research 376, 106692. https://doi.org/10.1016/j.precamres.2022.106692.
Treloar, P.J., Lawrence, D.M., Senghor, D., Boyce, A., Harbidge, P., 2015. The Massawa gold deposit, Eastern Senegal, West Africa: an orogenic gold deposit sourced from magmatically derived fluids? SP 393, 135–160. https://doi.org/10.1144/SP393.12.
Triboulet, C., Feybesse, J.-L., 1998. Les métabasites birimiennes et archéennes de la région de Toulepleu-Ity (Côte-d'lvoire): des roches portées à 8 kbar (≈ 24 km) et 14 kbar (≈ 42 km) au Paléoprotérozoïque. Comptes Rendus De L'académie Des Sciences - Series IIA - Earth and Planetary Science 327, 61–66. https://doi.org/10.1016/S1251-8050(98)80019-0.
Tshibubudze, A., Hein, K.A.A., Peters, L.F.H., Woolfe, A.J., McCuaig, T.C., 2013. Oldest U-Pb crystallisation age for the West African Craton From the Oudalan-Gorouol Belt of Burkina Faso. South African Journal of Geology 116, 169–181.
Tshibubudze, A., Hein, K.A.A., McCuaig, T.C., 2015. The relative and absolute chronology of strato-tectonic events in the Gorom-Gorom granitoid terrane and Oudalan-Gorouol belt, northeast Burkina Faso. Journal of African Earth Sciences, Tectonics, Mineralisation and Regolith Evolution of the West African Craton 112, 382–418. https://doi.org/10.1016/j.jafrearsci.2015.04.008.
Vanderhaeghe, O., Ledru, P., Thiéblemont, D., Egal, E., Cocherie, A., Tegyey, M., Milési, J.-P., 1998. Contrasting mechanism of crustal growth: geodynamic evolution of the Paleoproterozoic granite–greenstone belts of French Guiana. Precambrian Research 92, 165–193.
Vanin, D., Michaud, M., Thalenhorst, H., Reipas, K., 2004. Taparko-Bouroum Project, Burkina Faso. Unpublished. Technical Report 43–101.
Vegas, N., Naba, S., Bouchez, J.L., Jessell, M., 2008. Structure and emplacement of granite plutons in the Paleoproterozoic crust of Eastern Burkina Faso: rheological implications. International Journal of Earth Sciences 97, 1165–1180.
Vianna, S.Q., Lafon, J.M., Neto, J.M.M., Silva, D.P.B., de Mesquita Barros, C.E., 2020. U–Pb geochronology, Nd–Hf isotopes, and geochemistry of Rhyacian granitoids from the Paleoproterozoic Lourenço domain (Brazil), southeastern Guiana Shield. Journal of South American Earth Sciences 104, 102937.
Vidal, M., Gumiaux, C., Cagnard, F., Pouclet, A., Ouattara, G., Pichon, M., 2009. Evolution of a Paleoproterozoic weak type orogeny in the West African Craton (Ivory Coast). Tectonophysics 477, 145–159.
Walsh, G.J., Aleinikoff, J.N., Benziane, F., Yazidi, A., Armstrong, T.R., 2002. U–Pb zircon geochronology of the Paleoproterozoic Tagragra de Tata inlier and its Neoproterozoic cover, western Anti-Atlas, Morocco. Precambrian Research 117, 1–20. https://doi.org/10.1016/S0301-9268(02)00044-X.
Wane, O., Liégeois, J.-P., Thébaud, N., Miller, J., Metelka, V., Jessell, M., 2018. The onset of the Eburnean collision with the Kenema-Man craton evidenced by plutonic and volcanosedimentary rock record of the Masssigui region, southern Mali. Precambrian Research 305, 444–478. https://doi.org/10.1016/j.precamres.2017.11.008.
White, A.J., 2011. The nature and origin of gold mineralization at Damang mine. University of Oxford, Ghana.
White, A.J.R., Waters, D.J., Robb, L.J., 2013. The application of P–T–X(CO2) modelling in constraining metamorphism and hydrothermal alteration at the Damang gold deposit, Ghana. Journal Metamorphic Geology 31, 937–961. https://doi.org/10.1111/jmg.12051.
Wilde, A., Otto, A., McCracken, S., 2021. Geology of the Goulamina spodumene pegmatite field. Mali. Ore Geology Reviews 134, 104162.
Wille, S.E., Klemd, R., 2004. Fluid inclusion studies of the Abawso gold prospect, near the Ashanti Belt, Ghana. Mineralium Deposita 39, 31–45. https://doi.org/10.1007/s00126-003-0380-1.
Williams, H.R., 1988. The archaean kasila group of Western Sierra Leone: Geology and relations with adjacent granite-greenstone terrane. Precambrian Research 38, 201–213. https://doi.org/10.1016/0301-9268(88)90002-2.
Xu, C., Kynický, J., Song, W., Tao, R., Lü, Z., Li, Y., Yang, Y., Pohanka, M., Galiova, M.V., Zhang, L., 2018. Cold deep subduction recorded by remnants of a Paleoproterozoic carbonated slab. Nature Communications 9, 2790.
Yang, Q., Santosh, M., Shen, J., Li, S., 2014. Juvenile vs. recycled crust in NE China: Zircon U–Pb geochronology, Hf isotope and an integrated model for Mesozoic gold mineralization in the Jiaodong Peninsula. Gondwana Research 25, 1445–1468. https://doi.org/10.1016/j.gr.2013.06.003.
Yao, Y., Murphy, P.J., Robb, L.J., 2001. Fluid Characteristics of Granitoid-Hosted Gold Deposits in the Birimian Terrane of Ghana: A Fluid Inclusion Microthermometric and Raman Spectroscopic Study. Economic Geology 96, 1611–1643. https://doi.org/10.2113/gsecongeo.96.7.1611.
Zhao, H., Simonetti, A., Simonetti, S., Cao, X., Du, Y., 2024. A Geochemical and Isotopic Investigation of Carbonatites from Huangshuian, Central China: Implications for Petrogenesis and Mantle Sources. Minerals 14, 953.
Zitzmann, A., 1997. Geological, geophysical and geochemical investigations in the Bui belt area in Ghana. Geologisches Jahrbuch Reihe B, Heft.

Further reading

Allibone, A.H., Teasdale, J., Cameron, G., Etheridge, M., Uttley, P., Soboh, A., Appiah-Kubi, J., Adanu, A., Arthur, R., Mamphey, J., Odoom, B., Zuta, J., Tsikata, A., Pataye, F., Famiyeh, S., Lamb, E., 2002. Timing and structural controls on gold mineralization at the bogoso gold mine, Ghana, West Africa. Economic Geology 97, 949–969. https://doi.org/10.2113/gsecongeo.97.5.949.
Allibone, A.H., Hayden, P., Cameron, G., Duku, F., 2004. Paleoproterozoic gold deposits hosted by albite-and carbonate-altered tonalite in the Chirano District, Ghana, West Africa. Economic Geology 99, 479–497.
Allou, A.B., Lu, H.-Z., Guha, J., Carignan, J., Naho, J., Pothin, K., Yobou, R., 2005. Une Corrélation Génétique entre les Roches Granitiques, et les Dépôts Éluvionnaires, Colluvionnaires et Alluvionnaires de Columbo-Tantalite d'Issia, Centre-Ouest de la Côte d'Ivoire. Exploration and Mining Geology 14, 61–77.
AMIRA, 2013. P934A – West African Exploration Initiative – Stage 2 Final report.
Amponsah, P.O., Salvi, S., Béziat, D., Siebenaller, L., Baratoux, L., Jessell, M.W., 2015. Geology and geochemistry of the shear-hosted Julie gold deposit, NW Ghana. Journal of African Earth Sciences 112, 505–523. https://doi.org/10.1016/j.jafrearsci.2015.06.013.
Appiah, H., 1991. Geology and mine exploration trends of Prestea Goldfields, Ghana. Journal of African Earth Sciences (and the Middle East) 13, 235–241.
Augustin, J., Gaboury, D., 2017. Paleoproterozoic plume-related basaltic rocks in the Mana gold district in western Burkina Faso, West Africa: Implications for exploration and the source of gold in orogenic deposits. Journal of African Earth Sciences 129, 17–30. https://doi.org/10.1016/j.jafrearsci.2016.12.007.
Ballo, I., Hein, K.A.A., Guindo, B., Sanogo, L., Ouologuem, Y., Daou, G., Traore, A., 2016. The Syama and Tabakoroni goldfields, Mali. Ore Geology Reviews 78, 578–585. https://doi.org/10.1016/j.oregeorev.2015.10.019.
Billa, M., 1998. Calage des minéralisations aurifères et guides de prospection pour de nouveaux objectifs sur le permis d'exploration Ity (Côte-d'Ivoire) (No. BRGM 2717). BRGM - La Source.
Brownscombe, W., 2009. The Tinga anomaly: A new style of gold mineralization in Ghana? M. Sc. thesis 117.
Dampare, S.B., Nyarko, B.J.B., Osae, S., Akaho, E.H.K., Asiedu, D.K., Serfor-Armah, Y., Nude, P., 2005. Simultaneous determination of tantalum, niobium, thorium and uranium in placer columbite-tantalite deposits from the Akim Oda District of Ghana by epithermal instrumental neutron activation analysis. Journal of Radioanalytical and Nuclear Chemistry 265, 53–59.
Davis, D.W., Hirdes, W., Schaltegger, U., Nunoo, E.A., 1994. U-Pb age constraints on deposition and provenance of Birimian and gold-bearing Tarkwaian sediments in Ghana, West Africa. Precambrian Research 67, 89–107. https://doi.org/10.1016/0301-9268(94)90006-X.
Dia, A., 1988. Caractéres et signification des complexes magmatiques et métamorphiques du secteur de Sandikounda-Laminia (Nord de la boutonnière de Kédougou, Est du Sénégal): un modèle géodynamique du Birimien de l'Afrique de l'Ouest. Ph. D. thesis 350.
Diene, M., Gueye, M., Diallo, D.P., Dia, A., 2012. Structural Evolution of a Precambrian Segment: Example of the Paleoproterozoic Formations of the Mako Belt (Eastern Senegal, West Africa). IJG 03, 153–165. https://doi.org/10.4236/ijg.2012.31017.
Ennih, N., Liégeois, J.P., 2008b. The boundaries of the West African craton, with a special reference to the basement of the Moroccan metacratonic Anti-Atlas belt. In: Ennih, N., Liégeois, J.-P. (Eds.), The Boundaries of the West African Craton. Geological Society, London, Special Publications, 297, pp. 1e17.
Foster, R.P., Piper, D.P., 1993. Archaean lode gold deposits in Africa: crustal setting, metallogenesis and cratonization. Ore Geology Reviews 8, 303–347.
Fougerouse, D., 2011. Le gisement d'or d'Inata (Burkina Faso) Timing de la phase aurifère.
Goldfarb, R.J., Groves, D.I., Gardoll, S., 2001. Orogenic gold and geologic time: a global synthesis. Ore Geology Reviews 18, 1–75.
Griffin, W.L., Wang, X., Jackson, S.E., Pearson, N.J., O'Reilly, S.Y., Xu, X., Zhou, X., 2002. Zircon chemistry and magma mixing, SE China: in-situ analysis of Hf isotopes, Tonglu and Pingtan igneous complexes. Lithos 61, 237–269.

Gueye, M., Ngom, P.M., Diène, M., Thiam, Y., Siegesmund, S., Wemmer, K., Pawlig, S., 2008. Intrusive rocks and tectono-metamorphic evolution of the Mako Paleoproterozoic belt (Eastern Senegal, West Africa). Journal of African Earth Sciences 50, 88–110.

Kaboré, B.E., 2004. Datation d'une rhyolite porphyrique dans le secteur de Tiébélé (Nabenia). Rap BUMIGEB 8.

Kone, J., Vanderhaeghe, O., Diatta, F., Baratoux, L., Thebaud, N., Bruguier, O., Ndiaye, P. M., Duchene, S., Pitra, P., Ganne, J., 2020. Source and deposition age of the Dialé-Daléma metasedimentary series (Kédougou-Kénièba Inlier, Senegal) constrained by U–Pb geochronology on detrital zircon grains. Journal of African Earth Sciences 165, 103801. https://doi.org/10.1016/j.jafrearsci.2020.103801.

Lambert-Smith, J.S., 2014. The geology, structure and metallogenesis of the world class Loulo-Bambadji Au district in Mali and Senegal. Kingston University, West Africa.

Lambert-Smith, J.S., Rocholl, A., Treloar, P.J., Lawrence, D.M., 2016b. Discriminating fluid source regions in orogenic gold deposits using B-isotopes. Geochimica et Cosmochimica Acta 194, 57–76. https://doi.org/10.1016/j.gca.2016.08.025.

Leake, M.H., 1992. The petrogenesis and structural evolution of the early proterozoic Fetekro Greenstone Belt, Dabakala region. University of Portsmouth, NE Cote D'Ivoire.

Lebrun, E., Miller, J., Thébaud, N., Ulrich, S., McCuaig, T.C., 2017a. Structural controls on an orogenic gold system: the world-class Siguiri Gold District, Siguiri Basin, Guinea, West Africa. Economic Geology 112, 73–98. https://doi.org/10.2113/econgeo.112.1.73.

Lebrun, E., Thébaud, N., Miller, J., Roberts, M., Evans, N., 2017b. Mineralisation footprints and regional timing of the world-class Siguiri orogenic gold district (Guinea, West Africa). Mineralium Deposita 52, 539–564. https://doi.org/10.1007/s00126-016-0684-6.

Legros, H., Mercadier, J., Villeneuve, J., Romer, R.L., Deloule, E., Van Lichtervelde, M., Dewaele, S., Lach, P., Che, X.-D., Wang, R.-C., Zhu, Z.-Y., Gloaguen, E., Melleton, J., 2019. U-Pb isotopic dating of columbite-tantalite minerals: Development of reference materials and in situ applications by ion microprobe. Chemical Geology 512, 69–84. https://doi.org/10.1016/j.chemgeo.2019.03.001.

Liégeois, J.-P., Claessens, W., Camara, D., Klerkx, J., 1991. Short-lived Eburnian orogeny in southern Mali. Geology, tectonics, U-Pb and Rb-Sr Geochronology. Precambrian Research 50, 111–136.

Masurel, Q., 2016. 4D evolution of the Sadiola-Yatela gold district, Kédougou-Kénieba inlier, West Africa. University of Western Australia Crawley, WA. PhD Thesis.

Masurel, Q., Morley, P., Thébaud, N., McFarlane, H., 2021. Gold Deposits of the ~15-Moz Ahafo South Camp, Sefwi Granite-Greenstone Belt, Ghana: Insights into the Anatomy of an Orogenic Gold Plumbing System. Economic Geology 116, 1329–1353. https://doi.org/10.5382/econgeo.4829.

Masurel, Q., Thébaud, N., Miller, J., Ulrich, S., Hein, K.A.A., Cameron, G., Béziat, D., Bruguier, O., Davis, J.A., 2017b. Sadiola Hill: A World-Class Carbonate-Hosted Gold Deposit in Mali, West Africa. Economic Geology 112, 23–47. https://doi.org/10.2113/econgeo.112.1.23.

Milési, J.-P., Heinry, C., Sylvain, J.-P., 1989. Minéralisations aurifères de l'Afrique de l'ouest leurs relations avec l'évolution lithostructurale au Proterozoique inférieur. Bureau De Recherches Géologiques et Minières.

Mole, D.R., Fiorentini, M.L., Thebaud, N., McCuaig, T.C., Cassidy, K.F., Kirkland, C.L., Wingate, M.T.D., Romano, S.S., Doublier, M.P., Belousova, E.A., 2012. Spatio-temporal constraints on lithospheric development in the southwest–central Yilgarn Craton, Western Australia. Australian Journal of Earth Sciences 59, 625–656. https://doi.org/10.1080/08120099.2012.691213.

Mortimer, J., 1990. Evolution of the early Proterozoic Toumodi Volcanic Group and associated rocks. Ivory Coast, Portsmouth Polytechnic.

Mortimer, J., 1992. Lithostratigraphy of the early Proterozoic Toumodi Volcanic Group in central côte d'ivoire: implications for Birrimian stratigraphic models. Journal of African Earth Sciences (and the Middle East) 14, 81–91.

Olson, S.F., Diakite, K., Ott, L., Guindo, A., Ford, C.R.B., Winer, N., Hanssen, E., Lay, N., Bradley, R., Pohl, D., 1992. Regional setting, structure, and descriptive geology of the middle Proterozoic Syama gold deposit, Mali, West Africa. Economic Geology 87, 310–331. https://doi.org/10.2113/gsecongeo.87.2.310.

Parra-Avila, L.A., Belousova, E., Fiorentini, M.L., Baratoux, L., Davis, J., Miller, J., McCuaig, T.C., 2016. Crustal evolution of the Paleoproterozoic Birimian terranes of the Baoulé-Mossi domain, southern West African Craton: U–Pb and Hf-isotope studies of detrital zircons. Precambrian Research 274, 25–60.

Perrouty, S., Jessell, M.W., Bourassa, Y., Miller, J., Apau, D., Siebenaller, L., Velásquez, G., Baratoux, L., Aillères, L., Béziat, D., Salvi, S., 2015. The Wassa deposit: A poly-deformed orogenic gold system in southwest Ghana – Implications for regional exploration. Journal of African Earth Sciences 112, 536–547. https://doi.org/10.1016/j.jafrearsci.2015.03.003.

Peters, L.F.H., 2013. The volcanology, geochemistry and metallogenic potential of the Goren Volcano-sedimentary belt, northeast Burkina Faso, West Africa. University of Witwatersrand. MSc Thesis.

Salvi, S., Amponsah, P.O., Siebenaller, L., Béziat, D., Baratoux, L., Jessell, M., 2016a. Shear-related gold mineralization in Northwest Ghana: The Julie deposit. Ore Geology Reviews 78, 712–717. https://doi.org/10.1016/j.oregeorev.2015.08.008.

Salvi, S., Sangaré, A., Driouch, Y., Siebenaller, L., Béziat, D., Debat, P., Femenias, O., 2016b. The Kalana vein-hosted gold deposit, southern Mali. Ore Geology Reviews 78, 599–605. https://doi.org/10.1016/j.oregeorev.2015.10.011.

Salvi, S., Velásquez, G., Miller, J.M., Béziat, D., Siebenaller, L., Bourassa, Y., 2016c. The Pampe gold deposit (Ghana): Constraints on sulfide evolution during gold mineralization. Ore Geology Reviews 78, 673–686. https://doi.org/10.1016/j.oregeorev.2015.11.006.

Sylvester, P.J., Attoh, K., 1992. Lithostratigraphy and composition of 2.1 Ga greenstone belts of the West African Craton and their bearing on crustal evolution and the Archean-Proterozoic boundary. The Journal of Geology 100, 377–393.

Tourigny, G., Tranos, M.D., Masurel, Q., Kreuzer, O., Brammer, S., Owusu-Ansah, K., Yao, D., Hayford, T., 2019. Structural controls on granitoid-hosted gold mineralization and paleostress history of the Edikan gold deposits, Kumasi Basin, southwestern Ghana. Miner Deposita 54, 1033–1052. https://doi.org/10.1007/s00126-018-0858-5.

Traoré, Y.D., Siebenaller, L., Salvi, S., Béziat, D., Bouaré, M.L., 2016. Progressive gold mineralization along the Syama corridor, southern Mali (West Africa). Ore Geology Reviews 78, 586–598. https://doi.org/10.1016/j.oregeorev.2015.11.003.

Tshibubudze, A., Hein, K.A.A., 2016. Gold mineralisation in the Essakane goldfield in Burkina Faso, West African craton. Ore Geology Reviews 78, 652–659. https://doi.org/10.1016/j.oregeorev.2015.10.030.

Tunks, A.J., Selley, D., Rogers, J.R., Brabham, G., 2004. Vein mineralization at the Damang Gold Mine, Ghana: controls on mineralization. Journal of Structural Geology 26, 1257–1273. https://doi.org/10.1016/j.jsg.2003.11.005.